

# Journal of Materials Chemistry A

Accepted Manuscript



This is an *Accepted Manuscript*, which has been through the Royal Society of Chemistry peer review process and has been accepted for publication.

*Accepted Manuscripts* are published online shortly after acceptance, before technical editing, formatting and proof reading. Using this free service, authors can make their results available to the community, in citable form, before we publish the edited article. We will replace this *Accepted Manuscript* with the edited and formatted *Advance Article* as soon as it is available.

You can find more information about *Accepted Manuscripts* in the [Information for Authors](#).

Please note that technical editing may introduce minor changes to the text and/or graphics, which may alter content. The journal's standard [Terms & Conditions](#) and the [Ethical guidelines](#) still apply. In no event shall the Royal Society of Chemistry be held responsible for any errors or omissions in this *Accepted Manuscript* or any consequences arising from the use of any information it contains.

## Chemical sensors based on polymer composites with carbon nanotubes and graphene. The role of the polymer.

Horacio Salavagione<sup>\*1</sup>, Ana M. Díez-Pascual<sup>\*1</sup>, Eduardo Lázaro<sup>2</sup>, Soledad Vera<sup>2</sup>,

Marián A. Gómez-Fatou<sup>1</sup>

<sup>1</sup>Department of Polymer Physics, Elastomers and Energy Applications, Institute of Polymer Science and Technology (ICTP-CSIC), Juan de la Cierva 3, 28006 Madrid, Spain

<sup>2</sup>Analytical Chemistry, Physical Chemistry and Chemical Engineering Department, Faculty of Biology, Environmental Sciences and Chemistry, Alcalá University, E-28871 Alcalá de Henares, Madrid, Spain

### ABSTRACT

This review provides an overview of recent research on chemical sensors based on polymer composites with carbon nanotubes (CNTs) and graphene (G) for quantitative and qualitative analysis in diverse application fields such as biosensing (DNA, enzymes, proteins, antigens and metabolites), chemical and gas sensing using electrochemical and optical detection methods. Both, CNTs and G show outstanding electrical, chemical, electrochemical and optical properties that make them ideal candidates to be used in chemical sensors. The incorporation of polymers in the development of this type of sensors not only improves the CNT and G dispersion, but also enhances some of their properties like redox behaviour and biocompatibility, and provides additional properties such as photoelectric or swelling capacity. Moreover, unique synergistic effects arising from the combination of the matrix and nanofiller contributions are described by means of several examples highlighting the most important achievements in this field. Special emphasis has been placed throughout the review on analysing the role of the polymer in the different sensing platforms. The combination of polymers with carbon nanomaterials for the preparation of chemical sensors is opening up exciting areas of research due to their biocompatibility, excellent sensitivity and selectivity.

---

<sup>\*</sup>Corresponding authors. E-mail addresses: [horacio@ictp.csic.es](mailto:horacio@ictp.csic.es) (H. Salavagione), [adiez@ictp.csic.es](mailto:adiez@ictp.csic.es) (A. M. Díez-Pascual)

**Contents**

1. Introduction
  2. Polymer composites incorporating carbon nanotubes and graphene
    - 2.1. *Polymer/carbon nanotubes composites*
    - 2.2. *Polymer/graphene composites*
  3. Chemical sensors based on polymer composites
    - 3.1 *Chemical sensors based on polymer/carbon nanotubes*
      - 3.1.1 *Optical sensors*
      - 3.1.2 *Electrochemical sensors*
    - 3.2 *Chemical sensors based on polymer/graphene*
      - 3.2.1 *Optical sensors*
      - 3.2.2 *Electrochemical sensors*
    - 3.3 *Chemical sensors based on polymer/graphene/carbon nanotubes*
  4. Conclusions and future perspectives
- References

### *Abbreviations*

AA: acrylamide  
AAC: ascorbic acid  
ABSA: aminobenzene sulphonic acid  
ACBK: acid chromeblue K  
ADP: adenosine 5'-diphosphate  
AIBN: 2,2-azobisisobutyronitrile  
AMP: adenosine 5'-monophosphate  
AntB1: aflatoxin B1 antibody  
anti-HSA IgG: anti-mouse immunoglobulin G  
AO: ascorbate oxidase  
AP: acetaminophen  
APS: ammonium peroxodisulfate  
APASA: 2-acrylamido-2-methyl-1-propane sulfonic acid  
APTES: 3-aminopropyl triethoxysilane  
ATP: adenotriphosphate  
BSA: bovine serum albumin  
BMIMBF<sub>4</sub>: (1-butyl-3-methylimidazoliumtetrafluoroborate)  
BQ: benzoquinone  
CA: creatinineamidohydrolase  
CCE: ceramic carbon electrode  
CCP: cationic conjugated polymer  
CEF: cefotaxime  
CHOX: cholesterol oxidase  
CI: creatineamidinohydrolase  
CL: chemiluminiscence  
CMG:chemically modified graphene  
CNT: carbon nanotube  
CP: conducting polymers  
CPE: carbon paste electrode  
CR: congo red  
CS: chitosan  
CTC: chlorotetracycline  
CTP: cytidine 5'-triphosphate  
CV: cyclic voltammetry  
CVD: chemical vapour deposition  
DA: dopamine  
DAP: 3,4-diaminophenyl  
DEX: dextran  
DNP: 2,4-dinitrophenol  
DPASA: diphenyl amine 4-sulfonic acid  
DPASV: differential pulse anodic stripping voltammetry  
DPV: differential pulse voltammetry  
DSPE-3PEO: 1,2-distearoysl-n-glycero-3-phosphoethanolamine-coupled branched methoxyPEG  
DTAB : dodecyltrimethylammonium bromide  
EDC: N-ethyl-N'-(3-dimethylaminopropyl) carbodiimide  
EGDMA: ethylene glycol dimethacrylate

EIS: electrochemical impedance spectroscopy  
ELISA: enzyme-linked immunosorbent assay  
EMIM-BF<sub>4</sub>: 1-ethyl-3-methyl-imidazoliumtetra-fluoroborat  
EP: epinephrine  
FAD: flavin adenine dinucleotide  
FAM: carboxyl fluorescein  
FI-CL: flow injection chemiluminiscence  
Fluo: fluorescein  
FRET: Fluorescence resonance energy transfer  
FT-IR: Fourier transform infrared spectroscopy  
FUAA: 5-fluorouracil-N-acetylacrylamide  
G: graphene  
GABA:  $\gamma$ -amino butyric acid  
GABAD: *o*-phthalaldehyde/sulphite derivative of GABA  
GBP: glucosebinding protein  
GCE: glassy carbon electrode  
GO: graphene oxide  
GOD: glucose oxidase  
GQDs: graphene quantum dots  
GS: graphene sheets  
GTP: guanosine 5'-triphosphate  
GUA: guaiacol,2-methoxyphenol  
HA: hyaluronic acid  
Hb: hemoglobin  
HQ: hydroquinone  
HRP: horseradishperoxidase  
IL: ionic liquid  
ITO: indium tin oxide  
Lac: laccase enzyme  
LBL: layer by layer  
LDH: lactate dehydrogenase  
LEV: levofloxacin  
LOD: limit of detection  
LSV: linear sweep voltametry  
MAA: methacrylic acid  
MEF: mefenamicacid  
MIP: molecularimprinted polymer  
MNP: magnetic nanoparticles  
MO: morphine  
MSN:mesoporous silica nanoparticle  
MWCNT: multi-walled carbon nanotube  
NADH: nicotinamide adeninedinucleotide  
NAPD: N-acryloyl pyrrolidine-2, 5-dione  
NAS: N-acryloxysuccinimide  
NHS: N-hydroxysuccinimide  
NIR: near-infrared  
NP: nanoparticle  
NTA: NR,NR-bis(carboxymethyl)-L-lysine  
4-NP: paranitrophenol

NW: network  
OPDA: o-phenylenediamine  
OTA: ochratoxin A  
P3MT: poly-(3-methylthiophene)  
PAA: polyacrylic acid  
PABSA: poly(aminobenzenesulphonic acid)  
PAIHP: polyaminoimide  
PAM: polyacrylamide  
PANI: polyaniline  
PANIw: polyaniline nanowires  
PB: Prussian blue  
PBA: phenyl boronic acid  
PBPN: poly(benzyl methacrylate-r-ethylene glycol methacrylate-r-N-acryloxysuccinimide)  
PCDA: 10,12-penacosadiynoic acid  
PDA: polydiacetylene  
PDDA: poly(diallyldimethylammonium chloride)  
PDPB: poly(2,5-di-(2-thienyl)-1-pyrrole-1-(p-benzoic))  
PEG: polyethylene glycol  
PEDOT: poly(3,4-ethylenedioxythiophene)  
PFP: poly [(9,9-bis(6'-N,N,N-trimethylammonium)hexyl)-fluorenylene-phenylenedibromide]  
PGE: pyrolytic graphite electrode  
PLPEG-COOH: 1,2-distearoyl-*sn*-glycero-3-phosphoethanolamine-N-[carboxy(polyethylene glycol)]  
PmPV: poly(m-phenylenevinylene-co-2,5-dioctoxy-p-phenylenevinylene)  
PolyBz: polybenzidine  
PML/RARA: promyelocyticleukemia/retinoic acid receptor alpha  
POPDA: poly(o-phenylenediamine)  
PPEG8: polyethylene glycol, eight-membered branched polymer  
PpABA: poly(para-aminobenzoic acid)  
PPNP: porous platinum nanoparticle  
PPV: poly(p-phenylenevinylene)  
PPy: polypyrrole  
PQ11: poly[(2-ethyl dimethylammonioethyl methacrylate ethyl sulfate)-co-(1-vinylpyrrolidone)]  
PS: polystyrene  
PSS: poly(styrenesulfonic acid)  
PTMS: phenyltrimethoxysilane  
PVA: poly(vinyl alcohol)  
PVDF: poly(vinylidene fluoride)  
PVI-Os: cross-linked [Os(bpy)<sub>2</sub>Cl]<sup>+2+</sup> complexed poly(1-vinylimidazole)  
PVP: poly(vinyl pyrrolidone)  
QCA: quinoxaline-2-carboxylic acid  
QDs: quantum dots  
RGO: reduced graphene oxide  
R-N<sub>2</sub><sup>+</sup> X<sup>-</sup>: diazonium compounds  
SDBS: sodium dodecylbenzenesulfonate  
SDS: sodium dodecylsulfate

SEM: scanning electron microscopy  
SERS: surface-enhanced Raman scattering  
SG: sulphonated graphene  
SMZ: sulfamethoxazole  
SO: sarcosineoxidase  
SPCE: screen-printed carbon electrode  
SPANI: sulfonated polyaniline  
SPEEK: sulphonated poly(ether-ether-ketone)  
SPR: surface plasmon resonance  
ssDNA: single-strand DNA  
STM: scanning tunnelling microscopy  
SWCNT: single-walled carbon nanotube  
SWV: square-wave voltammetry  
TDI: 2,4-toluene diisocyanate  
TEM: transmission electron microscopy  
TEOS: tetraethoxysilane  
TMP: trimethoprim  
TiNP: TiO<sub>2</sub> nanoparticles  
TNT: 2,4,6 trinitrotoluene  
TRGO: thermally reduced graphene oxide  
TRIM: trimethylolpropane trimethacrylate  
Ty: tyrosinase  
UA: uric acid  
VA: 4-vinyl aniline  
VE: vitamin E  
VOC: volatile organic compounds

## 1. Introduction

Sensitivity, selectivity, and a rapid and cost effective detection of target molecules are the main drivers for the development of new chemical sensors and biosensors for their use in a wide range of fields from environmental, security, agriculture or food applications, to healthcare including clinic diagnosis and treatment of diseases amongst others. During the last decade the incorporation of nanomaterials to chemical sensors and biosensors has boosted the advances in this area leading to relevant enhancements in their performance.<sup>1,2</sup>

Carbon nanotubes (CNTs) and graphene (G) are two of the most innovative nanomaterials with unique electronic, optical, mechanical, chemical and electrochemical properties.<sup>3,4,5,6,7,8,9,10,11,12,13,14,15,16,17,18</sup> In recent years these novel carbon nanomaterials are attracting enormous interest for their use in sensors and biosensors in various transduction modes from electrical and electrochemical to optical detection, and important advantages have been reported with respect to conventional ones.<sup>19,20,21,22,23,24,25,26,27,28,29,30,31,32,33,34,35,36,37,38</sup> Among the exceptional properties of these two carbon allotropes, their large surface area, high electrical conductivity and very efficient electrocatalytic behaviour are the most relevant for electrochemical applications. Their excellent fluorescence quenching ability has been exploited in optical sensors. Both nanomaterials have the same composition with  $sp^2$ -hybridized carbon atoms although with different structure changing from the flat two-dimensional sheet of graphene to the rolling up of graphene sheets in tubes in CNTs. This feature affects their properties and plays a major role in the architecture design of sensors. Differences in the synthetic routes to obtain both carbon materials may also affect the performance of the sensors with, for example, CNTs grown from metallic particles or the variety of graphene materials which are prepared by diverse methods. Moreover, functionalization and control of the surface

chemistry of these nanofillers are essential for their use as building blocks in sensors. Of special interest is the biofunctionalization of these nanomaterials with the ability of specific recognition to amplify the detection signal in biosensors.

On the other hand, polymers are one of the most widely exploited classes of materials due to the incredible variety of chemical moieties available and the subsequent compendium of properties, together with their relatively low cost, easy processing, and their potential for recycling and application as sustainable materials. The development of polymeric composites based on CNTs and graphene has drawn great attention as a route to obtaining new materials with new structural and functional properties superior to those of the pure components and enhanced performance in a broad range of technological sectors such as telecommunications, electronics, energy, biomedicine and transport industries.<sup>39,40,41,42,43,44,45,46</sup> In particular, these polymers composites may play different roles in chemical sensors and biosensors besides providing mechanical stability and improving the nanofiller dispersion, leading to enhanced sensitivity and selectivity. Although there are a number of recent reviews related to the use of CNTs and graphene in chemical sensors and biosensors,<sup>19,20,21,22,23,24,25,26,27,28,29,30,31,32,33,34,35,36,37,38</sup> to the best of our knowledge, there is no report devoted to carbon based polymer composites for this specific application (except for the just published work<sup>47</sup> related exclusively to conducting polymers/graphene composites for electrochemical sensors). This is the framework of the present revision in which the added value of incorporating polymers to these carbon nanomaterials based sensors is discussed. Among the different types of chemical sensors and biosensors, we will only focus on electrochemical and optical sensors, and we will revise from 2007 in which the first works related with the incorporation of graphene into polymers appeared in the literature. After introducing the exciting properties of both CNTs and graphene and the strategies used to efficiently

incorporate them into polymer matrices, the synergistic effects of combining these carbon nanofillers with the macromolecular systems for their application in different sensing platforms will be highlighted. Relevant examples of different roles of the polymers from coatings or immobilization supports to specific active functions will be shown. Finally, an outlook of future perspectives and challenges of polymer/CNT and polymer/graphene composites for their use in chemical sensors and biosensors will be presented.

## **2. Polymer composites incorporating carbon nanotubes and graphene**

The combination of CNTs and graphene with polymers provides a route to the creation of materials with countless applications almost in a combinatorial manner, because it does not only refer to the combination of two compounds but in the assembly of two families of materials.

### *2.1. Polymer/carbon nanotubes composites*

Carbon nanotubes are allotropes of carbon discovered by Iijima in 1991 with a seamless tubular structure formed by curling-up graphene sheets.<sup>3</sup> There are two main types of CNTs: single-walled CNTs (SWCNTs), which consist of a single tube of graphene, and multi-walled CNTs (MWCNTs) that are composed of several concentric tubes of graphene fitted one inside the other. Different techniques have been developed to synthesize CNTs, and detailed information about such methods can be found elsewhere.<sup>48,49</sup> CNTs have unique electronic, chemical and mechanical properties that make them leading materials for a variety of potential applications. They are one of the stronger and stiffer materials in terms of strength and elastic modulus<sup>4,5</sup> and also display very high electrical<sup>6</sup> and thermal<sup>7</sup> conductivity as well as thermal stability<sup>8</sup>.

It is well known that homogeneous CNT dispersion and strong interfacial adhesion with the matrix are critical issues in the development of polymer/CNT composites in order

to attain improved properties. Therefore, significant efforts have been directed towards developing methods to modify surface properties of CNTs, and several review articles describe in detail these functionalization strategies.<sup>40,50,51</sup> They can be divided into chemical functionalization and physical methods based on the interactions between the modification molecules and the CNTs. The chemical method involves the covalent bonding (grafting) of polymer chains to CNTs, and can be carried out via “*grafting to*” or “*grafting from*” routes. The first approach involves the synthesis of a polymer with reactive groups or radical precursor that is attached to the surface of pristine or functionalized nanotubes by addition reactions; its main disadvantage is that the grafted polymer content is limited because of the relatively low reactivity and high steric hindrance of macromolecules. In the *grafting from* strategy the polymer is grown from the CNT surface via *in situ* polymerization of monomers; this process is efficient and controllable, enabling the preparation of composites with high degree of grafting, although requires strict control of the amounts of each reactant and the polymerization conditions. Further, during the functionalization treatment a large number of defects are typically generated on the CNT sidewalls that can adversely impact their mechanical properties and even disrupt the electron system. Alternatively, CNT functionalization can be performed by plasma treatment,<sup>52</sup> an environmentally friendly method for modifying CNTs by directly introducing a high density of functional groups. In particular, for the functionalization with amine groups, nitrogen containing gases (NH<sub>3</sub> or NH<sub>3</sub> mixed with N<sub>2</sub> or N<sub>2</sub>/H<sub>2</sub>) are used, and the CNT surfaces can change from hydrophobic to hydrophilic, thus facilitating the dispersion within the matrix without altering the intrinsic mechanical properties of the tubes.

The non-covalent CNT modification consists in the physical adsorption and/or wrapping of polymers to the surface of the CNTs. The physical adsorption is achieved through van der Waals interactions while the polymer wrapping process occurs via  $\pi$ - $\pi$  interactions between

CNTs and polymer chains containing aromatic rings. This functionalization does not destroy the conjugated system of the CNT sidewalls, and therefore it does not affect the final structural properties of the material. Besides polymers, surfactants have also been employed to functionalize CNTs<sup>53,54,55,56</sup>. The physical adsorption of the surfactant on the CNT surface lowers the surface tension, effectively preventing the formation of aggregates. Furthermore, the surfactant-treated CNTs overcome the van der Waals attraction by electrostatic/steric repulsive forces. A comprehensive review of the mechanisms behind the improved dispersability of surfactant-modified CNTs has been reported<sup>57</sup>. Another non-covalent method for CNT functionalization is the endohedral method.<sup>58</sup> In this approach, guest atoms or molecules are stored in the inner cavity of CNTs through the capillary effect. Typical examples of endohedral functionalization are the insertion of inorganic nanoparticles such as Ag, Au or Pt or small biomolecules such as proteins or DNA.

Several methods have been reported for the preparation of polymer/CNT composites, including solution mixing, melt-blending and *in situ* polymerization. The most common method is solution mixing because it can be used to prepare small composite films. Typically, it involves three steps:<sup>59</sup> dispersion of CNTs in a suitable solvent by mechanical stirring or tip/bath sonication, mixing with the polymer matrix at room or elevated temperatures and finally precipitation or casting of the mixture. This method enables to drop-cast films with up to 60 wt. % CNT content, although can result in reagglomeration of the CNTs during the casting/evaporation process. Melt blending is a commonly used technique to fabricate thermoplastic/CNT composites. In addition, it is suitable for polymers that cannot be processed by solution techniques due to their insolubility in common solvents. It uses a high temperature and a high shear force to disperse the CNTs, and is compatible with industrial processes. The main benefit of this method is that it does not require solvents to disperse the CNTs, although is limited to low filler concentrations.

Depending on the final morphology/shape of the composites, the bulk materials can be processed by different techniques such as extrusion or melt-spinning to form a fibre, which frequently results in CNT alignment along the fibre axis. *In situ* polymerization is an efficient method to disperse CNTs in a thermosetting polymer. The CNTs are initially mixed with monomers, either in the presence or the absence of a solvent, and subsequently these monomers are polymerized through addition or condensation reactions with a curing agent at high temperature. One of the most important advantages of this method is the formation of covalent bonds between the functionalized CNTs and the matrix. Moreover, due to the small size of monomeric molecules, the homogeneity of the resulting composites is higher than those obtained via solution mixing or melt-blending. Likewise, it allows the preparation of composites with high CNT weight fraction.

Another recent approach to incorporate CNTs in a polymer matrix is based on the use of the latex technology.<sup>60</sup> Latex is a colloidal dispersion of discrete polymer particles in an aqueous medium. By using this technique, it is possible to disperse CNTs in polymers that are synthesized by emulsion polymerization, or that can be produced in the form of an emulsion. The method consists in the dispersion of the CNTs in an aqueous surfactant solution, followed by mixing the dispersion with polymer latex. After freeze-drying and subsequent melt-processing, a composite can be obtained. This route is a safe, environmentally friendly, versatile and low-cost method, and enables to incorporate CNTs into highly viscous matrices. New approaches have been developed in the last years to obtain composites with high CNT content, including densification,<sup>61</sup> spinning of coagulant,<sup>62</sup> layer-by-layer deposition<sup>63</sup> and pulverization.<sup>64</sup>

Up to date, a large number of papers have been reported on the mechanical properties of polymer/nanotube composites, and the improvements attained have been summarized in several reviews.<sup>65,66,67,68,69</sup> It has been found that composites incorporating chemically

modified nanotubes show better results,<sup>68</sup> since the strong interaction between the functionalized CNTs and the matrix greatly enhances the dispersion as well as the interfacial adhesion, thus strengthening the overall mechanical performance of the composite. Further, the polymer grafting strategy seems to be the most effective for improving dispersion and mechanical properties due to the strong chemical bonding between CNTs and polymers.<sup>65,70</sup> On the contrary, low reinforcement has been found for melt-processed samples incorporating pristine CNTs.<sup>67</sup> Composite fibers produced by melt spinning/drawing techniques display better reinforcement compared to bulk samples due to CNT alignment effects. Nevertheless, the improvements attained are in general significantly below the expectations according to the rule of mixtures or the Halpin–Tsai equations, and new functionalization routes/chemical techniques are still required.

On the other hand, CNTs have clearly demonstrated their great potential for enhancing the electrical conductivity of polymers by several orders of magnitude at very low percolation thresholds (<0.1 wt%).<sup>67,69,68,71</sup> The conductivity values attained strongly depend on the nanotube aspect ratio, degree of dispersion and alignment. Thus, CNTs with higher aspect ratio result in significantly lower percolation thresholds. Alignment of the CNTs within the matrix has a detrimental effect on this property, since there are fewer contacts between the tubes, leading to a reduction in electrical conductivity and a higher percolation threshold as compared to composites with randomly oriented nanotubes. Regarding the CNT functionalization, controversial results have been reported.<sup>69</sup> While some researchers found reduced conductivity due to disruption of the  $\pi$ -conjugation system, others found an improvement due to better dispersion. It appears that the disadvantages of functionalization with respect to CNT conductivity can be outweighed by the improved dispersion enabled by functionalization,<sup>71</sup> although no general conclusion can be drawn.

With regard to the thermal conductivity, only modest improvements have been reported<sup>69,72</sup> which generally fall well below the predictions by the rule of mixtures, attributed to the low thermal conductance of the CNT-polymer interface. The covalent grafting of polymers to CNTs is a strategy to reduce this high thermal interfacial resistance. However, such bonds decrease the intrinsic tube conductivity by acting as scattering centers for phonons propagating along the tubes, and the final result depend on a balance of both factors.<sup>69,70</sup> On the other hand, the use of aligned CNTs has been shown to be the most effective for enhancing the polymer thermal conductivity.

A lot of works have reported improved thermal stability of polymer/CNT composites compared to the neat polymers.<sup>69,70</sup> The nanotubes hamper the diffusion of volatile products and thereby delay the onset of degradation.<sup>73</sup> In particular, it has been found that SWCNTs have higher capability to reduce the mass loss rate of the composite compared to MWCNTs, CNFs or carbon black particles.<sup>69</sup>

## 2.2. Polymer/graphene composites

Graphene is an atomically thick, two-dimensional sheet composed of  $sp^2$  carbon atoms arranged in a honeycomb structure. It has extraordinary electronic, thermal, optical and mechanical properties<sup>9,10,11,12,13,14,15,16,17,18</sup> with some values that exceed those obtained in any other material. Graphene has excellent thermal conductivity ( $\sim 5000$  W/m.K),<sup>12</sup> superior electron mobility ( $25000$   $\text{cm}^2/\text{V.s}$ ),<sup>15</sup> the highest electrical conductivity known at room temperature ( $6000$  S/cm),<sup>16</sup> very large surface area ( $\sim 2630$   $\text{m}^2/\text{g}$ ), and complete impermeability to any gases.<sup>17</sup> It is a zero-gap semiconductor material, electroactive and transparent.<sup>18</sup> Moreover, with a Young's modulus of  $\sim 1$  TPa and ultimate strength of  $130$  GPa, is the strongest material ever measured.<sup>13</sup> These unique properties make graphene an ideal candidate for a variety of applications such as sensors, batteries, supercapacitors, fuel

cells, photovoltaic devices, composites, photocatalysis, and flexible electronics amongst others.<sup>11, 43,44,74,75</sup>

It is important to note that the term “graphene” used in the literature includes a wide range of graphene-like structures which differ in the preparation method and, consequently in the chemical structure (usually the oxidation level), shape, size and number of layers. In fact, there exist several methods employed to prepare graphene, each with specific characteristics of dimension, shape, quantity and quality.<sup>9,11,76,77,78,79,80,81,82,83</sup> Therefore the production methods are strongly related to the final application to which the graphene is directed.<sup>11</sup>

From the standpoint of polymer composites, the excellent mechanical and electrical properties that graphene would confer to the polymer matrices are those critical for obtaining lightweight materials with superior performance. Consequently, polymer/graphene composites continue to attract considerable interest due to the outstanding properties encountered with only small quantities of nanofiller incorporated to the polymer matrix.<sup>84,85,86</sup> The main reason for this lies in the nano-level dispersion of large surface-to-volume ratio fillers when compared to micro- and macro-scale additives. Outstanding properties are achieved with small quantities of filler producing lightweight materials with low density. Apart from its intrinsic outstanding properties, graphene may be the best filler for lightweight polymer composites due to its highest aspect ratio in 2D sheets with lateral dimensions in the micro-scale and only one atom thick. In comparison with carbon nanotubes, graphene sheets have higher surface-to-volume ratios owing to the inaccessibility of the inside surface of the nanotubes to the polymer molecules. The graphene/polymer composites have shown the potential to rival or even surpass the performance of their carbon nanotube-based counterparts.<sup>43,44,45,46,87,88,89,90,91,92.</sup> Further, graphene is obtained from naturally occurring graphite implying that lighter composites can be produced at lower costs.

Consequently this area of research has grown to represent one of the largest classes within the scope of materials science, and is rapidly becoming a key area in nanoscience and nanotechnology offering significant potential in the development of advanced materials in multiple and diverse application areas.

In order to efficiently transfer the graphene properties to the matrices in composites the key aspects are related to the molecular-level dispersion of graphene into the matrix and the strength of the graphene/polymer interface. In order to be “compatibilised” with polymers, graphene must be appropriately modified with adequate functional groups able to interact with specific chemical moieties in polymeric matrices, prior to their incorporation into the matrix. Control of the size, shape and surface chemistry of the reinforcing graphene is essential in the development of materials that can be used to produce devices, sensors and actuators based on the modulation of functional properties.

However, the low intrinsic reactivity of graphene limits the interfacial interactions with the polymer affecting the load transfer across the interface and the performance of the composites. Graphene oxide is an alternative to be used in polymer composites due to the presence of specific functionalities in the graphitic sheets. However, the main limitations of using GO is the formation of structural defects and vacancies that disrupt the  $sp^2$  network and dramatically worsen the electronic properties.<sup>82</sup> The reduction of GO restores the conductivity albeit, as some defects or vacancies are irreversible, it remains lower than that of pristine graphene. In this sense, RGO brings together features of both graphene and GO and may lead to materials with reasonably good conductivity, thermal stability and processability.

Bearing all of this in mind, it is clear that the possibility to functionalize graphene and graphene derivatives, covalently or through supramolecular interactions, to tailor their compatibility with the polymer matrix and get stable dispersions is an efficient route

to enhance the final properties of the composites. The extensive previous work developed with the other structurally similar carbon nanomaterials, carbon nanotubes and fullerenes, has paved the way for the chemical modification of graphene.

Among the strategies addressed to modify graphene, similarly to CNT the covalent linkage between graphene and polymers, either by *grafting from*<sup>46,93,94,95</sup> or *grafting to*<sup>96,97</sup> approaches, represents an interesting alternative for polymer composites.<sup>98</sup> In this type of materials the concept of interface changes from a traditional view of molecular interactions between components at a polymer – filler interface (e.g. van der Waals, hydrogen bonding, halogen bonding, etc.), to the concept of a single compound where graphene forms an integral part of the matrix.<sup>99</sup> Moreover, click chemistry reactions have been recently successfully used to modify graphene for its incorporation in polymer composites.<sup>100,101,102</sup> The click reactions are wide in scope, general, orthogonal, easy to perform; only readily available reagents are used, and they are insensitive to oxygen and water. Finally, an alternative approach is the non-covalent modification, which enables the attachment of molecules through  $\pi$ - $\pi$  stacking or hydrophobic (van der Waals) interactions, preserving the intrinsic electronic properties of graphene.<sup>46</sup>

The different strategies employed for graphene dispersion and functionalization influence, to a large extent, the mechanical, thermal, and electrical performance of the polymer/graphene composites.<sup>44,45,46,98,99</sup>

The three main strategies used for CNT based composites have also been reported for the preparation of polymer/graphene composites: melt-blending, solution-mixing and *in situ* polymerization of monomers.<sup>46,99</sup> The first approach, involves the direct mixing of graphene with the polymer in the molten state and subsequent extrusion or injection moulding. It has the advantages of absence of solvents and industrial applicability previously commented. However, the use of melt blending has been limited due to the thermal instability of most

chemically modified graphenes and that the dispersion of the filler is substantially inferior to that obtained with solution methods. The solution-mixing method is the most efficient to ensure good dispersion of the filler. It involves the dispersion of graphene in an appropriate solvent, the mixing between the previous solution/dispersion with a polymer-containing solution in the same (or miscible) solvents and the precipitation of the composites by addition of a non-solvent or, alternatively, the elimination of the solvent by evaporation or distillation. In the case of using GO or modified-GO as fillers an intermediate step is applied which consists in the chemical reduction of GO to RGO in the presence of the polymer that stabilises the reduced graphitic sheets avoiding their re-aggregation. In the *in situ* polymerization strategy, graphene is first dispersed in the liquid monomer (or pre-polymer), the initiator (or curing agent) is then added and subsequently the polymerization (or curing) is started either by heat or radiation. This strategy generates very efficient interactions between the filler and the polymer matrix through covalent bonds.

Regarding final performance of the composites the mechanical properties may be the most addressed.<sup>45,46</sup> However, although electrical conductivity has been also widely studied, thermal conductivity and gas barrier effect have been analysed in less extent. Here it is worth nothing that these properties are not all equally sensitive to the source of graphene, in terms of structural integrity of the  $sp^2$  network. While mechanical properties are normally improved independently of the graphene source employed, the quality of graphene is extremely important for both thermal and electrical conductivity since  $sp^3$  defects or vacancies scatters electrons and phonons.<sup>103</sup>

The high modulus of graphene, which is much higher than that for polymers and the large surface area of the platelets, allow a substantial increase in the composites mechanical properties.<sup>45</sup> In general, improvements in mechanical performance are related to the graphene dispersion. Also, the mechanical properties increase with graphene loading until a

certain limit value, where platelet aggregation occur thus leading to a decrease in the aspect ratio as well as to the creation of crack points.

The electrical conductivity is one of the most important challenges when graphene/composites are prepared. In these systems the bulk conductivity of insulating polymers increases several order of magnitudes when an appropriate amount of graphene is added, following normally a percolation behavior. In other words, to achieve electrical conductivity, the concentration of graphene must surpass the electrical percolation threshold, where a conductive network of filler particles is formed.<sup>104</sup>

In the case of thermal conductivity, its improvement is also related to the contact between particles that reduces thermal resistance. Although in principle the thermal conductivity in graphene/polymer composites can be rationalized with percolation theory,<sup>45</sup> the increase in the thermal conductivity has been more modest than in the case of electrical conductivity and much higher graphene loading need to be added to obtain reasonable improvement on the thermal conductivity.<sup>105</sup> This is believed to be due to the much smaller differences between thermal conductivity of graphene and polymers (compared with electrical conductivity). In most of the cases reported the thermal stability of the composites is improved.

### **3. Chemical sensors based on polymer composites**

#### *3.1 Chemical sensors based on polymer/carbon nanotubes*

##### *3.1.1 Optical sensors*

The discovery in 2002 of the band-gap fluorescence of SWCNTs<sup>106</sup> has motivated the use of these nanomaterials for optical sensing, particularly for biological systems. Their fluorescence in the NIR region (between 820 and 1600 nm), where absorption of biological tissues is generally negligible, inherent photostability and tissue transparency<sup>107</sup> are

attractive characteristics for the design of *in vitro* and *in vivo* sensors. The main mechanisms by which a target molecule can selectively modify their fluorescent (or photoluminescent) spectra are changes in emission wavelength and intensity caused by solvatochromism,<sup>108</sup> charge-transfer<sup>109</sup> and/or doping and redox reactions.<sup>110</sup> The dielectric environment around CNTs affects polarizability and can provoke a solvatochromic shift in the absorption and emission spectra. An analyte could change the dielectric environment directly, by replacing solvent molecules or by changing the conformation of the polymer-wrapping. The charge-transfer mechanism occurs when the analyte orbitals overlap with SWCNT/wrapping orbitals. Electron transfer leads to a change of ground states or excited states, which affects the fluorescence spectrum via altered rates of exciton quenching. In the doping and redox reactions, the analyte changes the number of defects of the carbon lattice and thus exciton decay routes. The key challenge is the modification of the nanotube surface in order to be selective for the analyte of interest. In the following section, we review the most recent advances in the development of optical sensors based on polymer/CNT composites, making special emphasis on the role of the polymer. The most representative examples reported to date on this topic are collected in Table 1.

In most of the studies summarized in Table 1, the polymer is used to non-covalently functionalize or wrap the CNTs.<sup>111,112,113,114,115,116,117,118,119,120</sup> The non-covalent functionalization of SWCNTs with water-soluble polymers<sup>112,115,116,118,120</sup> or polysaccharides<sup>111,114,117</sup> is an efficient strategy for producing stable CNT-based sensing materials in aqueous media. Many of these studies are based on the change in the NIR emission spectra of the SWCNTs, as explained above. Some of them focused on the development of continuous *in vivo* glucose sensors, which would help to alleviate different diabetes related problems. The main goal is to maintain blood glucose levels at physiological concentrations, and current sensors lack accuracy in reporting real concentrations. For

example, Barone and Strano<sup>111</sup> developed a sensor that operated based on the competitive binding between this analyte and phenoxy-derivatized dextran, a polysaccharide that acts as a glucose analogue for a protein binding site (Figure 1A). Firstly, the SWCNTs were wrapped in the polymer derivative via solution mixing. The subsequent addition of concanavalin A (conA), a plant lectin with four saccharide binding sites at physiological pH, provoked aggregation of the dextran-coated SWCNTs and decrease in their NIR fluorescence proportional to the conA concentration. The introduction of glucose caused dissolution of the aggregate along with a fluorescence recovery due to competitive binding between the glucose and the polymer for conA binding sites. The lineal response of the fluorescence vs. glucose concentration was found between  $3.8$  and  $11 \times 10^{-3}$ M, hence it needs to be engineered to respond in the physiological range of  $2$ - $30 \times 10^{-3}$ M. A more recent study on polymer/nanotube-based glucose sensors utilizes allosteric changes in conformation to modulate SWCNT fluorescence emission.<sup>112</sup> In particular, SWCNTs wrapped in carboxylated-poly(vinyl alcohol) (PVA) were grafted to glucose binding protein (GBP) by covalently linking the carboxylic groups of the polymer to amine groups of the lysine moieties of the protein (Figure 1B). In the presence of glucose, the attached GBP undergoes a conformational change from an open to a closed structure as it absorbs a glucose molecule that results in a decrease of the SWCNT fluorescence. This fluorescence is recovered as the GBP returns to its initial open state, releasing the glucose molecule and demonstrating sensor reversibility.

Systems based on polymer-wrapped CNTs that selectively detect analytes like nitric oxide (NO) have also been developed, and the first was prepared by coating SWCNTs with 3,4-diaminophenyl-functionalized dextran via five synthetic steps in solution followed by dialysis.<sup>114</sup> The polymer wrapping imparted rapid and selective NIR fluorescence detection of NO by the donation of lone-pair electrons from amines that conferred more electron

density and mobility to the SWCNTs. The resulting sensors were capable of spatiotemporally detecting NO produced inside macrophage cells by activation of the NO synthase within the cells. The detection limit of the dextran-SWCNT hybrid was  $7 \times 10^{-8}$  M, about 12 times larger than that obtained with metal–fluorescein probes. Further optimization can be expected by varying the number of the diamino groups per polymer chain. Zhang *et al.*<sup>115</sup> tried to synthesize a PVA-wrapped SWCNT composite for the detection of NO. However, the NIR fluorescence of this compound remained unaltered in the presence of the oxide, which could be due to direct reaction between the analyte and the polymer through its hydroxyl groups. Another plausible explanation might be pore blocking due to the formation of organo-nitrite after reaction with NO. In contrast, the PVA-SWCNT fluorescence was quenched by reducing agents such as nicotinamide adenine dinucleotide (NADH), L-ascorbic acid and melatonin. The authors suggested that these molecules donate electrons directly to the conduction bands of PVA-SWNT, and extra electrons in the conduction bands can then quench excitons through a non-radiative Auger recombination.<sup>121</sup> Regardless of mechanism, the abovementioned examples demonstrate that the type of polymer adsorbed on the CNTs strongly influences the selectivity of the complex, and this has important implications for the sensor applications of carbon nanotubes. The same authors have designed a SWCNT probe for adenotriphosphate (ATP) detection.<sup>116</sup> In that study, luciferase enzyme was conjugated to the carboxylic acid group of poly(ethylene glycol) (PEG) that wrapped the SWCNTs. Upon exposure of this complex to ATP in the presence of D-luciferin, the luciferase on the SWCNTs selectively converted ATP to adenosine 5'-monophosphate (AMP) and simultaneously oxidized D-luciferin to oxyluciferin, which quenched the SWCNT NIR fluorescence. This sensor has high sensitivity, with a LOD of  $2.4 \times 10^{-7}$  M ATP. Moreover, it presents high selectivity towards ATP even in the presence of potentially interfering molecules such as AMP, adenosine 5'-diphosphate (ADP), cytidine

5'-triphosphate (CTP) and guanosine 5'-triphosphate (GTP). The capability of this sensor to spatially and temporally detect ATP in living cells was also demonstrated, making it the first CNT-based optical sensor for the recognition of ATP *in vivo*. Another example of biosensing polymer/SWCNT systems based on the quenching of the NIR fluorescence has been reported by Reuel *et al.*<sup>117</sup>. They fabricated a sensor array using recombinant lectins as glycan recognition sites tethered via histidine tags to Ni<sup>2+</sup> complexes that acted as fluorescent quenchers for semiconducting SWCNTs wrapped in a chitosan hydrogel (Figure 2). They used an automated printing method to develop the sensor chips. Thus, alternating layers of chitosan-wrapped SWCNTs and glutaraldehyde were printed and allowed to crosslink overnight. The crosslinked hydrogel acted as a polymer matrix and provided immobilized support to the embedded SWCNTs. This sensor allows measuring binding kinetics of model glycans in real time similarly to the surface plasmon resonance (SPR) technique. Its detection limit was found to be 2 µg of glycosylated protein or 100 ng of free glycan to 20 µg of lectin.

The formation of surfactant-polymer complexes that wrap the SWCNTs is another strategy employed for the development of pH optical nanosensors, which show promising applications for intracellular monitoring. This approach relies on combining CNTs previously suspended in cationic or neutral surfactants with a polymer that can be polymerized *in situ* to entrap the nanotube-surfactant micelles. The surfactant-polymer system provides an efficient and stable barrier between the SWCNTs and their local environment. Duque *et al.*<sup>113</sup> wrapped SWCNTs in sodium dodecylbenzene sulfonate (SDBS) and mixed them with biocompatible poly(vinyl pyrrolidone) (PVP). NIR fluorescence spectra of the composites demonstrated their linear response in the pH range of 1-6. Further, their effectiveness as sensors in the surface of live human embryonic kidney

cells was demonstrated, and a model was proposed that accounts for the photoluminescence stability of these systems based on the morphological changes of PVP at different pH values.

Other studies dealing with SWCNTs wrapped in fluorescent-polymer derivatives investigated the changes in the UV-Vis spectra of the fluorescent polymer after binding to the SWCNTs.<sup>118,120</sup> In this regard, Nakayama-Ratchford *et al.*<sup>118</sup> used non-covalently functionalized SWCNTs with fluorescein-PEG in aqueous solution. The hydrophobic aromatic moiety of fluorescein interacts with the CNT sidewalls via  $\pi$ - $\pi$  stacking, whilst the hydrophilic groups of PEG interact with water, resulting in highly stable complexes even after heating to 70 °C for 2 days. The polymer functionalization imparts solubility to the nanotubes in physiological buffers and simultaneously affords fluorescent labels. Plots of fluorescence vs. pH revealed a linear behaviour in the range of 5.7-8.5 pH, indicative of the suitability of these systems for detection, imaging and cell sorting in biological applications. Similar sensors for saccharide recognition were developed by Mu *et al.*<sup>120</sup> by wrapping SWCNTs in phenyl boronic acids (PBA) conjugated to a polyethylene glycol, eight-membered, branched polymer (PPEG8), which allows aqueous dispersion of the CNTs. Upon addition of a fluorophore, the complex became fluorescent in the UV-Vis region. Further addition of saccharide resulted in a decrease in the fluorescence intensity that was proportional to the amount of saccharide, leading to a LOD of  $1 \times 10^{-2}$  M. The synthesized PBA-PPEG8 polymers demonstrated strong saccharide binding selectivity. Thus, by conjugating different recognition groups to the amphiphilic polymers, sensors for specific saccharides could be developed.

Sensors based on conductive polymers like polyaniline (PANI)<sup>119</sup> and acid-functionalized MWCNTs have been recently synthesized by *in situ* polymerization using sulphonic acid as a dopant. A very uniform wrapping of PANI over the CNTs was attained, resulting in highly transparent and water soluble composites. Fluorescence measurements in

the UV-Vis region revealed their suitability for pH sensing in the range of 1-12. Moreover, the pH dependent change in the oxidation state of the PANI was easily reflected by the change in colour of the composite solution, which can be efficiently used for the development of colorimetric pH sensors.

Optical sensors based on CNTs covalently functionalized by polymers have also been fabricated. Ghini *et al.*<sup>122</sup> described the covalent anchoring of carboxylic-acid functionalized MWCNTs to fluorescein (Fluo)-PEG derivatives via *in situ* polymerization. This type of functionalization was found suitable for providing water solubility to the system while preserving the fluorescence properties of the dye. The use of polyether spacers between the dye and the nanotube surface was used to reduce fluorescence quenching effects.

Other sensors involve a polymer that acts as a matrix<sup>123,124</sup> or immobilization support.<sup>125,126</sup> In this regard, Barone *et al.*<sup>123</sup> developed a glucose-responsive hydrogel-based sensor, since they found that hydrogel swelling is a mechanism that can reversibly induce solvatochromic shifting in the SWCNT NIR emission. The CNTs were embedded in a PVA hydrogel via solution mixing followed by addition of different amounts of glutaraldehyde that acted as crosslinking agent in the presence of H<sub>2</sub>SO<sub>4</sub> as catalyst. As the cross-linking density and hydration state of the hydrogel increased, the Raman G-band shifted to higher wavenumber, indicating deformation of the nanotube lattice, while the SWCNT fluorescence decreased in energy. The data were well-described by a model that accounts for changes in dielectric screening of the 1D exciton as the osmotic pressure induces conformational distortions in PVA by rotating more polar groups to the nanotube surface. Cross-linking with apo-glucose oxidase made the hydrogel glucose responsive, showing a fast and reversible response to the repeated cycling of 1 x 10<sup>-2</sup> M glucose. As a proof of concept, these sensors were implanted into a mouse tissue, demonstrating an excellent signal-to-noise ratio of 8.6. Similarly, Ahn *et al.*<sup>124</sup> prepared a sensor for protein

detection based on SWCNTs embedded within a chitosan matrix bearing an NR,NR-bis(carboxymethyl)-L-lysine (NTA) chelator (Figure 3). With this scaffold, Ni<sup>2+</sup> can bind and tether a hexahistidine tagged (His-tag) protein, which is directly reflected in a decrease in the SWNT NIR fluorescence intensity. This modulation results from changes in the intermolecular distance between the SWCNT and the Ni<sup>2+</sup> ion, which acts as a proximity quencher of the fluorescence. This sensor shows a detection limit of  $1 \times 10^{-11}$ M, and can also analyze protein-protein interactions.

Aqueous polymeric gels are typically used in optical measurements to provide an inert immobilizing environment. This approach was used by Cognet *et al.*<sup>125</sup> who developed a biosensor using sodium dodecylbenzenesulfonate (SDBS)-wrapped SWCNTs embedded in agarose gel. These composites exhibited reversible stepwise quenching of the SWCNT NIR fluorescence after exposure to acid, base, or diazonium reactants, providing highly efficient sensing of local chemical and physical perturbations. Therefore, they are useful for detecting local pH gradients in restricted environments, such as microfluidic channels or organelles inside biological cells. Analogously, Chen *et al.*<sup>126</sup> prepared an assay for protein detection based on SWCNTs functionalized with PEGylated phospholipids (DSPE-3PEO). A carboxylated PEG was grafted onto a gold-coated surface for protein immobilization. Proteins such as anti-mouse immunoglobulin G (anti-HSA IgG) were immobilized on the assay surface and detected either by surface-enhanced Raman scattering (SERS) using the G-mode intensity or by conventional fluorescence. The detection limit using SERS was about 1 fM, a three order of magnitude improvement compared to fluorescence-based detection.

### 3.1.2 Electrochemical sensors

The unique chemical and physical properties of CNTs have paved the way to new and improved sensing devices, in general, and electrochemical sensors, in

particular.<sup>19,20,21,22</sup> CNTs have huge surface area, mechanical strength, high electrical conductivity and efficient electrocatalytic behaviour.

Polymer/CNT composites based electrochemical transducers offer substantial improvements in the performance of amperometric methods. Selection of the working electrode material is an important step in the development of electrochemical sensors. There are several strategies for the modification of electrodes directed to improving the sensitivity and selectivity of electrochemical sensors. The presence of polymers and CNTs allows different architectures on the electrode surface, which enable a greater active surface, improved immobilization of the targets and a more efficient electron transfer. In this section, we will show different strategies to combine polymers with CNTs in order to create electrochemical sensors with enhanced performance. The most representative examples reported to date on this topic are listed in Table 2.

CNTs have been dispersed directly in several polymers such as Nafion<sup>127</sup>, polystyrene (PS)<sup>128</sup> or chitosan (CS),<sup>129,130,131,132,133</sup> via sonication to obtain a stable suspension by means of a wrapping process, or these polymers have been embedded in the network structure formed by CNTs or covalently grafted to the CNT surface. Nafion has been extensively applied as an electrode modifier due to its excellent antifouling capacity and powerful adsorption ability. In a recent work, Nigović *et al.*<sup>127</sup> have identified two drugs, morphine and ondansetron, which coexist in biological fluids in patients receiving chemotherapy. The electrochemical behaviour of ondansetron was studied at the glassy carbon electrode (GCE) modified with the MWCNT-Nafion polymer composite (MWCNT-Nafion/GCE). The oxidation peak potential was shifted from 1.32 V to 1.18 V compared to the bare electrode indicating excellent electrocatalytic activity of the immobilized film toward the drug molecule. The modified electrode exhibited noticeably enhanced voltammetric response due to the synergistic effect of nanomaterial

and polymer on the electron transfer rate. Also, the MWCNT-Nafion/GCE showed a high selectivity in the voltammetric performance of ondansetron and co-administrated drug morphine with potential difference of 430 mV. In this example the polymer was used not only as a binder to form a stable and uniform film with well dispersed CNTs at the electrode surface but also exploiting its adsorption capability. Nafion has also been used in the immobilization of the enzyme horseradish peroxidase (HRP) facilitating the manufacture of an electrochemical biosensor of H<sub>2</sub>O<sub>2</sub> with Au electrode modified with a suspension of PS and MWCNTs.<sup>128</sup> PS improved the enzyme stability and electrode selectivity, enabling an excellent electrocatalytic activity to the reduction of H<sub>2</sub>O<sub>2</sub>, with a linear response in the range of  $5.0 \times 10^{-7}$  -  $8.2 \times 10^{-4}$  M and a LOD of  $1.6 \times 10^{-7}$  M.

Chitosan (CS) is one of the most utilized biopolymers to disperse nanocarbon materials. It is a natural cationic polysaccharide that displays a number of properties including biocompatibility, hydrophilicity, non-toxicity, good mechanical stability, cost-effectiveness, and availability of reactive functional groups for chemical modifications. In this context, much research has been focused on the preparation of CNT-CS composites as platforms to develop sensors for pharmaceutical, environmental and biotechnical applications.<sup>129,130,131,132,133</sup> Babaei *et al.*<sup>129</sup> modified a GCE with a MWCNT-CS composite for the sensitive voltammetric detection of morphine (MO) and dopamine (DA) in human blood serum or urine. CS improved the electrode stability due to its antifouling property, high mechanical strength and water stability as well as the electron transfer, enabling the simultaneous qualitative and quantitative determination of DA and MO at physiologically relevant conditions. A very similar approach was reported by Wu *et al.*, who prepared a MWCNT-CS modified GCE to easily and rapidly detect Sudan I in hot chili powder samples.<sup>130</sup> Sudan I is a synthetic azo-colorant widely used in waxes and textile colorants, shoe polishes and food additives that is a potential carcinogen and

mutagen in humans. The biopolymer enhanced the adsorption of the analyte and the sensitivity of the electrode, leading to a LOD in the order of  $1.0 \times 10^{-8}$  M.

The use of ionic liquids (IL) in electrochemistry to prepare modified electrodes has widely increased because of their high chemical and thermal stability, low toxicity, high ionic conductivity, wide electrochemical potential window and the enhanced sensitivity response.<sup>134,135</sup> Over the last years, the preparation of modified electrodes with room-temperature ionic liquids and composites has attracted considerable attention in order to combine their unique advantages to develop electrochemical devices. For example, Kianipour and Asghari<sup>131</sup> modified a glassy carbon electrode in presence of CS, MWCNTs and 1-ethyl-3-methyl-imidazoliumtetra-fluoroborat (EMIM-BF<sub>4</sub>) as ionic liquid, for the simultaneous determination of ascorbic acid (AAC), uric acid (UA), acetaminophen (AP), and mefenamicacid (MEF), in human serum and urine samples, by differential pulse voltammetry (DPV). The presence of CS in the modified electrode improved the sensor repeatability due to its antifouling effect and led to more current peak separation between the analytes, enhancing the sensor selectivity.

A more complex sensor based on CS, MWCNTs and an ionic liquid has been developed by Shahdost-fard *et al.*<sup>132</sup> They prepared a highly sensitive adenosine aptasensor based on the covalent attachment of an aptamer onto MWCNT-IL-CS composite. CS improved the dispersion ability of the IL, leading to a uniform CNT distribution within the composite. The developed sensor showed lower cost, improved sensitivity, linear range and stability compared with other aptamer-based sensors that require a specific label. The obtained LOD was very low, about  $1.5 \times 10^{-10}$  M.

The introduction in the architecture of the electrode of metal nanoparticles that interact with the polymer-CNT mixture provides new environment detection. In this regard, Li *et al.*<sup>133</sup> prepared a H<sub>2</sub>O<sub>2</sub> biosensor based on a glassy carbon electrode modified

with a composite composed of CS-MWNTs, hemoglobin (Hb) and silver nanoparticles (AgNPs). The authors reported that the presence of AgPNs and MWCNTs increased the electron transfer between Hb and the electrode surface. Chitosan was not only used as a solubilizing agent for the MWCNTs but also provided a favorable microenvironment for hemoglobin in the composite acting as an immobilization matrix. The Hb in the composite exhibited excellent electrocatalytic activity to the reduction of H<sub>2</sub>O<sub>2</sub>, leading to a selective sensor with a LOD of  $3.5 \times 10^{-7}$  M.

Conducting polymers (CP) are of great interest for sensor applications as they can be interfaced with some molecules for an effective signal transduction. CP provide an excellent platform upon which to build biorecognition and/or signal transduction for the target analyte.<sup>136,137</sup> Different strategies have been developed for the formation of composite electrodes with these CP like the oxidative polymerization in a CNT-monomer mixture and the electropolymerization onto the surface of the electrode or electrode/CNT.

A sensitive amperometric sensor for the detection of hydroquinone (HQ) in cosmetics<sup>138</sup> was developed based on the excellent electrocatalytic property of MWCNT and poly(3,4-ethylenedioxythiophene), PEDOT. Acid-treated MWCNTs were dispersed in deionized water, and the monomer and subsequently FeCl<sub>3</sub>.6H<sub>2</sub>O were added to the above suspension, which was drop-casted on the carbon paste electrode (CPE). The authors concluded that the polymer/MWCNT composite considerably decreased the oxidation potential of hydroquinone and increased the charge transfer rate constant compared to the bare electrode, enabling a very sensitive detection of HQ, with a LOD of  $3.0 \times 10^{-7}$  M, significantly lower than some related reports. The same authors used the PEDOT-MWCNT/CPE in the manufacture of a sensor for determining nitrobenzene in real wastewater samples, where the role of the polymer was also to enhance the electrocatalytic activity.<sup>139</sup>

Among the conducting polymers commonly used, polyaniline (PANI) and polypyrrole (PPy) have been the most widely investigated. For example, a biosensor based on the inhibition of enzymes has been used for the amperometric detection of organophosphorous compounds, paraoxon, in presence of MWCNTs coated with PPy.<sup>140</sup> The PPy-MWCNT composite improved the enzyme adsorption and allowed very low amperometric detection without the use of a mediating redox potential, enhancing the sensor stability and reproducibility. Due to high porosity of the polymer and the high electrical conductivity of CNTs, a detection level of  $3.0 \times 10^{-9}$  M could be achieved. Another amperometric biosensor based on PPy-MWCNT composites covered by Prussian blue (PB) has been developed by Jin *et al.*<sup>141</sup> for enzymeless  $\text{H}_2\text{O}_2$  detection. PB has been extensively studied for its attractive electrochemical properties and applications in the field of biosensors since exhibits good performance for  $\text{H}_2\text{O}_2$  electroreduction. PPy-MWCNT nanofibers were prepared by an *in situ* chemical oxidative polymerization process<sup>142</sup>. TEM images of MWCNT-PPy composites reveal that PB nanoparticles (about 12–24 nm size) were randomly and homogeneously deposited on the surface of MWCNT/PPy nanofibers. Thus, the PPy enabled to control the size and morphology of the PB nanoparticles deposited onto the electrode. The synergistic effect among MWCNTs, PPy and PB improved the performance of the modified electrode for the  $\text{H}_2\text{O}_2$  detection, showing good sensitivity, wide linear range ( $4.0 \times 10^{-6}$ – $5.2 \times 10^{-4}$  M) and low LOD ( $8.0 \times 10^{-8}$  M).

Min and Yoo<sup>143</sup> have developed a composite, SWCNT-PPy, which acts as the electrode itself without support of an additional electrode like Pt or GCE. The composite electrode was prepared by chemical polymerization of the monomer onto carboxylic-acid functionalized-SWCNTs using  $\text{LiClO}_4$  as oxidant. For biosensor applications, tyrosinase (Ty) was covalently attached to the functionalized SWCNTs, and the Ty-SWNT -PPy

electrode was prepared in a similar way. The SWCNTs were thickly coated by the polymer and the SWNT-PPy composite exhibited many surface pores that could improve mass transfer. This electrode showed a large specific surface area and a highly reproducible current response, about 100 times larger than that of the GCE. The composite increased the amount of enzyme loading and the frequency of contacts between the electrode surface and electrons, thereby enhancing the electron transfer rate. The Ty-SWCNT-PPy composite electrode was used for amperometric detection of dopamine in the presence of ascorbic acid and showed high sensitivity and a low detection limit,  $5.0 \times 10^{-6} \text{M}$ .

PANI is, perhaps, the preferred polymer for electrochemical sensor applications due to its electrical conductivity, stability, facile synthesis and significant redox behaviour. Several studies have shown improvements in the performance of enzymatic sensors by depositing PANI/CNT composites onto electrodes. For example, Lee *et al.*<sup>144</sup> prepared a new nanomaterial, by grafting a layer of sulfonated polyaniline network (SPANI-NW) onto the surface of amine functionalized MWCNT, and effectively utilized for immobilization of an enzyme, glucose oxidase (GOD), and for the fabrication of a glucose biosensor. There are few limitations on the use of PANI, as the loss of electroactivity at pHs greater than 4.0. Moreover, SPANI is electroactive even at physiological pH and, in this case, the interconnected polymer network morphology would provide adequate microenvironment for the immobilization of an enzyme. In situ polymerization of a mixture of diphenyl amine 4-sulfonic acid (DPASA), 4-vinyl aniline (VA) and 2-acrylamido-2-methyl-1-propane sulfonic acid (APASA) was performed in the presence of MWNT-NH<sub>2</sub>. GOD was immobilized onto MWNT-SPANI-NW to fabricate the biosensor, with good performances for the electrochemical determination of glucose.

Hua *et al.*<sup>145</sup> have developed a PANI-MWCNT composite by blending the emeraldine base form of polyaniline and carboxy-functionalized MWCNTs in dried dimethyl sulfoxide. The FT-IR spectra, SEM images and conductivity values confirmed the deposition of PANI on the MWCNT surface and the doping of the PANI by the weak protonic acid of the carboxylic groups and the radical cations of MWCNT fragments. Horseradish peroxidase (HRP) was immobilized within the composite modified Au electrode to form HRP/PANI-MWCNT/Au for use as a H<sub>2</sub>O<sub>2</sub> sensor. The synergistic effect between protonated PANI and functionalized MWCNT causes that only a minimum amount of enzyme, 6.6 µg mL<sup>-1</sup>, is required for detection, the lowest reported to date for this type of sensors. The HRP/PANI-MWCNT/Au for H<sub>2</sub>O<sub>2</sub> detection exhibits a broad linear detection range with a detection limit of 8.6 x 10<sup>-6</sup> M.

Cross-linking and conjugation of biomolecules to different kinds of substrates is extensively used in biosensors. A conventional method for immobilization of NH<sub>2</sub>-containing biomolecules onto carboxyl-containing substrates via covalent amide bonds consists in the use of N-ethyl-N'-(3-dimethylaminopropyl) carbodiimide (EDC) and N-hydroxysuccinimide (NHS) catalytic system.<sup>146</sup> The EDC/NHS activation strategy has many merits: high conversion efficiency, mild reaction conditions, excellent biocompatibility with small effect on the bioactivity of target molecules, and much cleaner products than other crosslinking reagents such as glutaraldehyde and formaldehyde. Owing to these advantages, EDC/NHS activation of carboxylic acids and the following amidation reaction have been commonly applied in biomolecular conjugation and immobilization of proteins, DNAs, and so forth to many kinds of substrates like polymers<sup>147,148,149</sup> or carbon nanotubes.<sup>150,151</sup> Using EDC/NHS chemistry, Dhand *et al.*<sup>152</sup> have electrophoretically deposited onto an indium tin oxide (ITO)-coated glass plate a composite of PANI and MWCNTs for covalent immobilization of

cholesterol oxidase, CHOX. Results from linear sweep voltammetry (LSV) revealed that the anodic peak around 0.28 V, which corresponds to the oxidation of PANI, increases with the cholesterol concentration. This behaviour suggests that CHOX gets electrically contacted by the PANI-MWCNT modified electrode. The direct acceptance of electrons by the composite is attributed to enhanced charge transport due to electron hopping through the conductive MWCNTs that mediate electron transfer via the redox polymer. The CHOX/PANI-MWCNT/ITO bioelectrode can detect cholesterol in the range of  $1.29 \times 10^{-3}$ - $1.29 \times 10^{-2}$  M with high sensitivity and a fast response time.

A simple and versatile method to assemble dispersed CNTs into thin-films is the layer-by-layer (LBL) technique, which consists in the repeated, sequential immersion of a substrate into solutions of oppositely charged polyelectrolytes. This approach can result in composites with high nanofiller weight fraction and controlled internal structure, having the potential to reach the desired properties through tailored design. Thus, it is possible to obtain a homogeneous, porous, and three-dimensional CNT multilayer film with a large surface area provided by the assembly procedure that is repeated many times.<sup>153,154,155</sup> Using this approach, Gao *et al.*<sup>156</sup> developed a glucose biosensor based on a composite made by LBL electrodeposition of a redox polymer, cross-linked  $[\text{Os}(\text{bpy})_2\text{Cl}]^{+/2+}$  complexed poly(1-vinylimidazole) (PVI-Os), into a multilayer containing glucose oxidase (GOD) and SWCNTs on the surface of a screen-printed carbon electrode (SPCE). To facilitate the adsorption of the negatively charged GOD and SWCNTs, the SPCE was functionalized with cationic PVI-Os by electrodeposition. The aim of the electrodeposition of the redox polymer was to stabilize the multilayer and to wire the GOD. Figure 4 shows the effect of the number of layers upon the current signal by cyclic voltammetry (CV). As can be seen, the optimal number of layers is five, since after the sixth layer the signal decreases. Therefore, modified SPCEs with five layers of

GOD/SWCNT/PVI-Os were used as biosensors for glucose determination. The developed biosensor showed a linear range from 0.5 to 6.0 x 10<sup>-3</sup> M and a detection limit of 1.0 x 10<sup>-4</sup> M. To evaluate the electrode selectivity, the amperometric current responses to uric acid 0.32 mM, ascorbic acid 0.05 mM, and acetaminophen 0.20 mM, were examined together with glucose. AP exhibited no response. In contrast, large current responses were observed for AAC and UA. To solve the problem, Nafion was added on the surface of the composite-modified electrode, eliminating interferences due to AAC and UA.

The LBL approach has also been employed to develop a composite film incorporating SWCNTs, PPy and gold nanoparticles (AuNPs) that modified an Au electrode as a voltammetric sensor to sensitively detect epinephrine (EP) in the presence of AAC and UA.<sup>157</sup> The catalytic peak currents obtained from differential pulse voltammetry increased linearly with increasing EP concentration in the range of 4.0 x 10<sup>-9</sup> - 1.0 x 10<sup>-7</sup> M with a LOD of 2.0 x 10<sup>-9</sup> M. The hybrid composite displayed a synergistic effect that strongly catalyzed the electrooxidation reactions of EP and UA, enhancing their electrochemical reversibility and oxidation peak separation. Therefore, the PPy-AuNPs-SWCNT-modified Au electrode can selectively determine EP in the coexistence of a large amount of UA and AAC.

Electropolymerization offers several advantages compared to other methods, in particular the absence of catalyst other than the electrode, direct grafting of the doped film onto the electrode surface, in situ characterization by different techniques and easy control of the deposit properties. Polymers can be electrogenerated at CNT electrodes or CNTs can be attached to the electrode during electropolymerization. Many examples demonstrate the use of this approach in the specific electrochemical detection of relevant molecules.<sup>158,159,160,161,162,163,164,165,166,167,168,169</sup> For example, an electrode composed of

MWCNTs and poly-(3-methylthiophene), P3MT was developed by Agüi *et al.*<sup>158</sup> using this approach. MWCNTs were dispersed in Nafion and dropped on a GCE. Then, the modified electrode was immersed into 3-methylthiophene monomer solution and the electropolymerization was performed by CV. Thus the modified electrode improves the amperometric NADH detection due to a synergic effect of the electrocatalytic properties and the high active surface area of both the conducting polymer and the MWCNTs. This P3MT-MWCNT-(Nafion)/GCE electrode provides fast responses, a linear range between  $5.0 \times 10^{-7}$  and  $2.0 \times 10^{-5}$ M and a detection limit of  $1.7 \times 10^{-7}$ M. The same authors developed a lactate biosensor using a similar method.<sup>159</sup> Both designed biosensors<sup>158,159</sup> showed good repeatability of the measurements, good reproducibility in the inter-biosensor assays and a good selectivity, especially when they were coated with a Nafion film. The synergistic effect of the composite constituents towards the electrocatalytic oxidation of NADH allowed the bioelectrodes to operate at low potential values without the need for redox mediators, improving the analytical performance in comparison to similar biosensors incorporating only CNTs or conducting polymers.

The electropolymerization of PANI on CNTs can also develop electrochemical sensors with superior performance. For instance, Yadav *et al.*<sup>160</sup> developed a creatinine biosensor based on a mixture of creatinineamidohydrolase (CA), creatineamidinohydrolase (CI), and sarcosineoxidase (SO) coimmobilized covalently by EDC/NHS chemistry onto an electrodeposited carboxylated MWCNT-PANI composite film. A schematic representation of chemical reaction of the modified electrode is shown in Figure 5. The comparison of the cyclic voltammograms of electrodeposition of pure PANI and MWCNT/PANI composite revealed that the composite led to higher currents than the polymer counterpart, ascribed to its larger effective surface area, hence more conductive pathways that allow for faster kinetics. Therefore, the MWCNTs, acting as

electron transfer mediators, help to enhance the enzyme sensor response and to increase the sensitivity of the biosensor. The use of MWCNT-PANI composite provides a large surface area for the immobilization of CA, CI and SO, leading to a creatinine biosensor with good analytical performance in terms of low working potential, short response time, sensitivity, and high storage stability. Using the same approach, these authors developed a highly sensitive and rapid oxalate biosensor by covalently immobilizing oxalate oxidase enzyme onto a electrodeposited MWCNT-PANI composite via EDC/NHS chemistry.<sup>161</sup>

Electropolymerization has also been employed by Tiwari *et al.*<sup>162</sup> for the preparation of a composite electrode incorporating PANI and polyacrylic acid (PAA) deposited on a Nafion-MWCNT membrane supported over a Pt electrode. Nafion has hydrophobic and hydrophilic regions and can wrap around the hydrophobic nanotube surface, hence is found to be an ideal medium for MWCNT dispersion, enabling the formation of a homogeneous composite. Further, the Nafion-MWCNT membrane forced self-organization of PANI/PAA during electropolymerization with the MWCNTs acting as nucleating agents, increasing the crystallinity of the system. The sensor was applied to determination of ascorbic acid with a LOD of  $2.5 \times 10^{-7}$  M. The same analyte, AAC, has been determined with a sensor based on PANI doped with silicotungstic acid ( $\text{SiW}_{12}$ ) and SWCNTs.<sup>163</sup> This modified electrode was prepared through one-step electropolymerization of the suspension of  $\text{SiW}_{12}$  and SWCNTs dispersed in aniline on the electrode surface. The electrochemical polymerization process of PANI, SWCNT-PANI,  $\text{SiW}_{12}$ -PANI and  $\text{SiW}_{12}$ -SWCNT-PANI was studied. When SWCNTs were simultaneously deposited in the  $\text{SiW}_{12}$ -PANI film via electropolymerization, only two couples of redox peaks with increased peak currents appeared (Figure 6), which is very useful for its electrocatalytic application. The authors proposed that SWCNTs, with exceptional electric conductivity and large  $\pi$ -bonded surface, not only enhanced the

electron transfer of the electrode interface but also exhibited strong interaction with the conjugated structure of PANI via  $\pi$ - $\pi$  stacking, which improved the SiW<sub>12</sub> distribution and increased the electron delocalization in the PANI composite. Using the method of the calibration curve, two linear ranges were found with a LOD of  $5.1 \times 10^{-7}$  M. Compared with other studies on the electrochemical determination of AAC with PANI-based electrodes, the SiW<sub>12</sub>-SWCNT-PANI showed better analytical performance in terms of stability, repeatability, wider linear range and lower detection limit.

CuNPs have been added to MWCNT-PANI modified electrodes to develop sensors for the determination of ascorbic acid<sup>164</sup> and polyphenols.<sup>165</sup> For the preparation of the non-enzymatic AAC sensor<sup>164</sup>, aniline was electropolymerized onto an Au electrode through CV, and then the PANI-coated electrode was dipped into a suspension of carboxylated-MWCNTs. The functionalized MWCNTs were covalently attached to the PANI layer by forming amide bonds between their -COOH groups and the free terminal -NH<sub>2</sub> groups of PANI. The polymer enhanced the absorption of the nanoparticles onto the carboxylated-MWCNTs, thereby improving the electrocatalytic activity to AAC oxidation. The LSV response of the modified electrode to AAC showed linear dependence in the concentration range of  $5.0 \times 10^{-6}$ - $6.0 \times 10^{-4}$  M with a LOD of  $1.0 \times 10^{-6}$  M. This superior performance, combined with the ease of fabrication, good reproducibility, stability, rapid response and selectivity to ascorbic acid in the presence of common interfering, make this electrode ideal for routine AAC detection.

For the determination of polyphenols via an enzymatic method,<sup>165</sup> the preparation procedure of the carboxylated-MWCNT-PANI/Au was identical to that described above. In this case, CuNPs were electrochemically deposited on the electrode in a 0.1% of chitosan solution by cyclic voltammetry. Then purified laccase enzyme was immobilized onto the CuNPs-CS-MWCNT-PANI modified gold electrode surface by glutaraldehyde

coupling. The fabrication scheme of this biosensor is shown in Figure 7. When the modified CuNPs-CS-MWCNT-PANI/Au electrode was treated with glutaraldehyde, its -CHO group at one end get attached to the -NH<sub>2</sub> groups of CS, while the other -CHO group get linked to free -NH<sub>2</sub> groups of enzyme through C=N bonds, and consequently the enzyme is covalently anchored, Figure 7. Both polymers played an important role in the biosensor: PANI enhanced the adsorption of the CuNPs, increasing the electroactive area, and CS promoted the attachment of the enzyme. A linear relationship between the current and the tested polyphenol, guaiacol, was found in the concentration range from  $1.0 \times 10^{-6}$  to  $5.0 \times 10^{-4}$  M, with a LOD of  $1.56 \times 10^{-7}$  M.

A stable and sensitive electrochemical sensor for the detection of dopamine, based on the electrodeposited conducting polymer, PEDOT, doped with MWCNTs, was reported by Xu *et al.*<sup>166</sup>. The PEDOT-CNT/CPE exhibited good catalytic properties toward the electrochemical reaction of DA, and high selectivity, since it was not affected by the presence of ascorbic acid.

Raicopol *et al.*<sup>167</sup> prepared, in a one-step electropolymerization process, an amperometric glucose biosensor based on a composite of PPy with p-phenyl sulfonate-functionalized SWCNTs in presence of GOD. The polymer facilitated the enzyme immobilization by entrapment within the electropolymerized film. Upon introduction of a thin film of PB at the substrate electrode surface, the hybrid system showed synergy between the PB and the functionalized SWCNTs, which remarkably amplifies the electrode sensitivity when operated at low potentials. The biosensor displayed good analytical performance in terms of low detection ( $1.0 \times 10^{-5}$  M) and wide linear range ( $2.0 \times 10^{-5}$  -  $6.0 \times 10^{-3}$ ). Another amperometric glucose biosensor on LBL assembled SWCNTs and electropolymerized PPy layers has been reported by Shirsat *et al.*<sup>168</sup>. Homogeneous SWCNTs and PPy multilayer films were alternately assembled on platinum coated

polyvinylidene fluoride (PVDF) membrane. The GOD was immobilized on the LBL assembled film via physical adsorption by cross linking through glutaraldehyde. This glucose biosensor exhibited a linear response range from  $1.0 \times 10^{-3}$  -  $5.0 \times 10^{-2}$  M with high sensitivity. Since conducting PPy favors the increase of the amount of SWCNTs on platinum coated PVDF membrane and imparts superior transducing ability, the LBL approach of PPy and SWCNT provides excellent matrix for the immobilization of GOD enzyme.

An electrochemical sensor based on AuNPs-MWCNT-poly (1,5-naphthalenediamine) films modified GCE for the detection of cellobiose dehydrogenase gene was reported by Zeng *et al.*<sup>169</sup> The polymer was electropolymerized onto the GCE surface with a large number of amino groups, which enhanced the stability of the modified electrode. The resulting sensor also displayed high sensitivity, selectivity and reproducibility, with a detection limit of  $1.2 \times 10^{-16}$  M.

On the other hand, molecular imprinting is a very useful technique to incorporate specific substrate recognition sites into polymers. Molecularly imprinted polymers (MIPs) are prepared by creating a three-dimensional polymeric matrix around a template molecule. After the removal of the template, the resulting imprinted cavities with complementary shape and functional groups remain.<sup>170</sup> The analytical applications of MIPs include different techniques such as chromatography, capillary electrochromatography, extraction and sensors.<sup>171</sup> Nevertheless, imprinted materials prepared by conventional methods suffer from some drawbacks since their performances are often limited by slow mass transfer, irregular material shape, thick polymer matrices, and relatively low recognition sites per unit volume of the polymers. To overcome these problems, many approaches have been established to develop surface molecularly imprinting techniques, particularly for systems incorporating CNTs because of their

unique properties, including their remarkable electrical, chemical, mechanical, and structural properties. MIP-CNT composites have been used in several fields such as clinic assays,<sup>172,173,174,175,176</sup> pharmaceutical<sup>177,178,179,180,181</sup> or environmental analysis.<sup>182</sup>

A surface imprinting biosensor for bovine serum albumin (BSA) detection has been prepared using chitosan-coated magnetic nanoparticles modified multi-walled carbon nanotubes (MIPs-CS-MWCNTs) as a signal amplifier.<sup>172</sup> The MIPs were dispersed in CS solution and mixed with acyl-chloride-functionalized MWCNTs, and subsequently the MIP-CS-MWCNT suspension was cast onto the electrode surface. The presence of CS promoted the connection between the MIPs and MWCNTs. Then, a PPy film with the template protein was electrodeposited onto the modified electrode using cyclic voltammetry, and the BSA molecules were trapped within the polymer matrix as a result of their ability to interact with the pyrrole units. When the protein molecules were eluted, a microenvironment for recognition of BSA based on shape selection and positioning of the functional groups was created in the imprinting film. This sensor exhibited a good analytical performance with a wide detection linear range ( $1.0 \times 10^{-10}$ - $1.0 \times 10^{-4}$  g mL<sup>-1</sup>) and a LOD of  $2.8 \times 10^{-11}$  g mL<sup>-1</sup>.

Prasad *et al.*<sup>173</sup> have fabricated an electrochemical sensor based on a MIP for the detection of  $\gamma$ -amino butyric acid (GABA), an important inhibitory amino acid common in the human central nervous system, at ultra-trace level by differential pulse anodic stripping voltammetry (DPASV). Since the  $\gamma$ -aminobutyric acid is a non-electroactive compound, its *o*-phthalaldehyde/sulphite derivative was used as a template for the imprinting polymer, which was made from 5-fluorouracil-N-acetylacrylamide, FUA monomer and ethylene glycol dimethacrylate, EGDMA, as cross-linking agent. A very thin MIP film was grown on the surface of MWCNT-COOH-modified pyrolytic graphite electrode (PGE). Further, the functionalized MWCNTs were abrasively attached to the tip

of PGE, and remained as a stable layer between the electrode surface and the MIP film, providing a channelized electron transport that enhanced the binding signal. The resulting sensor showed a linear response in the concentration range of 0.75-205.19 ng mL<sup>-1</sup> and the lowest LOD (0.28 x 10<sup>-9</sup> g mL<sup>-1</sup>) compared to other reported methods.

A monolithic molecular imprinting sensor based on a ceramic carbon electrode (CCE), was prepared by Tong *et al.*<sup>174</sup> as a recognition element for cholesterol, one of the most frequently determined species in clinical diagnosis. The sensor was prepared by mixing the MWCNT-MIP composite, graphite powder and silicon alkoxide oxide and subsequently packing the resulting mixture into the electrode cavity of a Teflon sleeve. Since the MIP was homogeneously doped inside the CCE by simply mixing, this sensor could be easily reused by a smoothing treatment in case that the surface of the sensor is fouled. The raise in the MWCNT-MIP content led to an increase in the response current owed to a larger number of recognition sites on the electrode surface. The sensor exhibited excellent sensitivity with a linear range of 1.0 x10<sup>-8</sup>- 3.0 x 10<sup>-7</sup> M and a LOD of 1.0 x 10<sup>-9</sup> M.

The discrimination of enantiomers is a complex problem. In this regard, Prasad *et al.*<sup>175</sup> developed a MIP-MWCNT-modified PGE for electrochemical sensing of methionine enantiomers. L-methionine is one of the sulphur-containing amino acids that rules the main supply of sulphur in the diet, and also prevents disorders in hair and skin. Further, it helps to reduce the cholesterol level by increasing lecithin production in liver and maintaining normal growth of cells. For this purpose, benzidine and (D- or L-) methionine were initially attached to the surface of MWCNT/PGE via formation of amide bonds and subsequent electropolymerization. During this process, methionine molecules were instantly oxidized to methionine sulfone as print molecules involving electrostatically driven hydrogen-bond linkages in the polymer-template adduct. After

methionine sulfone extraction, a molecularly imprinted polymer film was coated over the electrode surface, which had several molecular cavities that selectively encapsulated D- or L-methionine in its oxidized form. The polymer increased the electrode surface area, thereby improving the electron transfer. Further, the combination of MWCNTs and the MIP film imparted high mechanical strength and excellent conductivity. The non-covalent interactions (electrostatic and H-bonding) between the analyte and MIP favoured enantio-selective discrimination between enantiomers, and it was possible to determine L-methionine in the linear range of  $11.7 - 206.3 \times 10^{-9} \text{ g mL}^{-1}$  with a LOD of  $2.9 \times 10^{-9} \text{ g mL}^{-1}$ . Using a similar approach, the same authors prepared a MIP composite incorporating titanium dioxide nanoparticles (TiNPs) and MWCNTs for the modification of a pyrolytic graphite electrode (PGE) as an enantioselective-sensing probe for aspartic acid isomers<sup>176</sup>. In this case, the polymer initiator chemically adsorbed to TiNPs was covalently attached with the MWCNT-modified PGE. Analogously, Kan *et al.*<sup>177</sup> prepared a biosensor for dopamine recognition by covalently grafting vinyl functionalized MWCNTs to a MIP matrix (a copolymer of methacrylic acid and trimethylolpropanetriacrylate (copoly (MAA-co -TRIM))). The presence of MIP enhanced the adsorption dynamics and selectivity for DA. Other MIP-based sensors for the determination of allopurinol (4-hydroxypyrazolo[3,4-d] pyrimidine)<sup>178</sup>, brucine (an anti-inflammatory and analgesic drug)<sup>179</sup>, lorazepam (a benzodiazepine that produces central depression of the central nervous system)<sup>180</sup>, tramadol (a synthetic monoamine uptake inhibitor and analgesic)<sup>181</sup> and parathion-methyl (an organophosphate pesticide)<sup>182</sup> have been recently developed (see Table 2), and the main role of the polymer was also to improve the adsorption kinetics and the selectivity for the analyte.

Sol-gel imprinting process is a promising way to enhance the performance of MIP films by forming a sol-gel inorganic framework around a template molecule, which leads

to a uniformly porous structure. Moreover, the larger number of active sites on the imprinted sol-gel film, increase the electrochemical signal compared to a mono-layer modified electrode. In this regard, a rapid, sensitive and selective molecularly imprinted electrochemical sensor for quinoxaline-2-carboxylic acid (QCA) determination was successfully constructed, by Yang *et al.*<sup>183</sup>, via stepwise modification of MWNTs-CS functional composite and a sol-gel MIP film on the surface of a GCE. MWNTs-CS composite was used to enhance the electron transfer rate and expand electrode surface area, and consequently amplify QCA reduction electrochemical response. To prepare the QCA-imprinted sol, QCA as template and 3-aminopropyl triethoxysilane (APTES) as functional monomer were mixed, following the addition of tetraethoxysilane (TEOS) as crosslinker. Finally, the MIP modified MWNTs-CS/GCE was fabricated by electrodeposition using cyclic voltammetry. The fabricated electrochemical QCA-imprinted sensor using MIP/sol-gel/MWNTs-CS/GCE as working electrode showed good performance with a low detection limit,  $4.44 \times 10^{-7}$  M, good reproducibility and reliability.

Zhang *et al.*<sup>184</sup> proposed a molecularly imprinted electrochemical sensor based on electrodepositing MIP sol-gel onto a MWCNT-Nafion modified GCE for the determination of 2-nonylphenol, a toxic xenobiotic compound classified as an environmental endocrine disrupter. In the sol-gel imprinting process, the amino groups of the functional monomer 3-aminopropyl triethoxysilane (APTES) and the benzene rings of the functional co-monomer (phenyltrimetroxysilane, PTMS) provide recognition sites through hydrogen bonds and  $\pi$ - $\pi$  stacking interactions with 2-nonylphenol. The presence of Nafion was found to be essential for improving MWCNT dispersability and preparing a homogeneous and well distributed MIP sol-gel film. Under optimal conditions, the

sensor showed a linear response from  $2.0 \times 10^{-7}$  M to  $3.6 \times 10^{-4}$  M, with a LOD of  $6.0 \times 10^{-8}$  M.

### *3.2 Chemical sensors based on polymer/graphene*

#### *3.2.1 Optical sensors*

Due to its extraordinary electrical, chemical, optical and electrochemical properties, graphene is an ideal candidate to be used as transducer in optical sensors and biosensors based on fluorescence, chemiluminescence and colorimetric detection systems.<sup>24,25,26,27</sup> Among the different graphene forms, graphene oxide (GO) and reduced graphene oxide (RGO) have advantageous characteristics to be used in these optical sensing platforms. Although GO has been reported to be fluorescent and have tunable photoluminescence properties<sup>185,186</sup>, it can also quench fluorescence. In fact, both GO and RGO have been reported to be highly efficient fluorescence quenchers with long-range energy-transfer.<sup>24,25,187</sup> This property has been exploited in two types of fluorescent based sensors. In “signal-on” sensors fluorescence intensity increases with the addition of the analyte due to a reaction with the fluorescent label which separates label and GO and can be correlated to the concentration of the analyte. “Signal-off” sensors use fluorescently labelled hybridized probes which are not fully adsorbed on GO but in the presence of the target they quench the fluorescence by adsorption by GO having these sensors lower sensitivity. Moreover, GO can also be used in other optical sensors as it has been reported to be a quencher of chemiluminescence and color.<sup>25</sup> A detailed description of the different approaches used for the incorporation of graphene in optical sensing applications and the enhancements in performance attained in particular in selectivity, limits of detection, and dynamic ranges can be found in several very recent reviews.<sup>22,24,25,27</sup>

In this section we will discuss the efforts that have been carried out to incorporate polymers in graphene-based optical sensors and the advantages and improvement of properties due to the macromolecular system. The main aim is to understand the role of the polymer in these sensing platforms. Table 3 summarizes the most representative published data on this subject. Although the number of papers related with optical sensors based on polymer/graphene composites is still scarce very promising results have already been obtained.

One of the most important effects observed for the combination of a polymer with GO in an optical sensor based on fluorescence detection has been reported by Sheng *et al.*<sup>188</sup> They developed a simple method to detect ochratoxin A (OTA) using graphene oxide as a quencher of the fluorescence of carboxyl fluorescein (FAM) attached to toxin-specific aptamer. OTA is one of the most abundant food-contaminating mycotoxin which can cause severe effects on human health. The authors designed a “signal-on” type sensor using an aptamer as recognition agent. Aptamers are selected single-strand oligonucleotides isolated from random-sequence DNA or RNA libraries by an *in vitro* selection process.<sup>189,190</sup> They can bind with high affinity and specificity to target molecules changing their conformation/structure before and after binding. When they are modified with fluorophores these structural changes may affect the fluorescence.<sup>189</sup> The strategy used for the detection of ochratoxin A is shown in Figure 8. Meanwhile in the absence of OTA, FAM modified aptamer was absorbed on GO via  $\pi - \pi$  stacking and quenched the fluorescence of FAM, in the presence of the target the aptamer folded to form antiparallel G-quadruplex structure which was resistant to adsorption onto the surface of GO. The fluorescence intensity could be measured as a function of OTA concentration. The sensing strategy showed excellent selectivity for OTA against other structure analogues but showed poor sensitivity due to some unspecific adsorption of the target onto GO. In order to prevent this effect, poly (vinyl

pyrrolidone) was used as a coating material of GO. The ratio of PVP concentration to GO was optimized to be higher enough to prevent the adsorption of OTA and increase the concentration of these molecules in the solution but not as high as to eliminate the adsorption of the aptamer as it is shown in Figure 9. Using this approach the limit of detection decreased from  $1.9 \times 10^{-6}$  M of the non-protected GO-based biosensor to  $1.87 \times 10^{-8}$  M in the PVP-protected and the linear range from  $2 \times 10^{-6}$  M and  $35 \times 10^{-6}$  M to  $5 \times 10^{-8}$  M and  $50 \times 10^{-8}$  M. In this case the role of the polymer although it was only as a coating material, proved to be crucial to lower the LOD of the sensor two orders of magnitude.

In other strategies the polymer plays a more active function as occurs when cationic conjugated polymers (CCP) which are fluorophores have been combined with GO in order to amplify the fluorescence response in the sensing platform.<sup>191,192</sup> Xing *et al.* developed a DNA sensor based on poly [(9,9-bis(6'-N,N,N-trimethylammonium) hexyl)-fluorenylene phenylene dibromide] (PFP), GO and a fluorescein (FAM)-labeled single-stranded DNA (P).<sup>191</sup> The design of simple, reliable and amplified nucleic acids sensors is of great interest because of its importance in medical diagnosis, gene expression analysis and biomedical studies. Conjugated polymers have been used to amplify the detection of DNA due to their light harvesting properties since more than a decade ago based on the fluorescence resonance energy transfer (FRET) mechanism which involves the transfer of energy from a donor fluorophore to an acceptor fluorophore.<sup>193,194</sup> However these sensors are limited by high background fluorescence which can be attributed to nonspecific electrostatic interactions between the DNA probe and CCP. These authors introduced GO in a traditional CCP based platform to reduce the background signal.<sup>191</sup> The polymer was PFP which is suitable as a donor in FRET. They observed that in the absence of the target (DNA) the fluorescence intensity of P was quenched after the addition of GO due to the strong adsorption of P on GO surface and the quenching effect of GO. When PFP was added to the P/GO complex the

FRET from PFP to P was inefficient indicating that PFP could not release P from GO surface. In the presence of target DNA, P hybridized with its target and upon the addition of PFP a strong FRET was observed (Figure 10). Moreover, they found a very important effect on the fluorescent response of the P-GO-PFP system depending on the order of incorporation of P and PFP. If P was added to PFP/GO complex, efficient FRET was obtained in contrast to the inefficient FRET observed when PFP was added to the P/GO complex as it is shown in Figure 11. Based on all these findings they optimized the experimental conditions of the system and concentration of the components and reduced significantly the background signal by introducing GO but maintaining the role of the polymer amplifying the fluorescence. The LOD was as low as  $4 \times 10^{-11}$  M, which is more than one order of magnitude lower than those previously reported for DNA detection methods using PFP.<sup>195,196,197</sup> The same authors demonstrated that this principle could be extended for the detection of other targets and they designed a low background and amplified signal platform for  $K^+$  based on the same system.<sup>192</sup> In the presence of  $K^+$ , P formed a G-quadruplex which separated P from GO and upon addition of PFP a FRET signal was observed. An enhanced sensitivity and selectivity was obtained opening up new expectations for further applications of the combination of GO with cationic conjugated polymers in biomedical analysis.

Very recently Zhang *et al.* have also combined GO with a conjugated polymer in an optical sensor but with a completely different approach.<sup>198</sup> They developed a hybrid organic-inorganic fluorescent system to detect 2,4,6 trinitrotoluene (TNT) in aqueous solution by fluorescence resonance energy transfer. The hybrid was prepared by introducing poly(p-phenylenevinylene) (PPV) into mesoporous silica nanoparticles (MSNs) by ion exchange and in situ polymerization (PPV-MSN). They functionalised the MSN surface with amino groups and by reaction between the COOH groups of GO and the  $NH_2$  groups of PPV-MSN they obtained the hybrid material (GO-PPV-MSN). The GO-PPV-MSN had a good

dispersion and strong fluorescence in aqueous solution which is essential for sensors to be applied in environmental applications. In this strategy the polymer was encapsulated in the channels of the mesoporous nanoparticles in order to avoid the direct interaction with GO with the corresponding fluorescence quenching and maintain the fluorescence properties in the hybrid material. They observed that in the presence of the target the amino groups of the surface of PPV-MSN bound TNT molecules from solution by forming Meisenheimer complex and this complex strongly suppressed the fluorescence emission of the hybrid GO-PPV-MSN through FRET mechanism. They also measured that the quenching efficiency was higher for GO-PPV-MSN than for PPV-MSN with TNT. Therefore, the incorporation of GO improved the detection sensitivity, being the LOD of TNT of  $1.3 \times 10^{-7}$  M in the hybrid material besides increasing the water solubility.

Another route in which polymers have been introduced in optical sensing platforms based on graphene is by molecular imprinting technology.<sup>170,199,200,201,,202,203,204</sup> Liu *et al.* prepared an optosensing platform based on a molecular imprinted polymer incorporating quantum dots (QDs) and graphene oxide for highly selective and sensitive specific recognition of vitamin E (VE).<sup>199</sup> Quantum dots are nanometre scale semiconductor crystals which have unique optical and photophysical properties and have been widely applied in optical sensing and biosensing.<sup>205,206</sup> In this system the authors combined the fluorescence characteristics of both CdSe/ZnS QDs and GO and added an ionic liquid (IL) to the surface of GO in order to improve its fluorescence stability and the binding with the QDs. The material was prepared in a one-step polymerization using AA as functional monomer, EGDMA as crosslinker and 2,2-azobisisobutyronitrile (AIBN) as initiator including reaction with VE driving template molecules into the surface of the composites. When the VE was removed by solvent extraction, imprinting binding sites were left in the composites that selectively bound the target (VE). The sensor was based on the changes in fluorescence

intensity due to VE binding and ascribed to fluorescence quenching between VE and MIP. The method showed high selectivity, sensitivity and fluorescence stability with a detection range and limit indicated in Table 3. In another example the MIP was incorporated in a graphene quantum dots (GQDs) sensor for determination of para-nitrophenol (4-NP).<sup>200</sup> Graphene quantum dots are graphene sheets smaller than 100nm with very interesting characteristics such as high fluorescent activity, low toxicity and excellent water solubility.<sup>207</sup> The MIP was based on APTES as functional monomer and TEOS as crosslinker and prepared by sol-gel polymerization on GQDs to coat the nanomaterial. The fluorescence of MIP-coated GQDs was efficiently quenched when interacted with 4-NP. This novel fluorescent sensor showed stable fluorescence, rapid response, good recognition specificity, wider linear range and lower detection limit (Table 3) for environmental application. In all these sensors the role of the polymer was to enhance selectivity by its high selective recognition and capture capabilities.

On the other hand, polymer/graphene composites have also been used in chemiluminescence-based sensors. Huamin *et al.* developed a flow injection chemiluminescence (FI-CL) sensor for the detection of sulfamethoxazole (SMZ) using chitosan/graphene oxide-molecular imprinted polymer (CG-MIP) as recognition element<sup>201</sup>. Again the MIP was introduced in the chemiluminescence (CL) analysis to improve selectivity and chitosan/GO was used to improve adsorption capacity. The SMZ-CG-MIP system was prepared in acetone using AA as functional monomer, EGDMA as crosslinker and AIBN as initiator. The CL sensor had improved selectivity and sensitivity. Chen *et al.* prepared an electrochemiluminescence biosensor for glucose based on graphene/Nafion/glucose oxidase modified glassy carbon electrode.<sup>208</sup> The performance of this sensor was enhanced in comparison with Nafion/GOD modified electrode. It was determined that the incorporation of the reduced graphene oxide accelerated the charge

transfer. In another example of an CL sensor Ru(bpy)<sub>3</sub><sup>2+</sup>/graphene/Nafion modified electrode was developed for oxalate analysis.<sup>209</sup> In both cases the role of the polymer was to modify the electrode and the incorporation of graphene in the composites enhanced the electroluminescence.

Finally, polymers have also been combined with graphene in colorimetric-based sensors. A very interesting example has been recently reported by Wang *et al.* in which polydiacetylene (PDA) and graphene were prepared as stacked composite films for the detection of environmentally hazardous volatile organic compounds (VOCs)<sup>210</sup>. Polydiacetylenes are  $\pi$ -conjugated polymers which exhibit an intense chromatic change from blue to red in response to external stimuli such as temperature, solvent, mechanical stress and ligand-receptor interactions<sup>211</sup>. Due to their properties PDAs have been employed as sensing platforms for the detection of biologically, environmentally and chemically important target molecules<sup>211</sup>. However, these PDA sensors have some limitations such as low sensitivity and difficulties for precise quantitative information. The combination with graphene provided an efficient and transparent support for the assembly of PDA increasing the absorbing area of gaseous molecules that enhanced the colorimetric signal of PDA. The composite films were prepared by self-assembly of diacetylene onto graphene sheet (GS) and polymerized by UV. The chromatic change observed in the presence of VOCs corresponded to conformational changes in PDA due to the interactions with VOCs which were clearly observed by scanning tunnelling microscopy (STM).

### 3.2.2 Electrochemical sensors

From an electrochemical point of view the potential scope of graphene electrodes is enormous since they maintain the properties of other carbonaceous materials like potential windows, inert electrochemistry, and good electrocatalytic activities for many redox

reactions, while provide new properties like high surface area and ultrafast charge mobility, which ensure high sensitivity and rapid response. The fundamental aspects of graphene electrochemistry<sup>28,29,30,31</sup> as well as the room of graphene electrodes in sensing<sup>32,33,34,35,37,212,213,214</sup> are beyond the scope of this review and the readers are directed to the aforementioned literature.

For electrochemical sensors, the utilization of graphene based polymer composites may combine the advantageous electrical, electronic, mechanical, and thermal properties of graphene with the countless functions of polymers very different in nature ranging from natural to synthetic or conventional to conducting polymers. In this section we will focus on the enhancements of graphene-based electrochemical sensors attained upon addition of different types of polymers. Table 4 condenses the most representative examples on this subject reported so far.

Thus, in some cases the graphene/polymer electrodes for sensing are composed of MIPs that have been previously described. The advantages of MIPs lie in the rapid and low-cost synthesis and the possibility of tuning selectivity by means of the appropriate selection of templates in the imprinting process.<sup>215,216,217,218</sup> In addition, the use of a thin layer of MIP on the electrode surface as recognition element of the sensor greatly improves the electrode selectivity.

In the case of electrochemical sensors the MIP consists principally of a conducting polymer like polypyrrol<sup>219,220,221</sup> and derivatives of polyaniline,<sup>222,223</sup> where the polymer is prepared by electropolymerization in the presence of the target (Figure 12). For example, a trimethoprim (TMP) sensor has very recently been prepared by electropolymerization of pyrrole on a graphene oxide-modified glassy carbon electrode.<sup>219</sup> Here the polymer plays a dual role since it acts as the template of the recognition element and also as transducer of the signal. Moreover they also may play a dual role in both the sensor electrode preparation and

the electrode performance. In the first case GO serves as a site where the analyte is immobilized during the preparation of the MIP because of the high concentration of oxygen-containing groups on GO assures strong hydrogen bonding interactions with the TMP. In addition, graphene improves the sensitivity of TMP detection as it significantly increases the peak current response measured by square wave voltammetry (SWV). A LOD of  $1.3 \times 10^{-7}$  M was obtained. Since trimethoprim is an antibacterial drug widely used in the prophylaxis and treatment of urinary, intestinal and respiratory infections, the authors succeeded on its quantification in urine samples.

In another very recent work, the MIP PPy was integrated with graphene and Au nanoparticles and the composite was employed for sensing of levofloxacin (LEV), another antibacterial agent.<sup>220</sup> While the role of the MIP is again the recognition element, the incorporation of the metal nanoparticles clearly ensures higher electrode surface that significantly increases the analyte signal. The authors deeply evaluated other variables during the MIP preparation (template/monomer ratio, number of polymerization cycles), template molecules elimination (type of solvent) and sensing (supporting electrolyte and incubation time) and they established the optimal conditions for LEV determination. They used differential pulse voltammetry as detection method, obtaining a LOD of  $0.53 \times 10^{-6}$  M. Moreover, the authors studied the selectivity of the PPy-RGO/AuNPs modified electrode by determining the responses of LEV in the presence of some interfering substances like chlorotetracycline, oxytetracycline, prulifloxacin and norfloxacin, and found that these species do not mask the LEV response proving the selectivity conferred to the sensor by the MIP. A composite electrode similar to both examples described above has been employed to determine quercetin, a flavonoid with antioxidant power, by DPV.<sup>221</sup>

Liu *et al.* have reported a sensor of a tetracycline antibiotic (chlorotetracycline, CTC) based on an electrogenerated MIP, poly(o-phenylenediamine) (POPDA) and reduced

graphene oxide (RGO) that combines the response amplification of RGO and the special recognition of MIP.<sup>222</sup> In this sensor  $[\text{Fe}(\text{CN})_6]^{3-}/[\text{Fe}(\text{CN})_6]^{4-}$  redox pair is used as an indirect electrochemical probe. The authors demonstrated that the oxidation of  $[\text{Fe}(\text{CN})_6]^{3-}$  to  $[\text{Fe}(\text{CN})_6]^{4-}$  did not take place when the template molecules were in the cavities of the polymer and it was recovered after template removal. Using DPV they found a linear correlation between the peak current variation of the  $[\text{Fe}(\text{CN})_6]^{3-}/[\text{Fe}(\text{CN})_6]^{4-}$  redox pair and the concentration of CTC in the range of 10 to 500  $\mu\text{M}$  and also succeeded in the determination of CTC in tap and wastewater samples.

POPDA was also employed in an electrochemical sensor for the determination of cefotaxime (CEF), displaying a rather more complex composition.<sup>223</sup> The bare GCE was firstly covered by a film of RGO having COOH groups at the edges (RGO-COOH). Then a dispersion composed of gold networks in an ionic liquid (1-butyl-3-methylimidazoliumtetrafluoroborate,  $[\text{BMIM}][\text{BF}_4]$ ) and porous platinum nanoparticles (PPNPs) was coated on the modified electrode. Finally, the OPDA was electropolymerized in the presence of CEF by cyclic voltammetry. Here, the RGO-COOH and the metal particles increase the electrode surface area leading to an increase in the current signal whilst the polymer plays again a recognition role. All variables including the concentration of each electrode component, the template/monomer ratio, the polymerization time, the incubation time and pH were optimized. Under optimal conditions the sensor displayed linear response to CEF in the range of  $3.9 \times 10^{-9}$  -  $8.9 \times 10^{-6}$  M (Figure 13). The performance of the MIP was evaluated in the presence of some interference that can be present in real samples like glucose, AAC, UA and glutamic acid, showing high selectivity to CEF. In addition, the interference of similar compounds such as ceftizoxime and ceftriaxone was assessed and the MIP proved to be selective to CEF.

Beyond molecules of biological interest, a similar system was used to detect some pollutant like, 2,4-dinitrophenol(DNP).<sup>224</sup> The electrode preparation is slightly different from the examples described above. First GO was dispersed in an ethanol solution containing APTES to produce an amino-functionalized GO. Then the imprinting step was conducted by oxidative polymerization of o-phenylenediamine (OPDA) with ammonium peroxydisulfate (APS) in the presence of DNP. Then the GO/POPDA was drop-casted on the bare electrode. The authors optimized parameters such as the thickness of the GO-POPDA film, pH, accumulation time and scan rate and obtained linearity in the range  $1.0 \times 10^{-6}$  M to  $1.5 \times 10^{-4}$  M of DNP. Regarding selectivity, the MIP-GO electrode works very well in the presence of inorganic ions ( $\text{Na}^+$ ,  $\text{K}^+$ ,  $\text{Fe}^{3+}$ ), typical organic interfering compounds, such as m-dihydroxybenzene, p-aminobenzoic acid, p-hydroxybenzoic acid, phenol, 3- and 4-nitrophenol. However similar compounds like nitrophenols (at 10-fold concentrations) were found to affect the determination to some extent as the nitro groups can also be reduced near the reduction potential of DNP.

Moreover, there is one example where a copolymer of methacrylic acid (MAA) and ethylene glycol methacrylate, prepared by free radical polymerization is employed as MIP in electrochemical sensors.<sup>225</sup> In this case, a composite of graphene sheets non-covalently functionalized with Congo red (GSCR) and poly(MMA-co-EGDMA) has been used to detect one of the most studied molecules with biological functions, the neurotransmitter dopamine. The Congo red (CR) is used to improve the solubility of graphene and the absorption of the target DA. The combination of MIP with graphene sheet assures outstanding recognition performance, rapid adsorption kinetics due to high ratio of surface-imprinted sites and large aspect ratio because there are a great number of effectively imprinted sites distributed along the GSCR-MIP surface. The electrode was tested in

complex solution containing epinephrine and AAC, the principal interfering of DA, and it showed good selectivity.

Other studies used composite electrode of different graphene derivatives with non-molecularly imprinted conducting polymers such as PANI<sup>226,227,228</sup> and its derivatives,<sup>229</sup> PPy<sup>230,231</sup> and poly(3,4-ethylenedioxythiophene) (PEDOT).<sup>232</sup>

Luo *et al.* reported the preparation of a water-dispersible PANI/graphene composite by in situ polymerization of aniline on the surface of poly(styrenesulfonic acid) (PSS) coated graphene nanosheets (PSS-GS).<sup>226</sup> The sulphonic acid has been widely employed as PANI dopant to achieve good electroactivity at physiological pH<sup>233,234</sup> and recently SG has also been used for this purpose.<sup>235</sup> In the present paper the PSS coated graphene plays the same role. Moreover, the PANI/graphene composite displays fast electron transfer and catalytic capability for the oxidation of AAC with a LOD of  $5 \times 10^{-6}$  M.

Similarly Bao *et al.* reported the preparation of nanostructured PANI microsheets by chemical polymerization with APS in the presence of GO, which serve as templates.<sup>227</sup> GCE-modified PANI/GO composites were used for the simultaneous determination of AAC, DA and UA, because they displayed strong, moderate and no electrocatalytic effect for AAC, DA and UA, respectively, that permitted to separate the electrochemical response of the three analytes.

A similar system based on the electropolymerization of PANI nanowires (PANIw) on GO-modified GCE has been successfully employed for DNA sensing.<sup>228</sup> The polymer nanowires confer to the electrode high effective surface area, thereby increasing its sensitivity. The sensing electrode was prepared in two steps: firstly, the PANIw-GO-GCE was immersed in a solution of single-strand DNA (ssDNA) probes to immobilize it on the electrode. Then, the ssDNA-PANIw-GO-GCE electrodes were immersed in the hybridization phosphate buffer solution containing the target DNA. For the sensing test the

well-known electroactive hybridization indicator, daunomycin was employed. Because the DNA assay is directly related to the surface coverage of DNA probes on the electrode, the behaviour of DNA hybridization can be affected by daunomycin. When hybridization happens, daunomycin is intercalated in the DNA duplex, which can show the electrochemical response compared with single-stranded DNA. The modified electrode displayed certain selectivity towards the specific DNA target and a linear range with the logarithmic values of the target sequence concentration from  $2.12 \times 10^{-6}$  to  $2.12 \times 10^{-12}$  M, with a LOD of  $3.23 \times 10^{-13}$  M.

Yang *et al.* reported the preparation of a composite of poly(aminobenzenesulphonic acid) (PABSA) and RGO by simultaneous polymerization of ABSA and reduction of GO via pulse potentiostatic method.<sup>229</sup> They used electrodes modified with this composite to detect target genes. For example, they immobilized specific probe DNA via  $\pi$ - $\pi$  stacking interaction between the conjugated composite and DNA bases. In this case the original electrochemical response of the composites disappeared (signal-off) because of the DNA on the surface blocked the electron transfer of PABSA/RGO. However, the hybridization between the probe pDNA and target complementary cDNA induced the product hybridized DNA to be released from the conjugated composite, accompanied with the self-signal regeneration of the composite ("signal-on") (Figure 14). Ultimately, they used the Bode plots obtained from electrochemical impedance spectroscopy (EIS) for the detection of promyelocytic leukemia/retinoic acid receptor alpha (PML/RARA) gene sequence (Figure 14), obtaining a very low limit of detection of  $3.7 \times 10^{-17}$  M.

Ye *et al.* prepared a sensor of nitrite composed of a composite of PPy and RGO dispersed in a 0.5 wt. % CS solution.<sup>230</sup> The natural polymer appears positively charged in acidic solutions due to the protonation of  $-\text{NH}_2$  groups in the polymer, and therefore CS attracts negatively charged nitrite ions ( $\text{NO}_2^-$ ), in order to concentrate it on the electrode

surface. On the other hand PPy promotes the electrochemical oxidation of  $\text{NO}_2^-$ , whilst graphene guarantees high surface area and electrical conductivity.

A PPy derivative, poly(2,5-di-(2-thienyl)-1-pyrrole-1-(p-benzoic)) (PDPB) has been employed in immunosensing.<sup>231</sup> The polymer was incorporated in a complex system with RGO, AuNPs, aflatoxin B1 antibody (AntB1) and the ionic liquid, 1,3-di(isobutyl)imidazolium bis(trifluoromethanesulfonyl)imide. PDPB plays a key role as it covalently binds the specific antibody, contributing to the sensor stability. Although the polymeric film reduces the electron transfer to some extent, the presence of RGO and AuNPs recover it. The  $[\text{Fe}(\text{CN})_6]^{3-}/[\text{Fe}(\text{CN})_6]^{4-}$  redox probe was used to quantify the aflatoxin B1 by Faradaic impedance spectroscopy obtaining a LOD in the order of  $\text{fmol.L}^{-1}$ .

A composite of PEDOT with RGO has also been employed for biosensing.<sup>232</sup> The sensor was prepared by simultaneous polymerization of EDOT and reduction of GO by cyclic voltammetry in the presence of ascorbate oxidase enzyme. The obtained graphene–PEDOT composite meets properties of graphene and the polymer like large specific area, high conductivity, good biocompatibility, and fast redox properties. As an enzyme model, ascorbate oxidase (AO) was entrapped onto the film-modified electrode and used to construct an electrochemical AAC biosensor. The modified electrode showed good electrocatalytic performance towards ascorbic acid with high selectivity, wide linear range as well as good reproducibility and stability.

Also a natural polymer, CS has been used in composites with graphene for sensing purposes.<sup>236,237,238</sup> The main role of CS is the biocompatibilization with the target analyte and has been utilized covalently linked to chemically modified graphene (CMG) for the determination of DNA<sup>236</sup> or in a multicomponent sensor with graphene, sulphonated poly(ether-ether-ketone) (SPEEK) and AuNPs for the detection of glucose.<sup>237</sup>

On the other hand, composites of the diverse forms of graphene with non-conducting polymers (very different in nature) have been used in biosensing<sup>239,240,241,242</sup> or sensing.<sup>243,244</sup> The polymer families range from typical polystyrene,<sup>240</sup> poly(acrylic acid)<sup>242</sup> or polyethylenimine<sup>244</sup> to more complex polymers like poly[(2-ethyltrimethylammonioethyl methacrylate ethyl sulfate)-co-(1-vinylpyrrolidone)] (PQ11)<sup>243</sup> or poly(benzyl methacrylate-*r*-ethylene glycol methacrylate-*r*-N-acryloxysuccinimide)(PBPN).<sup>239</sup> The last case is especially interesting as the amphiphilic polymer is composed of three blocks, each with a specific function, i.e. a hydrophobic part with a benzene ring that helps to immobilize the polymer on the RGO surface by  $\pi$ - $\pi$  interactions; a poly(ethylene glycol) methacrylate segment whose function is protein repulsion and an easy-removable activated ester, N-acryloxysuccinimide (NAS) as a component for bioconjugation.<sup>245</sup> The bare ITO electrode was modified with aminoethyl benzenediazonium salt and then covered with a layer of GO, which was afterward electrochemically reduced. The modified electrode was immersed in a solution containing PBPN and the antibody (anti-mouse IgG), and was covalently immobilized on the polymer layer by substitution of the succinimide moieties.<sup>239</sup> The immunosensing platform for the detection of an antigen, mouse IgG, was prepared by the sandwich enzyme linked immunosorbent assay (ELISA) protocol (Figure 15). More exactly, the target antigen (mouse IgG) was dropped on the anti-mouse IgG-immobilized surface and then horseradish peroxidase (HRP)-labeled anti-mouse IgG was also dropped on the resulting surface. After incubation, the immunosensor was placed in a solution containing hydroquinone (HQ) and H<sub>2</sub>O<sub>2</sub>. In the presence of H<sub>2</sub>O<sub>2</sub>, the HRP molecules catalyze the oxidation of HQ into benzoquinone (BQ), which is electrochemically reduced on the electrode surface, producing a high signal current. The authors reported a LOD of 100 fg.mL<sup>-1</sup>.

### 3.3 Chemical sensors based on polymer/graphene/carbon nanotubes

This last section is devoted to polymeric composites where graphene and CNT are used simultaneously. The combination of both carbon nanoforms is expected to deliver outstanding properties like superior electrochemical activity that is not achieved by any of these components alone. In fact, polymer composites based on graphene and carbon nanotubes hybrids have been prepared to develop better supercapacitors<sup>246</sup>, highly conductive transparent electrodes for energy conversion in solar cells<sup>247,248</sup> and for thermal interface materials<sup>249</sup>. This philosophy has been recently extended to the field of electrochemical sensors.<sup>250,251,252,253,254,255,256</sup> But in the best of our knowledge, there are no examples on optical sensors combining these two carbon nanoforms with polymers.

Similar to those described in the preceding sections, several of these examples use molecularly imprinted conducting polymers.<sup>250,251,252</sup> In an interesting study a complex electrode has been used for the determination of tryptamine.<sup>250</sup> In this case the electrode is composed of three different polymers, each with a specific function. The GCE is modified by a first layer comprising PPy and sulphonated graphene (SG) that improves the selectivity and the rapidness of response of the electrode. Then a second layer of a biocomposite composed of a polysaccharide, hyaluronic acid (HA) and MWCNTs is drop casted on the modified electrode. While the HA provides biocompatibility and hydrophilicity, the function of the MWCNTs is to enhance the current response. Finally the selectivity is provided by an aniline derivative polymer, poly(para-aminobenzoic acid) (PpABA) that is electropolymerized on the top of the HA/MWCNT-PPy/SG-GCE electrode in the presence of tryptamine molecules. In this study all experimental parameters including scan cycles, template/monomer ratio, carbon nanoforms loading, pH and temperature were deeply study and optimal conditions determined. In addition the tryptamine response was evaluated in the presence of analogues like tyramine, dopamine and tryptophan demonstrating the selectivity

of the modified electrode. Under optimal conditions a linear range from  $9.0 \times 10^{-8}$  to  $7.0 \times 10^{-5}$  mol.L<sup>-1</sup> and a LOD  $7.4 \times 10^{-8}$  mol.L<sup>-1</sup> were reported.

Other complex electrode composed of CS-silver NPs, graphene-MWCNTs and MIP PPy has been employed to determine neomycin.<sup>251</sup> In this case CS-Silver NPs and graphene-MWCNTs were prepared separately. The sensor was constructed as follow: first, a solution of CS-Silver NPs was casted on the electrode surface, and then a suspension of graphene-MWCNTs was added on the top. Subsequently, a PPy film was formed in the presence of the neomycin templates and the electrode washed with acetic acid and ethanol to remove the template. By using CV and amperometry it was reported that, under optimal conditions, the linear range of the sensor range from  $9.0 \times 10^{-9}$  to  $7.0 \times 10^{-6}$  mol.L<sup>-1</sup>, with a LOD of  $7.63 \times 10^{-9}$  mol.L<sup>-1</sup>.

In another study a carbon electrode covered with graphene was casted with a film of diazonium functionalized SWCNT bearing aniline moieties and then a MIP PANI was electrodeposited in the presence of bovine serum albumin (BSA).<sup>252</sup> DPV experiments showed a wide linear range ( $1.0 \times 10^{-10}$  to  $1.0 \times 10^{-4}$  g.mL<sup>-1</sup>) with a low detection limit of  $6.2 \times 10^{-11}$  g.mL<sup>-1</sup> for BSA.

Due to good adsorption, compatibility and excellent film-forming ability CS was used with CNTs/graphene hybrids as a sensor of organophosphate pesticides<sup>253</sup> and an immunosensor.<sup>254</sup> In the former the electrode preparation is simple and rapid since it is based on a one-step electrodeposition procedure.<sup>253</sup> With this electrode methyl parathion, as a model of organophosphate pesticides, was linearly detected between  $7.6 \times 10^{-9}$  to  $1.9 \times 10^{-6}$  mol.L<sup>-1</sup>, with a LOD of  $1.9 \times 10^{-9}$  mol.L<sup>-1</sup>. In the latter a layer by layer assembling approach was employed to build the immunosensor.<sup>254</sup> This device was used to detect procalcitonin, a marker of the identification of severe bacterial infections, with a linear response range from

$1 \times 10^{-11}$  to  $3.50 \times 10^{-7}$  g.mL<sup>-1</sup> and a LOD of  $5 \times 10^{-13}$  g.mL<sup>-1</sup>, under optimal experimental conditions.

A novel strategy based in a layer-by-layer assembly method through the electrostatic adsorption between positively charged poly(diallyldimethylammonium chloride) (PDDA) and negatively charged MWCNT and graphene has also been employed to build a sandwich-type electrochemical immunosensor using human IgG as a model target.<sup>255</sup> The detection limit of the immunosensor was  $2.0 \times 10^{-10}$  g mL<sup>-1</sup> and a good linear relationship between the current signals and the concentrations of human IgG ( $1.0 \times 10^{-9}$  to  $5.0 \times 10^{-7}$  g mL<sup>-1</sup>) were reported.

#### 4. Conclusions and future perspectives

In summary, polymer/CNT and polymer/graphene based sensors have demonstrated their great potential in a wide variety of challenging chemical sensing and biosensing applications. The synergistic effect of the intrinsic properties of both carbon nanomaterials such as NIR fluorescence or fluorescence quenching, high electrical and thermal conductivity, chemical stability and mechanical strength with the tuneable properties of polymers in terms of their chemical structure and functionality, combined with their low cost, easy processability, and, in many cases, recyclability and sustainability, make these polymer composites ideal for the development of new types of chemical sensors.

Most examples described in this review show an enhancement in sensing performance with these polymer composites compared to current sensors in the literature, although only in few publications the sensing parameters with and without the polymer in the same sensor are compared. Likewise, the data reported to date reveal the different roles that polymers play for the development of ultrasensitive and highly selective sensors and biosensors based on CNT and graphene. Polymers can provide the immobilization support

and encapsulate or coat the carbon nanomaterial or the electrode to prevent or favour adsorption. They can enhance the electrocatalytic behaviour, amplify the fluorescence and improve selectivity. In this regard, molecular imprinting polymers can play a dual role in these sensors providing recognition sites and, for example, also enhancing the electron transfer.

Polymers can also improve the CNT or graphene dispersion or provide biocompatibility and water dispersion ability. They can be incorporated in the sensing platforms with many different preparation methods and architectures from in situ polymerization or electropolymerization, to solution mixing, molecular imprinting or layer by layer techniques, among others.

On the other hand, the combination of graphene derivatives (GO) with conjugated polymers has been very effective to amplify the fluorescence response in optical sensors for biomedical analysis. Polymer/graphene electrochemical sensors have shown enhanced detection sensitivity and selectivity and rapidness of response of the electrode depending of the nature of the polymer or combination of polymers and their synergistic effects with the graphene derivatives.

Nevertheless, there are a number of challenges to be addressed to fulfil the application of polymer/CNT and polymer/graphene composites for sensing applications. Firstly, due to the elevated cost of high purity and quality CNTs, the synthesis process of these composites is expensive. Moreover, the processing is still not fully controlled. For instance, nanotube dispersion is difficult to be optimized, and CNT aggregates are frequently formed, which limit the composite properties. Despite covalent and non-covalent functionalization of CNTs are generally successful in overcoming this limitation, some of these approaches are tedious and hence, difficult to scale up. In this sense, graphene has a cost advantage over CNTs since it can be obtained from naturally

occurring graphite and catalysts are not needed for this. However, the properties of graphene and its derivatives strongly depend on their quality and, in this regard; mass-scale production of high quality graphene is still a challenge. Moreover, although significant advances have been made on the functionalization of graphene and its interactions with polymers, much research effort is still necessary to incorporate them efficiently in multicomponent advanced devices. In addition, the toxicological impact of both types of composites has not been investigated in detail, and needs to be carefully analyzed prior to use them in living biological systems

Most advances have been done mainly in polymer/CNT based sensors although the application of polymer/graphene composites in biosensors is growing very quickly parallel to the developments and achievements in graphene itself and in polymer/graphene based materials.

The straight question that arises for the future perspectives in this field is which composites are better to be used in chemical sensors? Those based on graphene or carbon nanotubes? The answer is not straightforward neither general for both types of sensors analysed through this review. The advantages of using CNT or graphene/polymer composites would depend on the specific application taking into account the differences in the surface chemistry, redox behaviour, conductivity and optical properties of both carbon nanomaterials and their complex interactions with the polymeric matrix.

Regarding optical sensors, it is not possible to establish a direct comparison since there is lack of literature dealing with the same polymer reinforced with CNTs and graphene. Focusing on the same analyte (i. e. glucose) and composites prepared by the same method (i.e. solution mixing), it is found that samples with RGO (Ref. 208) display wider linear range and enhanced sensitivity than those incorporating SWCNTs (Ref. 111 and 112). However, it should be noted that these SWCNT-based sensors are based on the change in

the NIR emission spectra of the SWCNTs, while that incorporating RGO is an electrochemiluminescence biosensor in which the RGO accelerates the charge transfer. Higher potential of GO-based sensors can be envisaged considering comparative studies on the nanoquenching effects of CNTs and GO toward DNA fluorophores in the absence of polymer, which revealed superior quenching abilities of GO in both the quenching efficiency and kinetics.<sup>257</sup> Future applications in sensing and biosensing, specially based on the exceptional tunable optical properties of graphene derivatives combined with the multifunctionalities of polymers, are foreseen.

In the case of electrochemical sensors, both carbon nanoforms have wide potential window, are chemically inert, and show electrocatalytic activity for several reactions. Furthermore in CNT or graphene/polymer composites for electrochemical sensors, where the electronic transport is fundamental to assure a fast and sensitive response, both carbon nanoforms display exceptional intrinsic electric conductivities for signal transducing. However, their geometries are noticeably different causing different effect on the effective conductivities of composites. In this case, it has been demonstrated that graphene is more effective in conductivity enhancement than CNT.<sup>258</sup> Strictly analysing the role of the carbon nanostructures, the differences in concentration and distribution of edges and defects must be contemplated since it is known that a high density of edge-plane-like defective sites provide many active spots and is beneficial for accelerating electron transfer between the electrode and analytes in solution.<sup>259,260,261,262</sup> For example, in the case of DA graphene has displayed better sensing performance than both SWCNTs<sup>263</sup> and MWCNTs,<sup>264</sup> and effective separation of its electrochemical signal from interfering agents.

Apart from the rapidness and sensitivity, the other key factor is the selectivity or specificity of the devices. In this matter, the role of the polymer with broader chemistry than the carbon nanoform is of paramount importance and the larger the type of polymers

that can be composed with the carbon nanostructures, the higher the number of sensing devices that can be prepared and the number of analytes that can be determined. In addition, sometimes the polymer function is to increase the processability of the carbon nanoforms. In this case the possibility of polymer wrapping of CNTs (not possible in the case of graphene) makes that a great variety of these materials can be used increasing the range of electrodes that can be prepared, and thus specificity, selectivity and versatility. However, in the case of graphene this limitation can be addressed just using a graphene derivative like GO, which has a wide variety of oxygen-containing groups, each with specific chemistry that make possible tailor-modification of graphene.

Along this revision we didn't find sensors composed of the same polymeric system to detect the same target in order to compare the sensing performance of CNT and graphene. However, the cases of determining dopamine in ref. 177 and 225 show several similarities. In both cases a GCE modified with molecularly imprinted MMA -based copolymer was employed to detect dopamine. In this case the key factor lies in the MIP that allows for selectivity and sensitivity for the DA recognition, being the amounts of carbon nanoforms enough to assure a good electrochemical response and similar LOD were obtained in both cases. Therefore in this type of sensors the role of the polymer should not be ignored and to focus only on carbon nanostructures would be a mistake. In the future we envisage that the scope of graphene/polymer electrochemical sensors will increase considerably and that graphene-based composites with new families of polymer, some of them already employed with CNTs will be prepared and its sensing performance evaluated. Especially interesting is the case of disposable sensors where the cost of preparation is decisive, and graphene that can be prepared from naturally occurring graphite represents a better option than CNT.

The combination of graphene and carbon nanotubes, principally in the form of 3D structures in polymers represents a very interesting strategy, which has only begun to be

investigated for sensing. Expanding this philosophy could represent a breakthrough as a great synergistic effect can be produced, where the high concentration of edge planes in graphene provide high sensitivity and fast analysis and the polymer wrapped carbon nanotubes facilitate the devices preparation without losing the electron transport properties. Thus, the preparation of CNT/graphene hybrid polymer composites may constitute one of the future research lines in this field, where layer-by-layer assembling emerges as a simple approach to construct highly efficient, sensitive and selective devices. Although no examples have been reported so far about optical sensors, it is expected that hybrid graphene/CNT composites will be prepared and tested as sensing devices in the near future.

Therefore, although several milestones have been achieved, ongoing research efforts are necessary to design new polymer/CNT and polymer/graphene devices with improved performance and reproducibility compared to other materials that could be employed for chemical sensing and biosensing both in vivo and in vitro applications. The scope of these polymer composites is expected to continue growing with the development of more versatile fabrication strategies to build complex architectures being the understanding and control of the interphases of these materials the key factor. If all the aforementioned drawbacks are properly addresses, it can be expected that the merits of these polymer composites-based sensors will have an important impact in the future of sensors based on carbon nanomaterials.

### **Acknowledgments**

The authors wish to thank the MINECO, Spain, for financial support under the grants MAT 2009-09335 and MAT2010-21070-C02-01. HJS acknowledges the MINECO

for a Ramón y Cajal Senior Research Fellowship. AD would like to thank the CSIC for a JAE postdoctoral contract co-financed by the EU.

**Figure captions**

**Figure 1.** Schematic representation of polymer-wrapped SWCNT systems used for glucose detection: (A) Introduction of concanavalin A (ConA) to phenoxy-derivatized dextran-wrapped SWCNT initiates nanotube agglomeration, resulting in a decrease in nanotube fluorescence. The addition of glucose, which binds to ConA, separates the nanotube bundles with the recovery of fluorescence. (B) PVA-wrapped SWCNT is covalently tethered to GBP. Upon addition of glucose, the GBP undergoes a conformational change, resulting in a change in the SWCNT fluorescence intensity. Adapted from ref.111 and 112, copyright 2006, 2011 with permission from Wiley Inter-Science.

**Figure 2.** Schematic representation of chitosan-SWCNT sensors for glycan lectin detection. (A) The chitosan wrapped SWCNT sensors are processed to include tethered NTA groups and chelated  $\text{Ni}^{2+}$  so that His-tagged lectins can attach to the sensors. (B) Ensemble measurement setup: the chitosan-SWCNT gel is spotted onto glass chips which are excited by a laser, and the emission spectra are analyzed. Reprinted from ref.117, copyright 2011, with permission from American Chemical Society.

**Figure 3.** (A) Sensor array fabricated using SWCNT/Chitosan (CS). A SWCNT/CS suspension is spotted on glass and functionalized with Ni-NTA to bind His-tag proteins. (B) Optical and NIR fluorescence image of the SWCNT/CS array. (C) Signal transduction mechanism for detection of protein-protein interactions: a NIR fluorescence change from the SWCNT occurs when the distance between the  $\text{Ni}^{2+}$  quencher and SWCNT is altered upon analyte protein binding. Reprinted from ref 124, copyright 2011, with permission from American Chemical Society.

**Figure 4.** Cyclic voltammograms of SPCE modified with different numbers of GOX/SWCNT/PVI-Os layers in the presence of 10 mM glucose. The layer number is shown in the figure. The potential scan rate was 10 mV/s. Inset: structure of the redox polymer PVI-Os. Reprinted from ref. 156, copyright 2011, with permission from Elsevier.

**Figure 5.** Schematic representation of chemical reaction involved in the fabrication of enzyme/MWCNT/PANI/Pt modified electrode. Reprinted from ref. 160, copyright 2011, with permission from Elsevier.

**Figure 6.** CVs of the electropolymerization process in aniline (A), CNTs + aniline (B), SiW<sub>12</sub>+aniline (C) and CNTs+SiW<sub>12</sub>+aniline (D), respectively. Reprinted from ref. 163, copyright 2013, with permission from Springer.

**Figure 7.** Scheme of chemical sequence of electropolymerization of CuNPs-CS-cMWCNT-PANI on gold electrode and chemical reaction of immobilization of laccase enzyme. Reprinted from ref. 165, copyright 2011, with permission from Elsevier.

**Figure 8.** Schematic illustration of graphene oxide sensing platform for detection of ochratoxin A. Reprinted from ref. 188, copyright 2011, with permission from Elsevier.

**Figure 9.** (A) Effect of PVP concentration on the fluorescence intensity of graphene oxide/FAM-modified aptamer without (black bar) and with (red bar) existence of ochratoxin A. (B) Columns bars were obtained by subtracting the value of black columns

bars from the value of corresponding red columns bars, Error bars were obtained from three experiments. Reprinted from ref.188, copyright 2011, with permission from Elsevier.

**Figure 10.** Schematic representation of GO-based low background-signal platform for the detection of target DNA. Reprinted from ref.191, copyright 2013, with permission from American Chemical Society.

**Figure 11.** Normalized FRET-induced fluorescence spectra of P-GO-PFP system under different addition order: (A) addition of PFP into P/GO complex and (B) addition of P into PFP/GO complex by exciting at 370 nm. Reprinted from ref. 191, copyright 2013, with permission from American Chemical Society.

**Figure 12.** Schematic illustration of fabrication of a graphene/MIP-based sensor. (i) Drop casting of graphene derivatives; (ii) electropolymerization in the presence of the target; (iii) washing/elution of the template; (iv) incubation; (v) sensing.

**Figure 13.** DPVs of the POPDA-GNWs@IL/PPNPs-RGO-COOH-GCE sensor in a Britton-Robinson buffer solution (pH 2.0) containing CEF of different concentrations:  $1.0 \times 10^{-10}$  to  $8.9 \times 10^{-6}$  mol L<sup>-1</sup>. Inset shows the calibration curve of CEF. Reprinted from ref. 223, copyright 2014, with permission from Elsevier.

**Figure 14.** (A) Representative CVs of the pDNA-PABSA/RGO-CPE before (a) and after hybridization reaction (hybridized with  $1.0 \times 10^{-10}$  mol L<sup>-1</sup> cDNA, (b) recorded in  $0.30$  mol L<sup>-1</sup> phosphate buffer solution (pH 7.0); (B) Representative Bode plots of pDNA-

PABSA/RGO-CPE before (a) and after being hybridized with its complementary PML/RARA gene sequence of different concentrations:  $1.0 \times 10^{-16} \text{ molL}^{-1}$  (b) to  $1.0 \times 10^{-8} \text{ molL}^{-1}$  (j). (C) The plot of  $\Delta \log Z$  vs the logarithm of target sequence concentrations. Reprinted from ref. 229, copyright 2013, with permission from American Chemical Society.

**Figure 15.** Schematic representation of the preparation of the electrochemical immunosensing platform. (A) Electrodeposition of AEED, deposition of GO on the AEED-modified surface, and electrochemical reduction of GO to ERGO. (B) Attachment of poly(BPN) on the ERGO-modified surface, and detection of mouse IgG through a sandwich ELISA protocol, and electrochemical reduction of enzymatically produced BQ on the sensor surface. Reprinted from ref. 239, copyright 2012, with permission from American Chemical Society.

## References

- <sup>1</sup> A. Tuantranont. *Nanomaterials for sensing applications: Introduction and Perspectives*, in *Applications of Nanomaterials in Sensors and diagnosis*. (Ed. A.Tuantranont), Springer, Springer Series on Chemical Sensors and Biosensors vol.14, 2013, Chap. 1, p 1.
- <sup>2</sup> F. G Banica. *Nanomaterials applications in chemical sensors in Chemical Sensors and Biosensors: Fundamentals and Applications*. (Ed. F-G Banica), John Wiley & Sons Ltd, UK, 2012, Chap. 8, p 135.
- <sup>3</sup> S. Iijima, *Nature*, 1991, **354**, 56–58.
- <sup>4</sup> S. Belluci, *Phys. Status Solidi C*, 2005, **2**, 34–47.
- <sup>5</sup> M. F. Yu, O. Lourie, M. J. Dyer, K. Moloni, T. F. Kelly and R. S. Ruoff, *Science*, 2000, **287**, 637–640.
- <sup>6</sup> S. Hong and S. Myung, *Nat. Nanotechnol.*, 2007, **2**, 207–208.
- <sup>7</sup> E. Pop, D. Mann, Q. Wang, K. Goodson and H. Dai, *Nano Lett.*, 2005, **6**, 96–100.
- <sup>8</sup> E. Thostenson, C. Li, and T. Chou, *Compos. Sci. Technol.* 2005, **65**, 491–516.
- <sup>9</sup> K.S Novoselov, A. K. Geim, S. V. Morozov, D. Jiang, Y. Zhang, S. V. Dubonos, I. V. Grigorieva, A. A. Firsov, *Science* 2004, **306**, 5696, 666-669.
- <sup>10</sup> A. K. Geim, K.S. Novoselov. *Nat Mater* 2007, **6**, 183-91.
- <sup>11</sup> K. S. Novoselov, V. I. Falko, L. Colombo, P. R. Gellert, M. G. Schwab, K. Kim. *Nature* 2012, 490, 192-200.
- <sup>12</sup> A. A. Balandin, S. Ghosh, W. Bao, I. Calizo, D. Teweldebrhan, F. Miao, C. N. Lau. *Nano Lett* 2008, **8**, 8902-7.
- <sup>13</sup> C. Lee, X. Wei, J. W. Kysar, J. Hone. *Science* 2008, **321**, 385-8.
- <sup>14</sup> K. S. Novoselov, Z. Jiang, Y. Zhang, S. V. Morozov, H. L. Stormer, U. Zeitler, J. C. Maan, G. S. Boebinger, P. Kim, A. K. Geim. *Science* 2007, **315**, 1379.
- <sup>15</sup> A. S. Mayorov, R. V. Gorbachev, S. V. Morozov, L. Britnell, R. Jalil, L. A. Ponomarenko, P. Blake, K. S. Novoselov, K. Watanabe, T. Taniguchi, A. K. Geim. *Nano Lett* 2011, **11**, 2396-2399.
- <sup>16</sup> X. Du, I. Skachko, A. Barker, E. Y. Andrei. *Nature Nanotech.* 2008, **3**, 491-495.

- <sup>17</sup> J. S. Bunch, S. S. Verbridge, J. S. Alden, A. M. van der Zande, J. M. Parpia, H. G. Craidhead, P. L. McEuen. *Nano Lett.* 2008, **8**, 2458-2462.
- <sup>18</sup> R. R. Nair, P. Blake, A. N. Grigorenko, K. S. Novoselov, T. J. Booth, T. Stauber, N. M. R. Peres, A. K. Geim. *Science* 2007, **320**, 1308.
- <sup>19</sup> A.J.S. Ahammad, J.J. Lee, Md, A. Rahman. *Sensors* 2009, **9**, 2289-2319.
- <sup>20</sup> P. Yáñez-Señedo, J, M, Pingarrón, *Trends Anal. Chem.* 2010, **29**, 939-953.
- <sup>21</sup> C. Gao, Z. Guo, J-H Liu, Z-J. Huang. *Nanoscale*, 2012, **4**, 1948-1963.
- <sup>22</sup> B. Perez-Lopez, A. Merkoçi, *Microchimica Acta*, 2012, **179**, 1-16
- <sup>23</sup> S. Ghosh, S. M. Bachilo, R. A. Simonette, K. M. Beckingham and R. B. Weisman, *Science*, 2010, **330**, 567-581.
- <sup>24</sup> S. Kochmann, T. Hirsch, O. S. Wolfbeis, *Trends in Analytical Chemistry*, 2012, **39**, 87-113.
- <sup>25</sup> E. Morales-Narvaez, A. Merkoçi, *Advanced Materials*, 2012, **24**, 3298-3308.
- <sup>26</sup> M. Pumera, *Materials Today*, 2012, **14**, 308-315.
- <sup>27</sup> T. Kuila, S. Bose, P. Khanra, A. K. Mishra, N. H. Kim, J. H. Lee, *Biosensors and Bioelectronics*, 2011, **26**, 4637-4648.
- <sup>28</sup> D. A. C. Brownson, D. K. Kampouris, C. E. Banks, *Chem. Soc. Rev.* 2012, **41**, 6944-6976.
- <sup>29</sup> M. Pumera, *Chem. Soc. Rev.*, 2010, **39**, 4146-4157.
- <sup>30</sup> D. Chen, L. Tanga, J. Li, *Chem. Soc. Rev.*, 2010, **39**, 3157-3180.
- <sup>31</sup> D. A. C. Brownson, C. E. Banks, *Analyst*, 2010, **135**, 2768-2778.
- <sup>32</sup> S. Wu, Q. He, C. Tan, Y. Wang, H. Zhang, *Small*, 2013, **9**, 1160-1172
- <sup>33</sup> T. Premkumar, K. E. Geckeler, *Prog. Polym. Sci.* 2012, **37**, 515
- <sup>34</sup> Y. Shao, J. Wang, H. Wu, J. Liu, I. A. Aksay, Y. Lin. *Electroanalysis* 2010, **22**, 1027-1036.
- <sup>35</sup> X.M. Chen, G-H. Wu, Y-Q. Jiang, Y-R Wang, I. Chen, *Analyst*, 2011, **136**, 4631
- <sup>36</sup> K. R. R., W. Yang, J. J. Gooding, P. Thordarson, F. Braeta, *Electroanalysis*, 2011, **23**, 803-826.
- <sup>37</sup> M. Pumera, A. Ambrosi, A. Bonanni, E.L.K. Chang, H. L. Poh, *Trends Anal. Chem.* 2010, **29**, 954-965.
- <sup>38</sup> A. Martin, A. Escarpa, *Trends Anal. Chem.* 2014, **56**, 13-26.

- <sup>39</sup> N. G. Sahoo, S. Rana, J. W. Cho, L. Li, S. H. Chan. *Progress in Polymer Science*, 2010, **35**, 837-867.
- <sup>40</sup> P. Ma, N. A. Siddiqui, G. Marom, J. Kim. *Composites: Part A*, 2010, **41**, 1345-1367.
- <sup>41</sup> J.N. Coleman, U. Khan, Y.K. Gunko. *Adv. Mater.*, 2006, **18**, 689-706.
- <sup>42</sup> P. Pandey, M. Datta, B.D. Malhotra. *Anal. Lett.*, 2008, **41**, 159-209.
- <sup>43</sup> X. Huang, X. Qi, F. Boey, H. Zhang. *Chem. Soc. Rev.*, 2012, **41**, 666-86.
- <sup>44</sup> H. Kim, A. A. Abdala, C. W. Macosko. *Macromolecules*, 2010, **43**, 6515-30.
- <sup>45</sup> J. R. Potts, D. R. Dreyer, C. W. Bielawski, R. S. Ruoff. *Polymer*, 2011, **52**, 5-25.
- <sup>46</sup> T. Kuilla, S. Bhadra, D. Yao, N. H. Kim, S. Bose, J. H. Lee. *Prog. Polym. Sci.*, 2010, **35**, 1350-75.
- <sup>47</sup> W. Lei, W. Si, Y. Xu, Z. Gu, Q. Hao. *Microchim. Acta*. 2014, **181**, 707-722.
- <sup>48</sup> J. Prasek, J. Drbohlavova, J. Chomoucka, J. Hubalek, O. Jasek, V. Adam, R. Kizek. *J. Mater. Chem.*, 2011, 21, 15872-15884.
- <sup>49</sup> A. Szabó, C. Perri, A. Csató, G. Giordano, D. Vuono and J. B. Nagy, *Materials*, 2010, **3**, 3092-3140.
- <sup>50</sup> A. Hirsch and O. Vostrowsky, *Top. Curr. Chem.*, 2005, **245**, 93-237
- <sup>51</sup> D. Tasis, N. Tagmatarchis, A. Bianco and M. Prato, *Chem. Rev.*, 2006, **106**, 1105-1136
- <sup>52</sup> Z. Chen, X. J. Dai, P. R. Lamb, D. R. de Celis Leal, B. L. Fox, Y. Chen, J. du Plessis, M. Field and X. Wang, *Plasma Process. Polym.* 2012, **9**, 733-741.
- <sup>53</sup> S. Cui, R. Canet, A. Derre, M. Couzi and P. Delhaes, *Carbon*, 2003, **41**, 797-809
- <sup>54</sup> M. S. Strano, V. C. Moore, M. K. Miller, M. J. Allen, E. H. Aroz, C. Kittrell, R. H. Hauge and R. E. Smalley, *J. Nanosci. Nanotechnol.*, 2003, **3**, 81-86.
- <sup>55</sup> Y. Geng, M. Y. Liu, J. Li, X. M. Shi and J. K. Kim. *Composites Part A*, 2008, **39**, 1876-1883.
- <sup>56</sup> J. Yu, N. Grossiord, C. E. Koning and J. Loos. *Carbon* 2007, **45**, 618-623
- <sup>57</sup> L. Vaisman, H. D. Wagner and G. Marom. *Adv. Colloid Interface Sci.*, 2006, **128-130**, 37-46.
- <sup>58</sup> V. Georgakilas, D. Gournis, V. Tzitzios, L. Pasquato, D. M. Guldi and M. Prato *J. Mater. Chem.*, 2007, **17**, 2679-2694.
- <sup>59</sup> S.-F. Wang, L. Shen, W.-D. Zhang and Y.-J. Tong. *Biomacromolecules*, 2005, **6**, 3067-3072.
- <sup>60</sup> N. Grossiord, J. Loos, O. Regev and C. E. Koning. *Chem. Mater.*, 2006, **18**, 1089-1099.

- <sup>61</sup>B. L. Wardle, D. S. Saito, E. J. Garcia, A. J. Hart, R. G. Villoria and E. A. Verploegen, *Adv. Mater.*, 2008, **20**, 2707–2714
- <sup>62</sup>B. Vigolo, A. Penicaud, C. Coulon, C. Sauder, R. Paillet, C. Journet, P. Bernier and P. Poulin, *Science*, 2000, **290**, 1331–1334.
- <sup>63</sup>A. A. Mamedov, N. A. Kotov, M. Prato, D. M. Guldi, J. P. Wickstead and H. Hirsch, *Nat. Mater.*, 2002, **1**, 190–194.
- <sup>64</sup>H. Xia, Q. Wang, K. Li and G. H. Hu, *J. Appl. Polym. Sci.*, 2004, **93**, 378–86.
- <sup>65</sup>J. N. Coleman, U. Khan, W. J. Blau, Y. K. Gun'ko, *Carbon* 2006, **44**, 1624–52.
- <sup>66</sup>A. M. Diez-Pascual, M. Naffakh, C. Marco, G. Ellis, M. A. Gómez-Fatou, *Prog. Mater. Sci.* 2012, **57**, 1106–1190.
- <sup>67</sup>Z. Spitalsky, D. Tasis, K. Papagelis, C. Galiotis *Progr. Polym. Sci.* 2010, **35**, 357-401
- <sup>68</sup>N. G. Sahoo, S. Rana, J. W. Cho, L. Li, S. H. Chan. *Progr. Polym. Sci.* 2010, **35**, 837–867
- <sup>69</sup>M. Moniruzzaman, K. I. Winey, *Macromolecules* 2006, **39**, 5194-5205
- <sup>70</sup>A. M. Diez-Pascual, G. Martinez, M. T. Martinez, M. A. Gomez, *J. Mater. Chem.* 2010, **20**, 8247-8256.
- <sup>71</sup>A. M. Diez-Pascual, M. Naffakh, J. M. González-Domínguez, A. Ansón, Y. Martínez-Rubi, M. T. Martínez, B. Simard, M. A. Gómez, *Carbon* 2010, **48**, 3500-3511.
- <sup>72</sup>Han Z, Fina A. *Prog Polym Sci.* 2011, **36**, 914-944.
- <sup>73</sup>A. M. Diez-Pascual, M. Naffakh M. A. Gómez, C. Marco, G. Ellis, J. M. González-Domínguez, A. Ansón, M. T. Martínez, Y. Martínez-Rubi, B. Simard, B. Ashrafi. *Nanotechnology* 2009, **20**, 315707.
- <sup>74</sup>J. H. Warner, F. Schaffel, M. Rummeli, A. Bachmatiuk. Graphene: fundamentals and emergent applications. Oxford: Elsevier; 2013, Chapter 3, p. 109.
- <sup>75</sup>C. Lee, X. Wei, Kysar JW, Hone J. *Critical reviews in Solid State and Materials Science* 2010, **35**, 52-71.
- <sup>76</sup>H. J. Salavagione, *J. Mater. Chem. A* 2014, **2**, 7138
- <sup>77</sup>X. Li, W. Cai, J. An, S. Kim, J. Nah, D. Yang, R. Piner, A. Velamakanni, I. Jung, E. Tutuc, S. K. Banerjee, L. Colombo, R. S. Ruoff. *Science*, 2009, **324**, 1312-4.
- <sup>78</sup>P. Sutter. *Nat. Mater.*, 2009, **8**, 171-2.
- <sup>79</sup>M. Cai, D. Thorpe, D. H. Adamson, H. C. Schniepp, *J. Mater. Chem.*, 2012, **22**, 24992–25002.

- <sup>80</sup> G. M. Morales, P. Schifani, G. Ellis, C. Ballesteros, G. Martínez, C. Barbero C, H. Salavagione. *Carbon*, 2011, **49**, 2809-16.
- <sup>81</sup> S. Stankovich, D. A. Dikin, R. D. Piner, K. A. Kohlhaas, A. Kleinhammes, Y. Y. Jia, Y. Wu, S. T. Nguyen, R. S. Ruoff. *Carbon*, 2007, **45**, 1558-65.
- <sup>82</sup> S. Park and R. S. Ruoff, *Nat. Nanotechnol.*, 2009, **4**, 217–224.
- <sup>83</sup> M. J. McAllister, J. L. Li, D. H. Adamson, H. C. Schniepp, A. A. Abdala, J. Liu J, M. Herrera-Alonso, D. L. Milius, R. Car, R. K. Prud'homme, I. A. Aksay. *Chem. Mater.*, 2007, **19**, 4396-404.
- <sup>84</sup> S. Stankovich, D. A. Dikin, G. H. B. Dommett, K. M. Kohlhaas, E. J. Zimney, E. A. Stach, R. D. Piner, S. T. Nguyen, R. S. Ruoff, *Nature* 2006, **442**, 282.
- <sup>85</sup> T. Ramanathan, A. A. Abdala, S. Stankovich, D. A. Dikin, M. Herrera-Alonso, R. D. Piner, D. H. Adamson, H. C. Schniepp, X. Chen, R. S. Ruoff, S. T. Nguyen, I. A. Aksay, R. K. Prud'Homme, L. C. Brinson, *Nature Nanotechnology* 2008, **3**, 327.
- <sup>86</sup> G. Eda G, M. Chhowalla, *Nano Letters*, 2009, **9**, 814.
- <sup>87</sup> T. K. Das, S. Prusty. *Polym. Plast. Tech. Eng.*, 2013, **52**, 319-31.
- <sup>88</sup> H. Salavagione, G. Martínez, G. Ellis. *Macromol Rapid Commun.*, 2011, **32**, 1771-89.
- <sup>89</sup> H. Salavagione, G. Martínez, G. Ellis. *Graphene-based polymer composites*, in Physics and Applications of Graphene-Experiments. (Ed. S. Mihailov), Intech, Rijeka, Croatia, 2011, p. 169.
- <sup>90</sup> R. Verdejo, M. M. Bernal, L. J. Romasanta, M. A. Lopez-Manchado. *J. Mater. Chem.*, 2011, **21**, 3301- 3310.
- <sup>91</sup> H. Salavagione. *Innovative Strategies to Incorporate Graphene in Polymer Matrices: Advantages and Drawbacks from an Applications Viewpoint* in Innovative Graphene Technologies: Developments & Characterisation. (Ed. A. Tiwari), Smithers-Rapra, Shawbury, U.K., 2013, p.175-221.
- <sup>92</sup> K. Hu, D. D. Kulkarni, I. Choi, V, V, Tsukruk. *Prog. Polym. Sci.* 2014, in press.
- <sup>93</sup> D. R. Dreyer, S. Park, C. W. Bielawski, R. S. Ruoff, *Chemical Society Reviews*, 2010, **39**, 228.
- <sup>94</sup> X. Tian, S. Sarkar, A. Pekker, M. L. Moser, I. Kalinina, E. Bekyarova, M. E. Itkis, R. C. Haddon, *Carbon*, 2014, **72**, 82-88.
- <sup>95</sup> E. Bekyarova, S. Sarkar, F. Wang, M. E. Itkis, I. Kalinina, X. Tian, R. C Haddon. *Acc. Chem. Res.*, 2012, **45(4)**, 673–682.

- <sup>96</sup> H. J. Salavagione, G. Martínez, M. A. Gómez. *Macromolecules*, 2009, **42**, 6331-4.
- <sup>97</sup> H. J. Salavagione, G. Martínez. *Macromolecules*, 2011, **44**, 2685-2692.
- <sup>98</sup> H. Salavagione, G. Martínez, G. Ellis. *Macromol Rapid Commun.*, 2011, **32**, 1771-89
- <sup>99</sup> H. Salavagione. Innovative Strategies to Incorporate Graphene in Polymer Matrices: Advantages and Drawbacks from an Applications Viewpoint in Innovative Graphene Technologies: Developments & Characterisation.(Ed. A. Tiwari), Smithers-Rapra, Shawbury, U.K., 2013, p.175-221.
- <sup>100</sup> M. Castelain, G. Martínez, P. Merino, J. A. Martín-Gago, J. L. Segura, G. Ellis, H. J. Salavagione. *Chem. A Eur. J.*, 2012, **18**, 4965-73.
- <sup>101</sup> M. Castelaín, G. Martínez, G. Ellis, H. J. Salavagione. *Chem. Comm.*, 2013, **49**, 8967-69.
- <sup>102</sup> M. Castelaín, G. Martínez, C. Marco, G. Ellis, H. J. Salavagione, *Macromolecules*, 2013, **46**, 8980.
- <sup>103</sup> S. Shenogin, A. Bodapati, L. Xue, R. Ozisik, P. Koblinski, *Appl. Phys. Lett.* 2004, **85**, 2229
- <sup>104</sup> Y.A. Balogun, R.C. Buchanan, *Compos Sci Technol* 2010, **70**, 892–900
- <sup>105</sup> K. M. F. Shahil, A. A. Balandin, *Nano Lett.*, 2012, **12**, 861–867
- <sup>106</sup> S. M. Bachilo, M. S. Strano, C. Kittrell, R. H. Hauge, R. E. Smalley and R. B. Weisman. *Science*, 2002, **298**, 2361–2366.
- <sup>107</sup> S. Wray, M. Cope, D. Delpy, J. Wyatt and E. Reynolds. *Biochim. Biophys. Acta*, 1988, **933**, 184–192.
- <sup>108</sup> J. H. Choi and M. S. Strano. *Appl. Phys. Lett.*, 2007, **90**, 223114-223116.
- <sup>109</sup> P. W. Barone, S. Baik, D. A. Heller and M. S. Strano. *Nat. Mater.*, 2005, **4**, 86-92.
- <sup>110</sup> S. Ghosh, S. M. Bachilo, R. A. Simonette, K. M. Beckingham and R. B. Weisman. *Science*, 2010, **330**, 567-581.
- <sup>111</sup> P. W. Barone and M. S. Strano. *Angew. Chem. Int. Ed.*, 2006, **45**, 8138 –8141.
- <sup>112</sup> H. Yoon, J-H Ahn, P. W. Barone, K. Yum, R. Sharma, A. A. Boghossian, J.-H. Han and M. S. Strano. *Angew. Chem. Int. Ed.*, 2011, **50**, 1828 –1831.
- <sup>113</sup> J. G. Duque, L. Cagnet, A. N. G. Parra-Vasquez, N. Nicholas, H. K. Schmidt and M. Pasquali. *J. Am. Chem. Soc.*, 2008, **130**, 2626-2633
- <sup>114</sup> J.-H. Kim, D. A. Heller, H. Jin, P. W. Barone, C. Song, J. Zhang, L. J. Trudel, G. N. Wogan, S. R. Tannenbaum and M. S. Strano. *Nat. Chem.* 2009, **1**, 473-481

- <sup>115</sup>J. Zhang, A. A. Boghossian, P. W. Barone, J.-H. Kim, D. Lin, D. A. Heller, A. J. Hilmer, N. Nair, N. F. Reuel and M. S. Strano. *J. Am. Chem. Soc.* 2011, **133**, 567–581
- <sup>116</sup>J.-H. Kim, J.-H. Ahn, P. W. Barone, H. Jin, J. Zhang, D. A. Heller and M. S. Strano. *Angew. Chem. Int. Ed.* 2010, **49**, 1456–1459.
- <sup>117</sup>N. F. Reuel, J.-H. Ahn, J.-H. Kim, J. Zhang, A. A. Boghossian, L. Mahal and M. S. Strano. *J. Am. Chem. Soc.*, 2011, **133**, 17923–17933
- <sup>118</sup>N. Nakayama-Ratchford, S. Bangsaruntip, X. Sun, K. Welsher and H. Dai. *J. Am. Chem. Soc.*, 2007, **129**, 2448–2449
- <sup>119</sup>M. V. Kulkarni and B. B. Kale. *Sensor Actuat. B*, 2013, **187**, 407–412.
- <sup>120</sup>B. Mu, T. P. McNicholas, J. Zhang, A. J. Hilmer, Z. Jin, N. F. Reuel, J.-H. Kim, K. Yum and M. S. Strano. *J. Am. Chem. Soc.*, 2012, **134**, 17620–17627.
- <sup>121</sup>G. Dukovic, B. White, Z. Zhou, F. Wang, S. Jockusch, M. L. Steigerwald, T. F. Heinz, R. A. Friesner, N. J. Turro and L. E. Brus. *J. Am. Chem. Soc.*, 2004, **126**, 15269–15276.
- <sup>122</sup>G. Ghini, C. Trono, A. Giannetti, G. L. Puleo, L. Luconi, J. Amadou, G. Giambastiani and F. Baldini. *Sensor Actuat. B*, 2013, **179**, 163–169.
- <sup>123</sup>P. W. Barone, H. Yoon, R. Ortiz-Garcia, J. Zhang, J.-H. Ahn, J.-H. Kim and M. S. Strano. *ACS Nano*, 2009, **3**, 3869–3877.
- <sup>124</sup>J.-H. Ahn, J.-H. Kim, N. F. Reuel, P. W. Barone, A. A. Boghossian, J. Zhang, H. Yoon, A. C. Chang, A. J. Hilmer and M. S. Strano. *Nano Lett.*, 2011, **11**, 2743–2752.
- <sup>125</sup>L. Cognet, D. A. Tsyboulski, J.-D. R. Rocha, C. D. Doyle, J. M. Tour and R. B. Weisman. *Science*, 2007, **316**, 1465–1468
- <sup>126</sup>Z. Chen, S. M. Tabakman, A. P. Goodwin, M. G. Kattah, D. Daranciang, X. Wang, G. Zhang, X. Li, Z. Liu, P. J. Utz, K. Jiang, S. Fan and H. Dai, *Nat. Biotechnol.* 2008, **26**, 285–1292.
- <sup>127</sup>B. Nigović, M. Sadiković and M. Sertić, *Talanta*, 2014, **122**, 187–194.
- <sup>128</sup>H. Zhao, Q. Sheng and J. Zheng, *Microchim. Acta*, 2012, **176**, 177–184.
- <sup>129</sup>A. Babaei, M. Babazadeh and H. R. Momeni, *Int. J. Electrochem. Sci.*, 2011, **6**, 1382–1395.
- <sup>130</sup>M. Wu, W. Tang, J. Gu, Q. Wang, P. He and Y. Fang, *Am. J. Anal. Chem.*, 2013, **4**, 1–6.
- <sup>131</sup>S. Kianipour and A. Asghari, *IEEE Sens. J.*, 2013, **13**, 2690–2698.

- <sup>132</sup>F. Shahdost-fard, A. Salimi, E. Sharifi and A. Korani, *Biosens. Bioelectron.*, 2013, **48**, 100-107.
- <sup>133</sup>Y. Li, Y. Li and Y. Yang, *J. Solid. State Electrochem.*, 2012, **16**, 1133-1140.
- <sup>134</sup>X.B. Lu, J. Q. Hu, X. Yao, Z. P. Wang and J. H. Li, *Biomacromolecules*, 2006, **7**, 975-980.
- <sup>135</sup>G. C. Zhao, M. Q. Xu, J. Ma and X. W. Wei, *Electrochem. Commun.*, 2007, **9**, 920-924.
- <sup>136</sup>C. Janáky and C. Visy, *Anal. Bioanal. Chem.*, 2013, **405**, 3489-3511.
- <sup>137</sup>G. Inzelt, *Conducting Polymers*, Monographs in Electrochemistry, Springer-Verlag, Berlin Heidelberg, 2012, Chapter 2.
- <sup>138</sup>G. Xu, B. Li and X. Luo, *Sens. Actuators, B*, 2013, **176**, 69-74.
- <sup>139</sup>G. Xu, B. Li, X. Wang and X. Luo, *Microchim. Acta*, 2014, **181**, 463-469.
- <sup>140</sup>N. Jha, S. Ramaprabhu, *J. Nanosci. Nanotechnol.*, 2010, **10**, 2798-2802
- <sup>141</sup>E. Jin, X. Bian, X. Lu and C. Wang, *J. Mater. Sci.*, 2012, **47**, 4326-4331.
- <sup>142</sup>T. M. Wu and S. H. Lin, *J. Polym. Sci. Part B Polym. Phys.*, 2006, **44**, 1413-1418.
- <sup>143</sup>K. Min and Y. J. Yoo, *Talanta*, 2009, **80**, 1007-1011.
- <sup>144</sup>K. P. Lee, S. Komathi, N. J. Nam and A. I. Gopalan, *Microchem. J.*, 2010, **95**, 74-79.
- <sup>145</sup>M. Y. Hua, Y. C. Lin, R. Y. Tsai, H. C. Chen and Y. C. Liu, *Electrochim. Acta*, 2011, **56**, 9488-9495.
- <sup>146</sup>Fischer, M. J. E. *Amine Coupling Through EDC/NHS: A Practical Approach*, N. J. de Mol, M. J. E. Fischer (Eds.), *Surface Plasmon Resonance*, Methods in Molecular Biology 627, Springer, 2010, Chapter 3
- <sup>147</sup>J. Dai, G. L. Baker and M. L. Bruening, *Anal. Chem.*, 2006, **78**, 135-140.
- <sup>148</sup>J. A. Phelps, S. Morisse, M. Hindi, M. C. Degat, E. Pauthe and P. R. Van Tassel, *Langmuir*, 2011, **27**, 1123-1130.
- <sup>149</sup>C. Wang, Q. Yan, H. B. Liu, X. H. Zhou and S. J. Xiao, *Langmuir*, 2011, **27**, 12058-12068.
- <sup>150</sup>Y. Gao and I. Kyratzis, *Bioconjugate Chem.*, 2008, **19**, 1945-1950.
- <sup>151</sup>Z. G. Wang, Y. Wang, H. Xu, G. Li and Z. K. Xu, *J. Phys. Chem. C*, 2009, **113**, 2955-2960.
- <sup>152</sup>C. Dhand, S. K. Arya, M. Datta and B. D. Malhotra, *Anal. Biochem.*, 2008, **383**, 194-199.

- <sup>153</sup>A. A. Mamedov, N. A. Kotov, M. Prato, D. M. Guldi, J. P. Wicksted and A. A. Hirsch, *Nat. Mater.*, 2002, **1**, 190-194.
- <sup>154</sup>J. H. Rouse and P. T. Lillehei, *Nano Lett.*, 2003, **3**, 59-62.
- <sup>155</sup>M. Zhang, Y. Yan, K. Gong, L. Mao, Z. Guo and Y. Chen, *Langmuir*, 2004, **20**, 781-785.
- <sup>156</sup>Q. Gao, Y. Guo, J. Liu, X. Yuan, H. Qi and C. Zhang, *Bioelectrochemistry*, 2011, **81**, 109-113.
- <sup>157</sup>X. Lu, Y. Li, J. Du, X. Zhou, Z. Xue, X. Liu and Z. Wang, *Electrochim. Acta*, 2011, **56**, 7261-7266.
- <sup>158</sup>L. Agüí, C. Peña-Farfal, P. Yáñez-Sedeño and J. M. Pingarrón, *Electrochim. Acta*, 2007, **52**, 7946-7952.
- <sup>159</sup>L. Agüí, C. Peña-Farfal, P. Yáñez-Sedeño and J. M. Pingarrón, *J. M. Electroanalysis*, 2009, **21**, 386-391.
- <sup>160</sup>S. Yadav, A. Kumar and C. S. Pundir, *Anal. Biochem.*, 2011, **419**, 277-283.
- <sup>161</sup>S. Yadav, R. Devi, S. Kumari, S. Yadav and C. S. Pundir, *J. Biotechnol.*, 2011, **151**, 212-217.
- <sup>162</sup>I. Tiwari, K.P. Singh, M. Singh and C. E. Banks, *Anal. Methods*, 2012, **4**, 118-124.
- <sup>163</sup>X. Zhang, G. Lai, A. Yu and H. Zhang, *Microchim. Acta*, 2013, **180**, 437-443.
- <sup>164</sup>N. Chauhan, J. Narang, R. Rawal and C. S. Pundir, *Synthetic Met.*, 2011, **161**, 2427-2433.
- <sup>165</sup>S. Chawla, R. Rawal and C. S. Pundir, *J. Biotechnol.*, 2011, **156**, 39-45.
- <sup>166</sup>G. Xu, B. Li, X.T. Cui, L. Ling and X. Luo, *Sens. Actuators, B. Chem.*, 2013, **188**, 405-410.
- <sup>167</sup>M. Raicopol, A. Prună, C. Damian and L. Pilan, *Nanoscale. Res. Lett.*, 2013, **8**, 316-323.
- <sup>168</sup>M.D. Shirsat, C.O. Too and G. G. Wallace, *Electroanalysis*, 2008, **20**, 150-156.
- <sup>169</sup>G. Zeng, Z. Li, L. Tang, M. Wu, X. Lei, Y. Liu, C. Liu, Y. Pang and Y. Zhang, *Electrochim. Acta*, 2011, **56**, 4775-4782.
- <sup>170</sup>L. Chen, S. Xu and J. Li, *Chem. Soc. Rev.*, 2011, **40**, 2922-2942.
- <sup>171</sup>K. Haupt, *Analyst*, 2001, **126**, 747-756.
- <sup>172</sup>H.J. Chen, Z.H. Zhanga, L.J. Luo and S. Z. Yao, *Sens. Actuators, B. Chem.*, 2012, **163**, 76-83.
- <sup>173</sup>B.B. Prasad, A. Prasad and M. P. Tiwari, *Electrochim. Acta*, 2013, **102**, 400-408.

- <sup>174</sup> Y. Tong, H. Li, H. Guan, J. Zhao, S. Majeed, S. Anjum, F. Liang and G. Xu, *Biosens. Bioelectron.*, 2013, **47**, 553-558.
- <sup>175</sup> B.B. Prasad, I. Pandey, A. Srivastava, D. Kumar and M. P. Tiwari, *Sens. Actuators, B. Chem.*, 2013, **176**, 863-874.
- <sup>176</sup> B.B. Prasad, A. Srivastava and M. P. Tiwari, *Mater. Sci. Eng. C*, 2013, **33**, 4071-4080.
- <sup>177</sup> X. Kan, Y. Zhao, Z. Geng, Z. Wang and J. J. Zhu, *J. Phys. Chem. C*, 2008, **112**, 4849-4854.
- <sup>178</sup> B. Rezaei and O. Rahmanian, *Sens. Actuators, B. Chem.*, 2011, **160**, 99-104.
- <sup>179</sup> P. Liu, X. Zhang, W. Xu, C. Guo and S. Wang, *Sens. Actuators, B. Chem.*, 2012, **163**, 84-89.
- <sup>180</sup> B. Rezaei, O. Rahmanian and A. A. Ensaifi, *Microchim. Acta*, 2013, **180**, 33-39.
- <sup>181</sup> A. Afkhami, H. Ghaedi, T. Madrakian, M. Ahmadi and H. Mahmood-Kashani, *Biosens. Bioelectron.*, 2013, **44**, 34-40.
- <sup>182</sup> D. Zhang, D. Yu, W. Zhao, Q. Yang, H. Kajiura, Y. Li, T. Zhou and G. Shi, *Analyst*, 2012, **137**, 2629-2636.
- <sup>183</sup> Y. Yang, G. Fang, G. Liu, M. Pan, X. Wang, L. Kong, X. He and S. Wang, *Biosens. Bioelectron.* 2013, **47**, 475-481.
- <sup>184</sup> J. Zhang, Y. Niu, S. Li, R. Luo and C. Wang, *Sens. Actuators, B. Chem.*, 2014, **193**, 844-850.
- <sup>185</sup> K.P. Loh, Q. Bao, G. Eda, M. Chhowalla. *Nat. Chem.* , 2010, **2**, 1015 – 1024.
- <sup>186</sup> Ch. tao, S. Li, W. Lai, Y. Yeh, H. Chen, I. Chen, L. Chen, k. Chen, T. Nemoto, S. Isoda, M. Chen, T. Fujita, G. Eda, H. Yamaguchi, M. Chhowalla, Ch. Wein. *Angew. Chem. Int. Ed.*, 2012, **51**, 6662 – 6666.
- <sup>187</sup> K. H. Zhao, R. M. Kong, X. B. Zhang, H. M. Meng, W. N. Liu, W. H. Tan, G. L. Shen, R. Q. Yu, *Anal. Chem.*, 2011, **83**, 5062–.
- <sup>188</sup> L. Sheng, J. Ren, Y. Miao, J. Wang, E. Wang. *Biosensors and Bioelectronics*, 2011, **26**, 3494 – 3499.
- <sup>189</sup> R. E. Wang, Y. Zhang, J. Cai, W. Cai, T. Gao. *Curr. Med. Chem.*, 2011, **18**, 4175 – 4184.
- <sup>190</sup> Y. Wang, Z. Li, J. Wang, J. Li, Y. Lin. *Trends in Biotechnology*, 2011, **29**, 205 – 212.
- <sup>191</sup> X. J. Xing, X. G. Liu, Y. He, Y. Lin, C. L. Zhang, H. W. Tang, D. W. Pang. *Biomacromolecules*, 2013, **14**, 117-123.

- <sup>192</sup> X. J. Xing, Y. Zhou, X. G. Liu, H. W. Tang, D. W. Pang. *Analyst*, 2013, **138**, 6301-6304.
- <sup>193</sup> B. S. Gaylord, A. J. Heeger, G. C. Bazan. *Proc. Natl. Acad. Sci. USA* 2002, **99**, 10954-10957.
- <sup>194</sup> Q. H. Xu, B. S. Gaylord, S. Wang, G. C. Bazan, D. Moses, A. J. Heeger. *Proc. Natl. Acad. Sci. USA*. 2004, **101**, 11634-11639.
- <sup>195</sup> F. He, Y. Tang, M. Yu, F. Feng, L. An, H. Sun, S. Wang, Y. Li, D. Zhu, G. C. Bazan. *J. Am. Chem Soc.*, 2006, **128**, 6764 - 6765.
- <sup>196</sup> X. L. Feng, X. R. Duan, L. B. Liu, L. L. An, F. D. Feng, S. Wang. *Langmuir*, 2008, **24**, 12138-12141.
- <sup>197</sup> F. He, F. Feng, X. Duan, S. Wang, Y. Li, D. Zhu. *Anal. Chem.*, 2008, **80**, 2239 - 2243.
- <sup>198</sup> H. Zhang, L. Feng, B. Liu, C. Tong, C. Lu. *Dyes and Pigments*, 2014, **101**, 122-129.
- <sup>199</sup> H. Liu, G. Fang, H. Zhu, Ch. Li, C. Liu, Sh.Wang. *Biosensors and Bioelectronics*, 2013, **47**, 127-132.
- <sup>200</sup> Y. Zhou, Z. Qu, Y. Zeng, T. Zhou, G. Shi. *Biosensors and Bioelectronics*, 2014, **52**, 317-323.
- <sup>201</sup> Q. Huamin, F. Lulu, X. Li, L. Li, S. Min, L. Chuannan. *Carbohydrate polymers*, 2013, **92**, 394-399.
- <sup>202</sup> S. Li, S. Cao, M. J. Whitcombe, S. A. Piletsky, *Prog. Polym. Sci.*, 2014, **39**, 145-163
- <sup>203</sup> R. Schirhagl, *Anal. Chem.*, 2014, **86**, 250-261
- <sup>204</sup> E. Turiel, a. Martin-Esteban, *Analytica Chimica Acta.*, 2010, **668**, 87-99
- <sup>205</sup> R. Freeman, I. Willner. *Chem. Soc. Rev.*, 2012, **41**, 4067-4085.
- <sup>206</sup> M. F. Frasco, N. Chaniotakis. *Chem. Soc. Rev.*, 2009, **9**, 7266-7286.
- <sup>207</sup> M. Bacon, S. J. Bradley, T. Nann Particle & Particle system characterization. 2014, DOI: 10.1002/ppsc.201300252
- <sup>208</sup> X. Chen, H. Ye, W. Wang, B. Qiu, Z. Lin, G. Chen. *Electroanalysis*, 2010, **22**, 2347-2352.
- <sup>209</sup> H. J. Li, J. A. Chen, S. Han, W. X. Niu, X. Q. Liu, G. B. Xu. *Talanta*, 2009, **79**, 165-170.
- <sup>210</sup> X. Wang, X. Sun, PA. Hu, J. Zhang, L. Wang, W. Feng, S. Lei, B. Yang, W. Cao. *Adv. Func. Mater.*, 2013, **23**, 6044-6050.

- <sup>211</sup> B. Yoon, S. Lee, J. M. Kim. *Chem. Soc. Rev.*, 2009, **38**, 1958-1968.
- <sup>212</sup> K. R. Ratinac, W. Yang, J. J. Gooding, P. Thordarson and F. Braeta, *Electroanalysis*, 2011, **23**, 803-826.
- <sup>213</sup> S. Guo and S. Dong, *J. Mater. Chem.*, 2011, **21**, 18503-18516.
- <sup>214</sup> Y. Fang and E. Wang, *Chem. Commun.*, 2013, **49**, 9526-9539.
- <sup>215</sup> M. J. Whitcombe, I. Chianella, L. Larcombe, S. A. Piletsky, J. Noble, R. Porter, A. Horgan, *Chem. Soc. Rev.*, 2011, **40**, 1547-1571.
- <sup>216</sup> P. S. Sharma, M. Dabrowski, F. D'Souza, W. Kutner. *Trends Anal. Chem.*; 2013, **51**, 146.
- <sup>217</sup> C. Malitesta, E. Mazzotta, R. A. Picca, A. Poma, I. Chianella, S.A. Piletsky. *Anal. Bioanal. Chem.* 2012, **402**, 1827-1846.
- <sup>218</sup> N. M. Bergmann, N. A. Peppas, *Prog. Polym. Sci.* 2008, **33**, 271-288.
- <sup>219</sup> H. da Silva, J. G. Pacheco, J. M. C. S. Magalhães, S. Viswanathan, C. Delerue-Matos. *Biosens. Bioelect.* 2014, **52**, 56-61.
- <sup>220</sup> F. Wang, L. Zhu, J. Zhang, *Sens. Actuators, B.* 2014, **192**, 642.
- <sup>221</sup> S. Sun, M. Zhang, Y. Li, X. He, *Sensors* 2013, **13**, 5493-5506.
- <sup>222</sup> Y. Liu, L. Zhu, Z. Luo, H. Tang, *Sens. Actuators, B.* 2013, **185**, 438-444.
- <sup>223</sup> G. Yang, F. Zhao, B. Zeng, *Biosens. Bioelect.* 2014, **53**, 447-452.
- <sup>224</sup> Y. Liu, L. Zhu, Z. Luo and H. Tang, *Sens. Actuators, B.* 2012, **171**, 1151-1158.
- <sup>225</sup> Y. Mao, Y. Bao, S. Gan, F. Li, L. N. *Biosens. Bioelect.*, 2011, **28**, 291-297.
- <sup>226</sup> J. Luo, S. Jiang, R. Liu, Y. Zhang, X. Liu, *Electrochim. Acta*, 2013, **96**, 103-109.
- <sup>227</sup> Y. Bao, J. Song, Y. Mao, D. Han, F. Yang, L. Niu, A. Ivaska, *Electroanalysis*, 2011, **23**, 878-884.
- <sup>228</sup> Y. Bao, H. Yang, Y. Hu, T. Yao, S. Huang, *Electrochim. Acta*, 2011, **56**, 2676-2681.
- <sup>229</sup> T. Yang, Q. Guan, X. Guo, L. Meng, m. Du, K. Jiao, *Anal. Chem.*, 2013, **85**, 1358-1366.
- <sup>230</sup> D. Ye, L. Luo, Y. Ding, Q. Chen, X. Liu, *Analyst*, 2011, **136**, 4563-4569.
- <sup>231</sup> Z. Linting, L. Ruiyi, L. Zaijun, X. Qianfang, F. Yinjun, L. Junkang, *Sens. Actuators, B.*, 2012, **174**, 359-365.
- <sup>232</sup> L. Lu, O. Zhang, J. Xu, Y. Wen, X. Duan, H. Yu, L. Wu, T. Nie, *Sens. Actuators, B.*, 2013, **181**, 567-574.

- <sup>233</sup> C. Sanchís, H. J. Salavagione, J. Arias-Pardilla, E. Morallón, *Electrochim. Acta*, 2007, **52**, 2978–2986.
- <sup>234</sup> C. Sanchís, H. J. Salavagione, E. Morallón, *J. Electroanal. Chem.* 2008, **618**, 67–73.
- <sup>235</sup> E. Coskun, E. A. Zaragoza-Contreras, H. J. Salavagione, *Carbon* 2012, **50**, 2235
- <sup>236</sup> S. Alwarappan, K. Cissell, S. Dixit, C. Z. Li, S. Mohapatra, *J. Electroanal. Chem.*, 2012, **686**, 69-72.
- <sup>237</sup> J. Sing, P. Khanra, T. Kuila, M. Srivastava, A. Das, N. H. Kim, B. J. Jung, D. Y. Kim, S. H. Lee, D. W. Lee, D. G. Kim, J. H. Lee. *Process Biochem.*, 2013, **48**, 1724-1735.
- <sup>238</sup> H. Gong, M. Sun, R. Fan, L. Qian. *Microchim. Acta*, 2013, **180**, 295-301.
- <sup>239</sup> A.-M. J. Haque, H. Park, D. Sung, S. Jon, S.-Y. Choi, K. Kim. *Anal. Chem.* 2012, **84**, 1871-1878.
- <sup>240</sup> W. Liu, J. Xiao, C. Wang, H. Yin, H. Xie, R. Cheng *Mater. Lett.* 2013, **10**, 70-73.
- <sup>241</sup> X. Lin, Y. Ni, S. Kokot. *J. Hazard. Mater.* 2013, **260**, 508-517.
- <sup>242</sup> Z. Wang, J. Xia, X. Qiang, Y. Xia, G. Shi, F. Zhang, G. Han, L. Xia, J. Tang. *Int. J. Electrochem. Sci.*, 2013, **8**, 6941-6950.
- <sup>243</sup> S. Liu, J. Tian, L. Wang, H. Li, Y. Zhang, X. Sun. *Macromolecules*, 2010, **43**, 10078-10083.
- <sup>244</sup> M. Song, J. Xu. *Electroanalysis*, 2013, **25**, 523-530.
- <sup>245</sup> D. Sung, D. H. Shin, S. Jon. *Biosens. Bioelect.*, 2011, **26**, 3967–3972.
- <sup>246</sup> D. Yu, L. Dai *J. Phys. Chem. Lett.*, 2010, **1**, 467–470
- <sup>247</sup> V. C. Tung, L.M. Chen, M. J. Allen, J. K. Wassei, K. Nelson, R. B. Kaner, Y. Yang *Nano Lett.* 2009, **9**, 1949-1955
- <sup>248</sup> T.K. Hong, D. W. Lee, H. J. Choi, H. S. Shin, B.S. Kim, *ACS Nano* 2010, **4**, 3861–3868
- <sup>249</sup> A. Yu, P. Ramesh, X. Sun, E. Bekyarova, M. E. Itkis, R. C Haddon. *Adv. Mater.* 2008 **20**, 4740.
- <sup>250</sup> X. Xing, S. Liu, J. Yu, W. Lian and J. Huang, *Biosens. Bioelectron.*, 2012, **31**, 277-283.
- <sup>251</sup> W. Lian, S. Liu, J. Yu, J. Li, M. Cui, W. Xu, J. Huang, *Biosens. Bioelect.*, 2013, **44**, 70-76
- <sup>252</sup> H. J. Chen, Z. H. Zhang, D. Xie, R. Cai, X. Chen, Y. N. Liu, S. Z. Yao. *Electroanalysis*, 2012, **24**, 2109

- 
- <sup>253</sup> Y. Liu, S. Yang, W. Niu, *Colloids and Surfaces B: Biointerfaces* 2013, **108**, 266-270
- <sup>254</sup> Y. S. Fang, H. Y. Wang, L. S. Wang, J. F. Wang, *Biosens. Bioelectron.*, 2014, **51**, 310
- <sup>255</sup> Y. Liu, Y. Liu, H. Feng, Y. Wu, L. Joshi, X. Zeng, J. Li, *Biosens. Bioelectron.* 2012, **35**, 63-68
- <sup>256</sup> C. H. Lien, K. H. Chang, C. C. Hu, D. S. H. Wang, *J. Electrochem Soc.* 2013, **160**, B107-B112.
- <sup>257</sup> F. Li, H. Pei, L. Wang, J. Lu, J. Gao, B. Jiang, X. Zhao, C. Fan, *Adv. Funct. Mater.* 2013, **23**, 4140-4148.
- <sup>258</sup> S. H. Xie, Y. Y. Liu and J. Y. Li, *Appl. Phys. Lett.* 2008, **92**, 243121
- <sup>259</sup> C.E. Banks, T.J. Davies, G.G. Wildgoose, R.G. Compton. *Chem. Commun.* 2005, 829–841
- <sup>260</sup> C. E. Banks, R. G. Compton, *Analyst* 2005, **130**, 1232–1239.
- <sup>261</sup> C. E. Banks, R. R. Moore, T. J. Davies, R. G. Compton, *Chem. Commun.* 2004, **16**, 1804–1805.
- <sup>262</sup> Y. Shao, J. Wang, H. Wu, J. Liu, I. A. Aksay, Y. Lin, *Electroanalysis*, 2010, **22**, 1027-1036.
- <sup>263</sup> S. Alwarappan, A. Erdem, C. Liu, C. Z. Li, *J. Phys. Chem. C* 2009, **113**, 8853.
- <sup>264</sup> Y. Wang, Y. M. Li, L. H. Tang, J. Lu, J. H. Li, *Electrochem. Commun.* 2009, **11**, 889

**Table 1.** Optical sensors based on polymer/carbon nanotubes composites.

Polymer	Nanofiller type	Processing method	Polymer function	Analyte	Detection method	Linear range (mol L <sup>-1</sup> )	LOD (mol L <sup>-1</sup> )	Ref.
Phenoxy-DEX	SWCNT	Solution mixing	Wrap the CNTs and prevent their aggregation	Glucose	NIR fluorescence	$3.8 \times 10^{-3} - 1.1 \times 10^{-2}$	-	111
Carboxylated PVA	SWCNT	Solution mixing	Wrap the CNTs. Enable allosterically controlled optical transduction	Glucose	NIR fluorescence	$2.5 \times 10^{-3} - 1 \times 10^{-2}$	-	112
PVP	SBDS wrapped-SWCNT	In situ polymerization	Wrap the CNTs and prevent their aggregation	Protons (H <sup>+</sup> )	NIR fluorescence	$10^{-1} - 10^{-6}$	-	113
DAP-functionalized dextran	SWCNT	Solution mixing/dialysis	Wrap the CNTs. Improve selectivity	NO	NIR fluorescence	$10^{-6} - 10^{-7}$	$7 \times 10^{-8}$ <sup>a</sup>	114
PVA	SWCNT	Solution mixing/dialysis	Wrap the CNTs. Improve selectivity	NADH L-ascorbic acid Melatonin	NIR fluorescence	-	-	115
PLPEG-COOH	SWCNT	Solution mixing	Wrap the CNTs. Improve selectivity and sensitivity	ATP	NIR fluorescence	-	$2.4 \times 10^{-7}$	116
CS hydrogel	SWCNT	Solution mixing/automated printing method	Wrap the CNTs. Act as matrix and immobilization support	Glyco-protein	NIR fluorescence	-	$2 \times 10^{-6}$ <sup>b</sup>	117

Table 1. (Continued)

Polymer	Nanofiller type	Processing method	Polymer function	Analyte	Detection method	Linear range (mol L <sup>-1</sup> )	LOD (mol L <sup>-1</sup> )	Ref.
Fluo-PEG	SWCNT	Solution mixing	Wrap the CNTs. Impart solubility and fluorescence	Protons (H <sup>+</sup> )	UV/Vis fluorescence	2.0x10 <sup>-6</sup> -3.2x10 <sup>-9</sup>	-	118
PANI	MWCNT-COOH	In situ polymerization	Wrap the CNTs. Impart solubility. Allow colorimetric detection	Protons (H <sup>+</sup> )	UV/Vis fluorescence/colorimetric	1x10 <sup>-1</sup> -1x10 <sup>-12</sup>	-	119
PBA-PPEG8	SWCNT	Solution mixing	Wrap the CNTs. Impart solubility and fluorescence	Saccharide	UV/Vis/NIR fluorescence	-	1x10 <sup>-2</sup>	120
Fluo-PEG	MWCNT-COOH	In situ polymerization	Covalently graft the CNTs. Provide solubility and fluorescence	Protons (H <sup>+</sup> )	UV/Vis fluorescence	1.6x10 <sup>-8</sup> -5x10 <sup>-6</sup>	-	122
PVA hydrogel	SWCNT	Solution mixing/ Gelation via crosslinking	Matrix. Induce solvatochromic shift	Glucose	NIR fluorescence	-	-	123
NTA-grafted to chitosan	SWCNT	Ultrasonication/ solution casting/ cross-linking	Matrix. Improve selectivity	His-tag Protein	NIR fluorescence	1x10 <sup>-5</sup> - 1x10 <sup>-7</sup>	1x10 <sup>-11</sup>	124

Table 1. (Continued )

Polymer	Nanofiller type	Processing method	Polymer function	Analyte	Detection method	Linear range (mol L <sup>-1</sup> )	LOD (mol L <sup>-1</sup> )	Ref.
Agarose gel	SDBS wrapped-SWCNT	Solution mixing/ freeze gelation	Immobilization support	Protons (H <sup>+</sup> ) OH <sup>-</sup> R-N <sub>2</sub> <sup>+</sup> X <sup>-</sup>	NIR fluorescence	-	-	125
PEG-COOH	DSPE-3PEO-functionalized SWCNT	solution mixing/ filtration	Immobilization support	anti-HSA IgG protein	UV/Vis fluorescence SERS	1x10 <sup>-9</sup> -1x10 <sup>-14</sup>	1x10 <sup>-15</sup>	126

<sup>a</sup>concentration at three times the noise value for a typical experiment with a signal-to-noise ratio of seven; <sup>b</sup>units in g

**Table 2.** Electrochemical sensors based on polymer/carbon nanotubes composites.

Polymer	Nanofiller type	Processing method	Polymer function	Composite electrode	Analyte	Detection method	Linear range (mol L <sup>-1</sup> )	LOD <sup>a</sup> (mol L <sup>-1</sup> )	Ref.
Nafion	MWCNT-COOH	Mixing	Enhancement electrocatalytic activity and adsorption. Wrapping	MWCNT-Nafion/GCE	Ondasetron Morphine	SWV	1.0x10 <sup>-7</sup> -5.0x10 <sup>-6</sup> 1.0x10 <sup>-7</sup> -4.0x10 <sup>-6</sup>	3.1x10 <sup>-8</sup> 3.2x10 <sup>-8</sup>	127
PS	MWCNT	Mixing	Increase stability of the enzyme and the electrode selectivity. Wrapping	Nafion-HRP/ PS-MWCNT/Au	H <sub>2</sub> O <sub>2</sub>	Chronoamperometry	5.0x10 <sup>-7</sup> -8.2x10 <sup>-4</sup>	1.6x10 <sup>-7</sup>	128
CS	MWCNT	Mixing	Antifouling Efficient electron transfer Wrapping	MWCNT-CS/GCE	Dopamine Morphine	DPV	1.0x10 <sup>-6</sup> -2.1x10 <sup>-4</sup> 2x10 <sup>-6</sup> -1.0x10 <sup>-4</sup>	1.9x10 <sup>-7</sup> 2.4x10 <sup>-7</sup>	129
CS	MWCNT	Mixing	Enhancement adsorption of analyte. Wrapping	MWCNT-CS/GCE	Sudan I	DPV	1.0x10 <sup>-7</sup> -1.0x10 <sup>-6</sup>	3.0x10 <sup>-8</sup>	130
CS	MWCNT	Mixing	Antifouling Wrapping	IL-MWCNT-CS/GCE	Ascorbic acid Uric acid Acetaminophen Mefenamicacid	DPV	4.0x10 <sup>-5</sup> - 4.0x10 <sup>-3</sup> 2.0x10 <sup>-6</sup> - 4.5x10 <sup>-4</sup> 1.0x10 <sup>-6</sup> - 4.0x10 <sup>-4</sup> 2.0x10 <sup>-6</sup> - 6.5x10 <sup>-4</sup>	4.1x10 <sup>-6</sup> 3.4x10 <sup>-7</sup> 2.4x10 <sup>-7</sup> 1.2x10 <sup>-6</sup>	131
CS	MWCNT	Mixing	Strong dispersion ability of the IL-CS film Wrapping	MWCNT-IL-CS/GCE	Adenosine	DPV	2.5 10 <sup>-10</sup> - 2.5 10 <sup>-9</sup> 1.0 10 <sup>-8</sup> - 5.0 10 <sup>-8</sup> 5.0 10 <sup>-8</sup> - 4.0 10 <sup>-7</sup>	1.5 10 <sup>-10</sup>	132
CS	MWCNT	Mixing	Biocompatibility and better microenvironment for Hb Wrapping	CS-MWCNT/Hb-AgNPs/GCE	H <sub>2</sub> O <sub>2</sub>	Chronoamperometry	6.2x10 <sup>-6</sup> -9.3x10 <sup>-5</sup>	3.5x10 <sup>-7</sup>	133
PEDOT	MWCNT-COOH	Mixing Polymerization <i>in situ</i> by an oxidant	Enhancement of electrocatalytic activity	PEDOT-MWCNT/CPE	HQ	DPV	1.1 10 <sup>-6</sup> - 1.25 10 <sup>-4</sup>	3.0 10 <sup>-7</sup>	138

Table 2. (Continued)

Polymer	Nanofiller type	Processing method	Polymer function	Composite electrode	Analyte	Detection method	Linear range (mol L <sup>-1</sup> )	LOD <sup>a</sup> (mol L <sup>-1</sup> )	Ref.
PEDOT	MWCNT-COOH	Mixing Polymerization <i>in situ</i> by an oxidant	Enhancement of the electrocatalytic activity	PEDOT-MWCNT/CPE	Nitrobenzene	Chronoamperometry	2.5 10 <sup>-7</sup> - 4.3 10 <sup>-5</sup>	8.3 10 <sup>-8</sup>	139
PPy	MWCNT	Mixing Polymerization <i>in situ</i> by an oxidant	Coating	ACE/PPy-MWCNT/GCE	Paraoxon	Amperometry	3.0x10 <sup>-9</sup> -7.0x10 <sup>-9</sup>	3.0x10 <sup>-9</sup>	140
PPy	MWCNT	Mixing Polymerization <i>in situ</i> by an oxidant	Provides the formation of PB nanoparticles Nanofibers	MWCNT-PPy-PB/GCE	H <sub>2</sub> O <sub>2</sub>	Chronoamperometry	4.0x10 <sup>-6</sup> -5.2x10 <sup>-4</sup>	8.0x10 <sup>-8</sup>	141
PPy	SWCNT-COOH	Mixing Polymerization <i>in situ</i> by an oxidant	Increases the amount of enzyme loading by the large specific surface area Coating	Ty-SWCNT-PPy	Dopamine	Chronoamperometry	5.0x10 <sup>-6</sup> - 5.0x10 <sup>-5</sup>	5.0x10 <sup>-6</sup>	143
SPANI	MWCNT-NH <sub>2</sub>	Mixing Polymerization <i>in situ</i>	Increases the amount of enzyme Enhancement of charge transport Grafting	GOD-(SPANI-NW)-MWNT/Pt	Glucose	Chronoamperometry	-	1.1x10 <sup>-7</sup>	144
PANI	MWCNT-COOH	Mixing	Enhancement of the conductivity Enhancement of the electrocatalytic activity and adsorption Coating	HRP/PANI-SWCNT/Au	H <sub>2</sub> O <sub>2</sub>	Chronoamperometry	8.6x10 <sup>-5</sup> -1.0x10 <sup>-2</sup>	8.6x10 <sup>-5</sup>	145
PANI	MWCNT-COOH	Electrophoretic	Enhancement of charge transport Wrapping	ChOX/PANI-SWCNT/ITO	Cholesterol	LSV	1.3x10 <sup>-3</sup> -1.3x10 <sup>-2</sup>	-	152
PVI-Os (Nafion)	SWCNT	Electrodeposition	Enhancement of electrocatalytic current LBL	[GOD/SWCNT-PVI-Os] <sub>n</sub> /SPCE	Glucose	Chronoamperometry	2.0x10 <sup>-4</sup> -7.5x10 <sup>-3</sup>	1.0x10 <sup>-4</sup>	156
PPy	SWCNT	Polymerization <i>in situ</i> by an oxidant	LBL	PPy-AuNPs-SWCNT/Au	Epinephrine	DPV	4.0x10 <sup>-9</sup> -1.0x10 <sup>-7</sup>	2.0x10 <sup>-9</sup>	157

Table 2. (Continued)

Polymer	Nanofiller type	Processing method	Polymer function	Composite electrode	Analyte	Detection method	Linear range (mol L <sup>-1</sup> )	LOD <sup>a</sup> (mol L <sup>-1</sup> )	Ref.
P3MT (Nafion)	MWCNT	Electropolymerization	Improvement of oxidation current (Wrapping)	P3MT-MWCNT-(Nafion)/GCE	NADH Cytochrome c FAD	Chronoamperometry	5.0x10 <sup>-7</sup> -2.0x10 <sup>-5</sup> 1.0x10 <sup>-7</sup> -4.0x10 <sup>-5</sup> -	1.7x10 <sup>-7</sup> 3.0x10 <sup>-8</sup> -	158
P3MT (Nafion)	MWCNT	Electropolymerization	Improvement of oxidation current (Wrapping)	LDH-MWCNT-(Nafion)- P3MT/GCE	Lactate	Chronoamperometry	1.0x10 <sup>-6</sup> -5.0x10 <sup>-4</sup>	5.6x10 <sup>-7</sup>	159
PANI	MWCNT	Electropolymerization	Increases the amount of enzyme loading by the large specific surface area	enzyme-MWCNT-PANI/Pt	Creatinine	Amperometry	1.0x10 <sup>-5</sup> -7.5x10 <sup>-4</sup>	1.0x10 <sup>-7</sup>	160
PANI	MWCNT-COOH	Electropolymerization	Increases the amount of enzyme loading by the large specific surface	OXOX-MWCNT-PANI/Pt	Oxalate	Amperometry	8.4x10 <sup>-6</sup> -27.2x10 <sup>-4</sup>	3.0x10 <sup>-6</sup>	161
PANI PAA (Nafion)	MWCNT	PANI Electropolymerization	Enhancement of the electrocatalytic activity Coating (Wrapping)	PANI-PAA-(Nafion-MWCNT)/Pt	Ascorbic acid	DPV	1.0x10 <sup>-6</sup> -1.0x10 <sup>-3</sup>	2.5x10 <sup>-7</sup>	162
PANI	SWCNT-COOH	Electropolymerization	Enhancement of the electrocatalytic activity	SiW12-SWCNT-PANI/CGE	Ascorbic acid	Chronoamperometry	1.0x10 <sup>-6</sup> -1.0x10 <sup>-5</sup> 1.0x10 <sup>-5</sup> -9.0x10 <sup>-3</sup>	5.1x10 <sup>-7</sup>	163
PANI	MWCNT-COOH	Electropolymerization	Enhancement of the absorption of CuNPs on cMWCNT	CuNPs-cMWCNT-PANI/Au	Ascorbic acid	LSV	5.0x10 <sup>-6</sup> -6.0x10 <sup>-4</sup>	1.0x10 <sup>-6</sup>	164
PANI (CS)	MWCNT-COOH	Electropolymerization	Enhancement of the absorption of CuNPs on cMWCNT (Promoting the union of enzyme)	Lac-CuNPs-CS-cMWCNT-PANI/Au	Polyphenols (Guaiacol)	CV	1.0x10 <sup>-6</sup> -5.0x10 <sup>-4</sup> (for GUA)	1.56x10 <sup>-7</sup> (for GUA)	165

Table 2. (Continued)

Polymer	Nanofiller type	Processing method	Polymer function	Composite electrode	Analyte	Detection method	Linear range (mol L <sup>-1</sup> )	LOD <sup>a</sup> (mol L <sup>-1</sup> )	Ref.
PEDOT	MWCNT-COOH	Electropolymerization	Enhancement of the electrocatalytic properties. Selectivity Wrapping	PEDOT-MWCNT/CPE	Dopamine	DPV	1.0x10 <sup>-7</sup> -2.0x10 <sup>-5</sup>	2.0x10 <sup>-8</sup>	166
PPy	SWCNT-PhSO <sub>3</sub> <sup>-</sup>	Electropolymerization	Wrapping	PPy/GOD/SWCNT-PhSO <sub>3</sub> <sup>-</sup> /PB/Pt	Glucose	Chronoamperometry	2.0x10 <sup>-5</sup> -6.0x10 <sup>-3</sup>	1.0x10 <sup>-5</sup>	167
PPy	SWCNT	Electropolymerization	Increasing the amount of the SWCNTs on Pt coated PVDF Enhancement of the immobilization of enzyme LBL	GOD-[SWCNT-PPy] <sub>n</sub> /Pt(PVDF)	Glucose	Chronoamperometry	1.0x10 <sup>-3</sup> -5.0x10 <sup>-2</sup>	-	168
poly (1,5-naphthalene diamine)	MWCNT-COOH	Electropolymerization	Improvement of the electrode stability, sensitivity and selectivity	poly (1,5-naphthalenediamine)-(CR-MWCNT)-GCE	DNA (CDH gene)	Chronoamperometry	5.0x10 <sup>-15</sup> -1.0x10 <sup>-10</sup>	1.2x10 <sup>-16</sup>	169
PPy (CS)	MWCNT-COCl	MIP by electropolymerization	Recognition (Promotes the connection between MNPs and MWCNTs) Entrapment of the protein.	PPy/MNP-CS-MWCNT/CPE	BSA	DPV	1.0x10 <sup>-10</sup> -1.0x10 <sup>-4</sup> <sup>b</sup>	2.8x10 <sup>-11</sup> <sup>b</sup>	172
Poly-FUAA	MWCNT-COOH	MIP by electropolymerization	Recognition. Enhance the electron transport	FUAA/ MWCNT/PGE	GABA	DPASV	0.75-205.19 <sup>c</sup>	0.28 <sup>c</sup>	173
Chitin	MWCNT	MIP by cross-linker with TDI	Recognition. Increase in the response current. (Wrapping)	Chitin-Cholesterol/MWCNT/CCE	Cholesterol	LSV	1.0x10 <sup>-8</sup> -3.0x10 <sup>-7</sup>	1.0x10 <sup>-9</sup>	174

Table 2. (Continued)

Polymer	Nanofiller type	Processing method	Polymer function	Composite electrode	Analyte	Detection method	Linear range (mol L <sup>-1</sup> )	LOD <sup>a</sup> (mol L <sup>-1</sup> )	Ref.
PolyBz	MWCNT-COOH	MIP by electropolymerization	Recognition. Increase surface area and improve electron transfer. Favour enantio-selective discrimination (Wrapping)	PolyBz/MWCNT/PGE	D- or L-methionine	DPCSV	11.7 -206.3 <sup>c,d</sup>	2.9 <sup>c,d</sup>	175
PolyNAPD	MWCNT	MIP by “surface-grafting from”	Recognition. Favour enantio-selective discrimination	NAPD/CHPA-TiNP-MWCNT/PGE	D- or L-aspartic acid	DPCSV	9.98-532.72 <sup>c,e</sup>	1.73 <sup>c</sup>	176
poly(MAA-co-TRIM)	MWCNT-CH=CH <sub>2</sub>	MIP by “grafting to”	Recognition. Improve the adsorption dynamics and the analyte selectivity	MAA-TRIM/MWCNT/GCE	Dopamine	Chronoamperometry	5.0x10 <sup>-7</sup> -2.0x10 <sup>-4</sup>	-	177
PolyMAA	MWCNT-COOH	MIP by cross-linker with EGDMA	Recognition. Improve electrocatalytic activity and selectivity	PolyMAA/MWCNT/GCE	Allopurinol	Chronoamperometry	1.0x10 <sup>-8</sup> -1.0x10 <sup>-6</sup>	6.88x10 <sup>-9</sup>	178
PoPD	SWCNT	MIP by electropolymerization	Recognition. Improve the affinity for the analyte.	PoPD/SWCNT/GCE	Brucine	LSV	6.2x10 <sup>-7</sup> -1.2x10 <sup>-5</sup>	2.1x10 <sup>-7</sup>	179
PoPD	MWCNT-COOH	MIP by electropolymerization	Recognition. Improve the adsorption dynamics and the analyte selectivity	AuNP/PoPD/MWCNT/GCE	Lorazepam	SWV	5.0x10 <sup>-10</sup> -1.0x10 <sup>-9</sup> 1.0x10 <sup>-9</sup> -1.0x10 <sup>-8</sup>	2.0x10 <sup>-10</sup>	180
PAIHP	MWCNT	MIP by cross-linker with EGDMA	Recognition. Improve sensitivity.	Nano-MIP/MWCNT/CPE	Tramadol	SWV	1.0x10 <sup>-8</sup> -2.0x10 <sup>-5</sup>	4.0x10 <sup>-9</sup>	181

Table 2. (Continued)

Polymer	Nanofiller type	Processing method	Polymer function	Composite electrode	Analyte	Detection method	Linear range (mol L <sup>-1</sup> )	LOD <sup>a</sup> (mol L <sup>-1</sup> )	Ref.
PAA	MWCNT-CH=CH <sub>2</sub>	MIP by cross-linker with EGDMA	Recognition. Improve selectivity and association/dissociation kinetics	PAA/MWCNT/GCE	Parathion-methyl	DPV	2.0x10 <sup>-7</sup> -1.0x10 <sup>-5</sup>	6.7x10 <sup>-8</sup>	165
APTES (functional monomer) (CS)	MWCNT-COOH	MIP by electropolymerization and cross-linker with TEOS	Recognition (Enhancement of charge transport. Enable the preparation of a homogeneous MIP sol-gel film. Wrapping)	APTES/MWNT-CS/GCE	QCA	DPV	2.0x10 <sup>-6</sup> -1.0x10 <sup>-3</sup>	4.44x10 <sup>-7</sup>	166
APTES (functional monomer) PTMS (functional comonomer) (Nafion)	MWCNT-COOH	MIP by electropolymerization and cross-linker with TEOS	Recognition. Enable the preparation of a homogeneous MIP sol-gel film. Enhancement of the electrochemical signal (Wrapping)	APTES-PTM(sol-gel)/MWNT-NF/GCE	2-nonylphenol	DPV	2.0x10 <sup>-7</sup> -3.6x10 <sup>-4</sup>	6.0x10 <sup>-8</sup>	167

<sup>a</sup> 3 S/N; <sup>b</sup> g mL<sup>-1</sup>; <sup>c</sup> ng mL<sup>-1</sup>; <sup>d</sup> for L-methionine; <sup>e</sup> for L-aspartic acid

**Table 3.** Optical sensors based on polymer/graphene composites.

Polymer	Nanofiller type	Processing method	Polymer Function	Analyte	Detection method	Linear range (mol L <sup>-1</sup> )	LOD (mol L <sup>-1</sup> )	Ref.
PVP	GO	Polymer coating	Prevent adsorption of target onto GO	Ochratoxin A	Fluorescence	5x10 <sup>-8</sup> -5x10 <sup>-7</sup>	1.87x10 <sup>-8</sup>	188
PFP (CCP)	GO	Solution mixing	Fluorescence amplification	DNA	Fluorescence	-	4x10 <sup>-11</sup>	191
PFP (CCP)	GO	Solution mixing	Fluorescence amplification	K <sup>+</sup>	Fluorescence	-	3.03x10 <sup>-6</sup>	192
PPV	GO	Ion exchange and in situ polymerization	Encapsulated in MSNs to maintain fluorescence	TNT	Fluorescence	-	1.3x10 <sup>-7</sup>	198
MIP <sup>a</sup>	GO/QDs/IL	Solution polymerization	Improve selectivity	Vitamin E	Fluorescence	2.3x10 <sup>-8</sup> -2x10 <sup>-4</sup>	3.5x10 <sup>-9</sup>	199
MIP <sup>b</sup>	GQDs	Sol-gel polymerization	Improve selectivity	Paranitrophenol	Fluorescence	2x10 <sup>-2</sup> -3x10 <sup>-3c</sup>	9x10 <sup>-6c</sup>	200
MIP <sup>a</sup>	Chitosan/GO	Solution polymerization	Improve selectivity	Sulfamethoxazole	Chemiluminescence	1x10 <sup>-7</sup> -2.3x10 <sup>-3</sup>	2.9x10 <sup>-8</sup>	201
Nafion	RGO/GOD	Solution mixing	Modification of electrodes	Glucose	Electro-chemiluminescence	2x10 <sup>-6</sup> -1x10 <sup>-4</sup>	1x10 <sup>-6</sup>	208
Nafion	RGO	Solution mixing	Modification of electrodes	Oxalate	Electro-chemiluminescence	1x10 <sup>-7</sup> -1x10 <sup>-4</sup>	5x10 <sup>-8</sup>	209
PDA	GS	UV Polymerization	Chromatic change	VOC	Colorimetric	-	-	210

<sup>a</sup>MIP composition: AA/EDGMA/AIBN ; <sup>b</sup>MIP composition: APTS/TEOS; <sup>c</sup>Units in g.L<sup>-1</sup>

**Table 4.** Electrochemical sensors based on polymer/graphene composites.

Polymer	Graphene derivative	Composite electrode	Polymer function	Analyte	Detection method	Linear range (mol L <sup>-1</sup> )	LOD (mol L <sup>-1</sup> )	Ref.
PPy	GO	PPy-GO-GCE	MIP, Recognition	Trimethoprim	SWV	1.0x10 <sup>-6</sup> -1.0x10 <sup>-4</sup>	1.3x10 <sup>-7</sup>	219
PPy	RGO	PPy-RGO/AuNPs-GCE	MIP, Recognition	Levofloxacin	CV, DPV	1.0x10 <sup>-6</sup> -1.0x10 <sup>-4</sup>	5.3x10 <sup>-7</sup>	220
PPy	GO	PPy-GO-GCE	MIP, Recognition	Quercetin	DPV	6.0x10 <sup>-7</sup> -1.5x10 <sup>-5</sup>	4.8x10 <sup>-8</sup>	221
POPDA	RGO	POPDA-RGO-GCE	MIP, Recognition	Chlorotetracycline	CV, DPV	1.0x10 <sup>-5</sup> -5.0x10 <sup>-4</sup>	-	222
POPDA	RGO-COOH	POPDA-GNWs@IL/PPNPs-RGO-COOH-GCE	MIP, Recognition	Cefotaxime	DPV	3.9x10 <sup>-9</sup> -8.9x10 <sup>-6</sup>	1.0x10 <sup>-10</sup>	223

Table 4.(Continued)

Polymer	Graphene derivative	Composite electrode	Polymer function	Analyte	Detection method	Linear range (mol L <sup>-1</sup> )	LOD (mol L <sup>-1</sup> )	Ref.
POPDA	GO	POPDA/GO-GCE	MIP, Recognition	2,4-dinitrophenol	DPV	1.0x10 <sup>6</sup> -1.5 x10 <sup>-4</sup>	-	224
P(MMA-co-EGDMA)	GSCR	GSCR/ P(MMA-co-EGDMA)-GCE	MIP, Recognition	Dopamine	LSV	1.0x10 <sup>-7</sup> -8.3x10 <sup>-4</sup>	-	225
PANI	PSS-GS	PANI/PSS-GS-GCE	Signal transduction	Ascorbic acid	CV	1.0x10 <sup>-4</sup> -1.0x10 <sup>-3</sup>	5.0x10 <sup>-6</sup>	226
PANI	GO	PANI/GO-GCE	Electrocatalyst	Ascorbic acid Dopamine Uric acid	CV	1.5x10 <sup>-4</sup> -1.05x10 <sup>-3</sup> 1.0x10 <sup>-6</sup> -1.4x10 <sup>-5</sup> 3.0x10 <sup>-6</sup> -2.6x10 <sup>-5</sup>	-	227
PANI <sub>w</sub>	GO	ssDNA-PANI <sub>w</sub> -GO-GCE	Signal transduction amplification, binding site for ssDNA probe	DNA	DPV	2.12x10 <sup>-6</sup> -2.12x10 <sup>-12</sup>	3.23x10 <sup>-13</sup>	228
PABSA	RGO	pDNA-PABSA/RGO-CPE	Signal transduction, water capability	DNA	EIS	1.0x10 <sup>-8</sup> -1.0x10 <sup>-16</sup>	3.7x10 <sup>-17</sup>	229

Table 4.(Continued)

Polymer	Graphene derivative	Composite electrode	Polymer function	Analyte	Detection method	Linear range (mol L <sup>-1</sup> )	LOD (mol L <sup>-1</sup> )	Ref.
PPy	RGO	PPy/RGO/CS-GCE	Signal generation	NO <sub>2</sub> <sup>-</sup>	Chronoamperometry	5.0x10 <sup>-7</sup> -7.22x10 <sup>-4</sup>	1.0x10 <sup>-7</sup>	230
PDPB	RGO	IL/ AntB <sub>1</sub> /Au/PDPB/RGO -Au	Sensor stabilization	Aflatoxin B <sub>1</sub>	EIS	3.0x10 <sup>-15</sup> -3.2x10 <sup>-13</sup>	1.0x10 <sup>-15</sup>	231
PEDOT	RGO	AO/PEDOT/RGO-GCE	Bio-compatibilization signal transduction	Ascorbic acid	Chronoamperometry	5.0x10 <sup>-6</sup> -4.8x10 <sup>-4</sup>	2.0x10 <sup>-6</sup>	232
CS	RGO	CMG-GCE	Bio-compatibilization	DNA	CV	-	-	236
CS PEEK	SPG	GOD/SPG/AuNPs/CS-ITO	Bio-compatibilization Water dispersion ability	Glucose	CV	5.0x10 <sup>-4</sup> -2.22x10 <sup>-2</sup>	5.1x10 <sup>-4</sup>	237
CS	GO	GO/PB/CS-GCE	-	H <sub>2</sub> O <sub>2</sub>	Chronoamperometry	1.0x10 <sup>-6</sup> -1.0x10 <sup>-3</sup>	1.0x10 <sup>-6</sup>	238

Table 4.(Continued)

Polymer	Graphene derivative	Composite electrode	Polymer function	Analyte	Detection method	Linear range (mol L <sup>-1</sup> )	LOD (mol L <sup>-1</sup> )	Ref.
PBPN	RGO	Anti-mouse IgG/PBPN/RGO-ITO	Immobilization to the electrode, protein repulsion, bioconjugation	Mouse IgG	CV	1.0x10 <sup>-13</sup> -1.0x10 <sup>-9</sup> <sup>a</sup>	1.0x10 <sup>-13</sup> <sup>a</sup>	239
PS	RGO	PS/RGO-GCE	Solubility for electrode preparation	Dopamine	DPV	5.0x10 <sup>-6</sup> -1.0x10 <sup>-4</sup>	-	240
P(ACBK) Nafion	GO	P(ACBK)/GO/Nafion-GCE	Electrocatalytic activity (PACBK) crosslinking agent to fix GO and GCE (Nafion)	β-agonists	LSV	1.0x10 <sup>-9</sup> -3.6x10 <sup>-8</sup> <sup>a</sup>	5.8x10 <sup>-10</sup> to 1.46x 10 <sup>-9</sup> <sup>a,b</sup>	241
PAA	EG	CuNPs/PAA/G-GCE	Solubilizing agent and chelating of Cu <sup>2+</sup> for CuNPs	Glucose	Chronoamperometry	3.0x10 <sup>-7</sup> -6.0x10 <sup>-4</sup>	8.0x10 <sup>-8</sup>	242
PQ11	RGO	Ag/RGO-GCE	Stabilize graphene in water Reducer for AgNPs formation	H <sub>2</sub> O <sub>2</sub>	CV	1.0x10 <sup>-4</sup> -2.0x10 <sup>-2</sup>	2.8x10 <sup>-5</sup>	243
PEI	GO	GO-COOH/PEI	Enhance electrocatalytic activity	Ammonia	CV	2.7x10 <sup>-5</sup> -1.2x10 <sup>-4</sup>	2.26x10 <sup>-5</sup>	244

<sup>a</sup> Values in g.mL<sup>-1</sup>; <sup>b</sup> Depending on the specific β-agonist

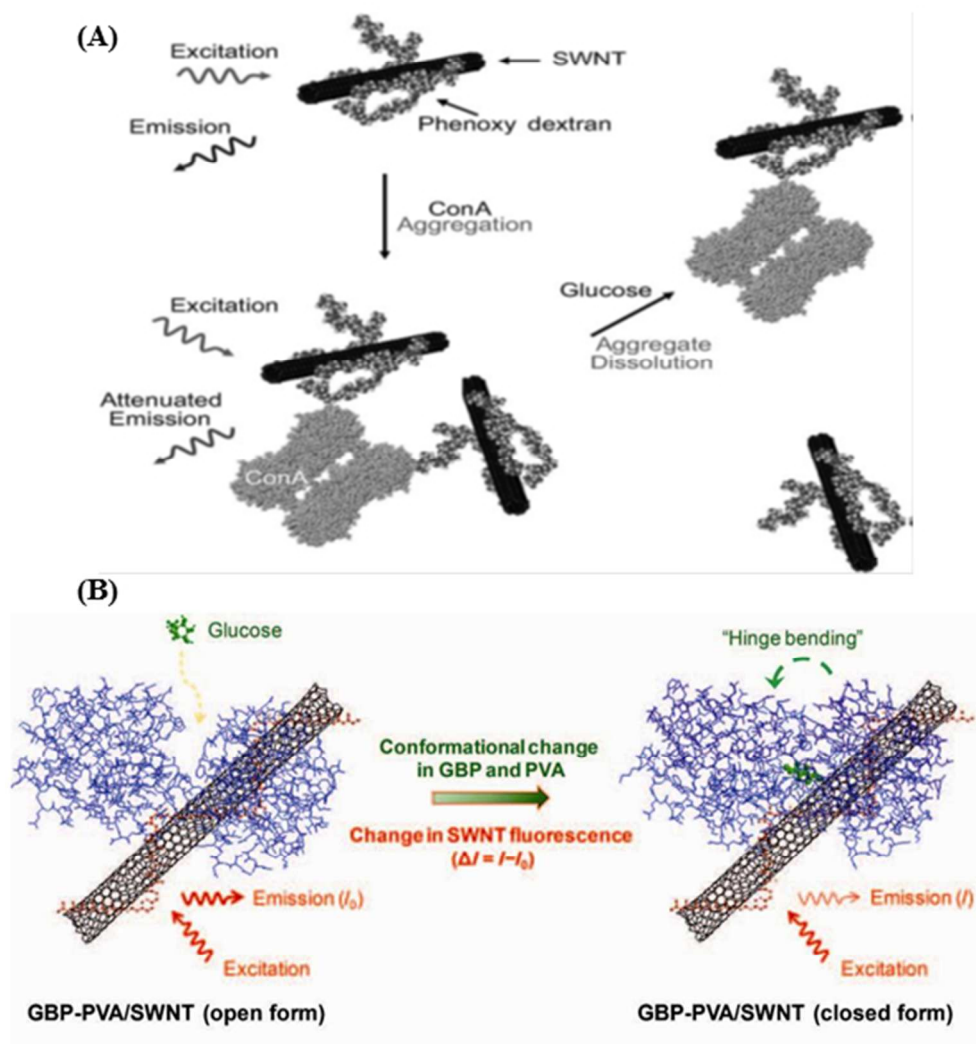


Figure 1. Schematic representation of polymer-wrapped SWCNT systems used for glucose detection: (A) Introduction of concanavalin A (ConA) to phenoxy-derivatized dextran-wrapped SWCNT initiates nanotube agglomeration, resulting in a decrease in nanotube fluorescence. The addition of glucose, which binds to ConA, separates the nanotube bundles with the recovery of fluorescence. (B) PVA-wrapped SWCNT is covalently tethered to GBP. Upon addition of glucose, the GBP undergoes a conformational change, resulting in a change in the SWCNT fluorescence intensity. Adapted from ref. 94 and 95, copyright 2006,2011 with permission from Wiley Inter-Science.

160x174mm (96 x 96 DPI)

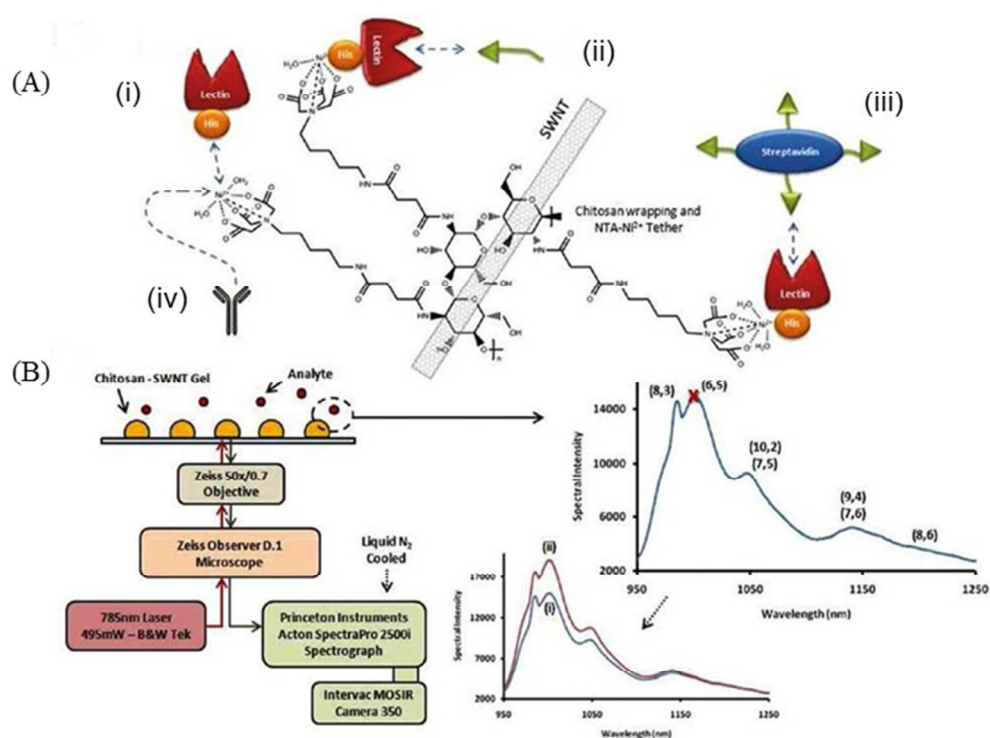


Figure 2. Schematic representation of chitosan-SWCNT sensors for glycan lectin detection. (A) The chitosan wrapped SWCNT sensors are processed to include tethered NTA groups and chelated Ni<sup>2+</sup> so that His-tagged lectins can attach to the sensors. (B) Ensemble measurement setup: the chitosan-SWCNT gel is spotted onto glass chips which are excited by a laser, and the emission spectra are analyzed. Reprinted from ref. 100, copyright 2011, with permission from American Chemical Society.  
192x148mm (96 x 96 DPI)

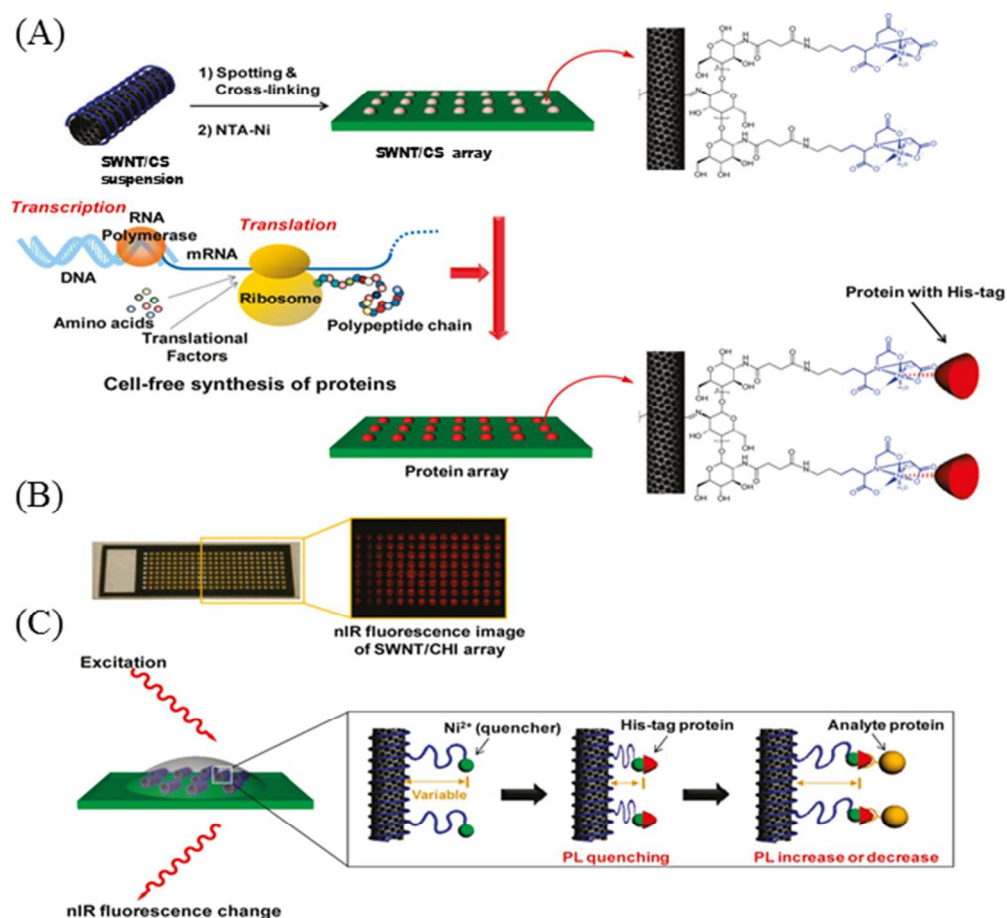


Figure 3. (A) Sensor array fabricated using SWCNT/Chitosan (CS). A SWCNT/CS suspension is spotted on glass and functionalized with Ni-NTA to bind His-tag proteins. (B) Optical and NIR fluorescence image of the SWCNT/CS array. (C) Signal transduction mechanism for detection of protein-protein interactions: a NIR fluorescence change from the SWCNT occurs when the distance between the Ni<sup>2+</sup> quencher and SWCNT is altered upon analyte protein binding. Reprinted from ref.107, copyright 2011, with permission from American Chemical Society.  
172x161mm (96 x 96 DPI)

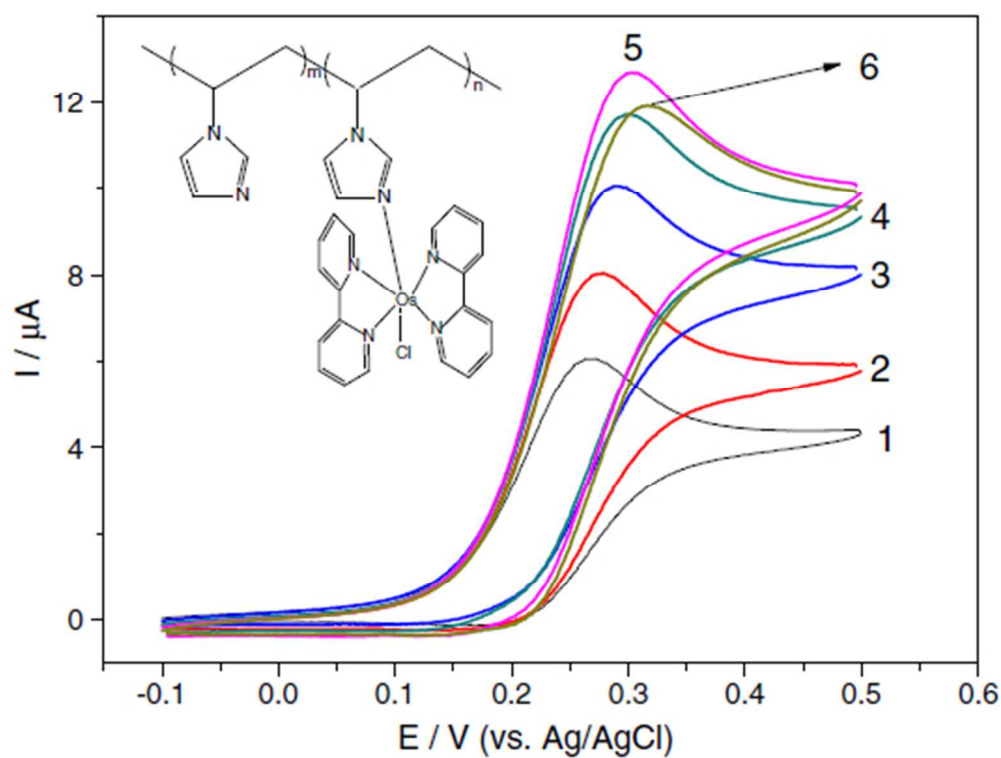


Figure 4. Cyclic voltammograms of SPCE modified with different numbers of GOX/SWCNT/PVI-Os layers in the presence of 10 mM glucose. The layer number is shown in the figure. The potential scan rate was 10 mV/s. Inset: structure of the redox polymer PVI-Os. Reprinted from ref 139, copyright 2011, with permission from Elsevier.  
141x110mm (96 x 96 DPI)

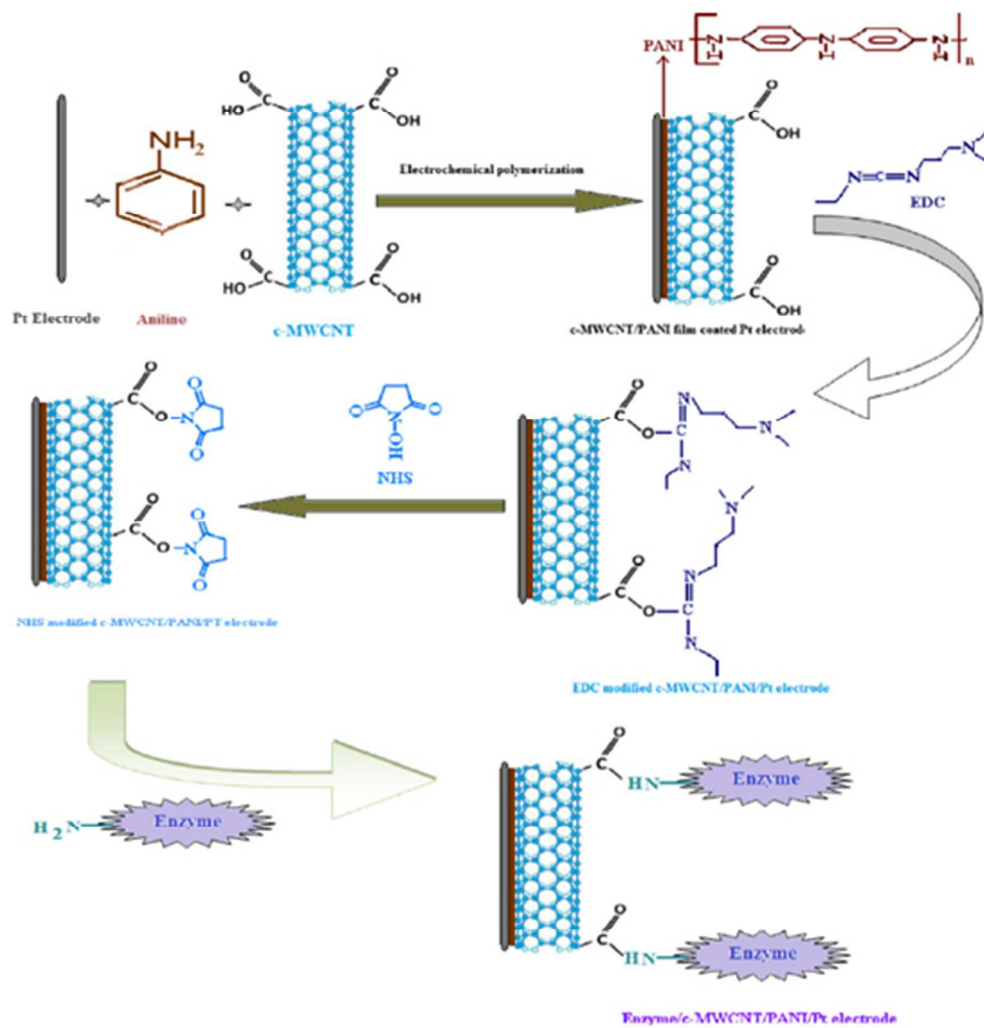


Figure 5. Schematic representation of chemical reaction involved in the fabrication of enzyme/MWCNT/PANI/Pt modified electrode. Reprinted from ref.143, copyright 2011, with permission from Elsevier.

147x150mm (96 x 96 DPI)

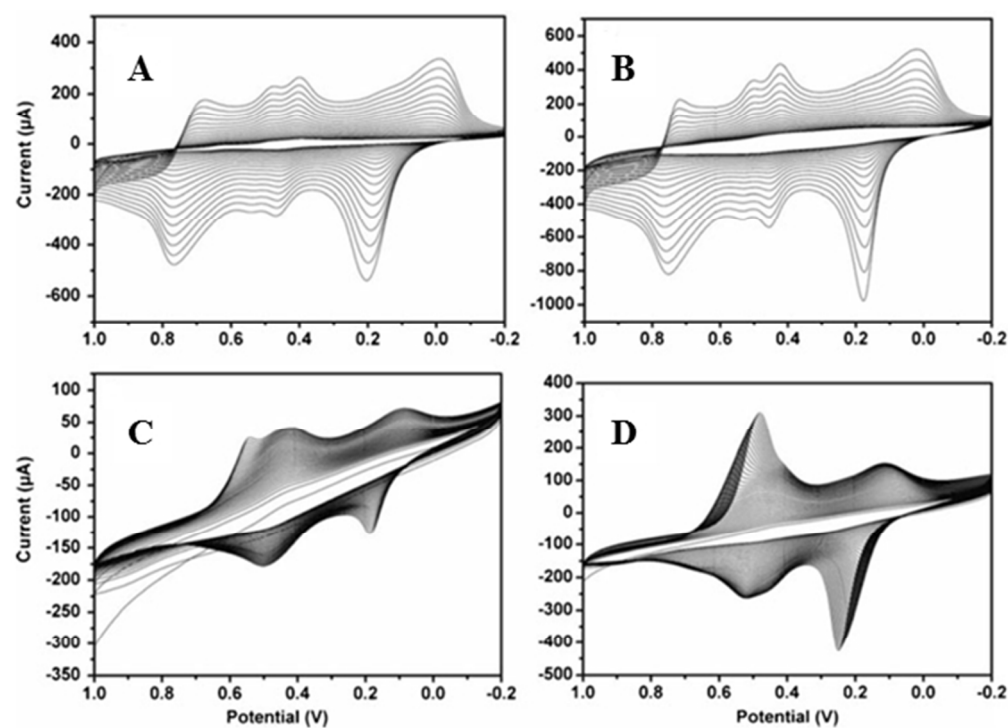


Figure 6. CVs of the electropolymerization process in aniline (A), CNTs+aniline (B), SiW12+aniline (C) and CNTs+SiW12+aniline (D), respectively. Reprinted from ref. 146, copyright 2013, with permission from Springer.

169x124mm (96 x 96 DPI)

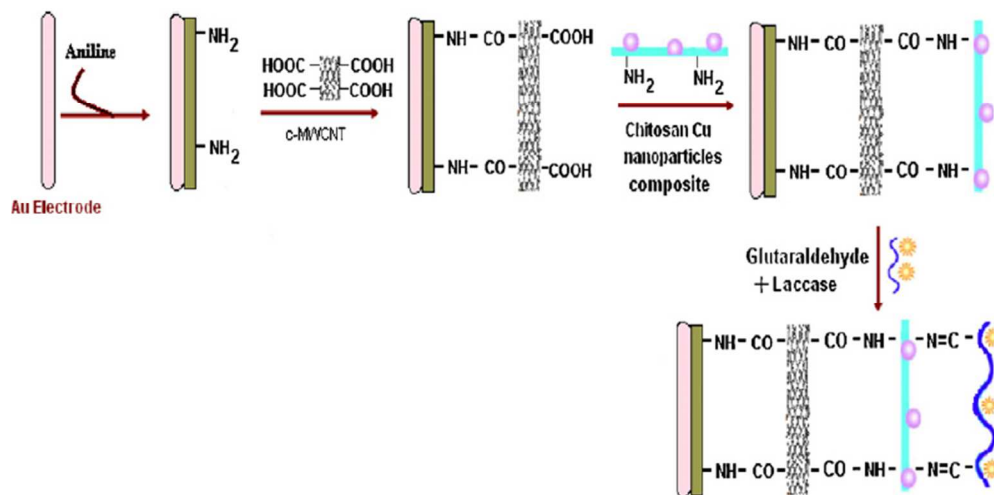


Figure 7. Scheme of chemical sequence of electropolymerization of CuNPs-CS-cMWCNT-PANI on gold electrode and chemical reaction of immobilization of laccase enzyme. Reprinted from ref. 148, copyright 2011, with permission from Elsevier.  
212x105mm (96 x 96 DPI)

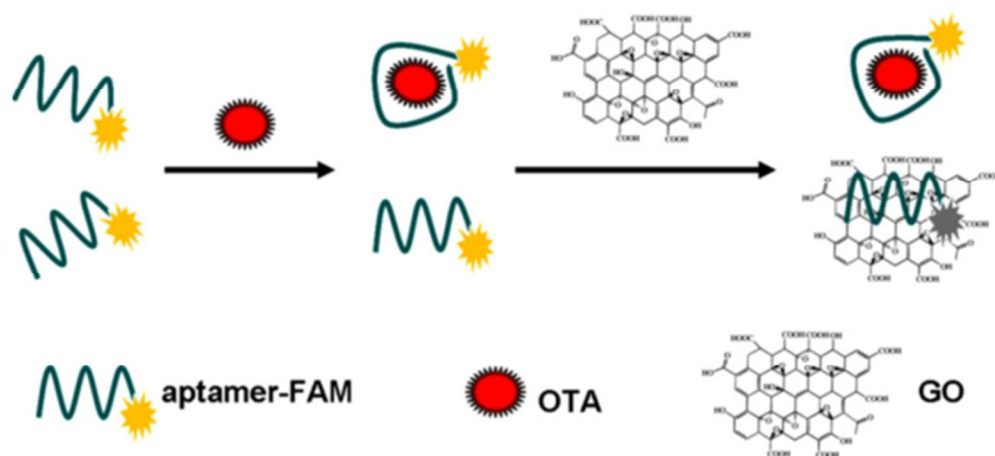


Figure 8. Schematic illustration of graphene oxide sensing platform for detection of ochratoxin A. Reprinted from ref. 171, copyright 2011, with permission from Elsevier. 179x82mm (96 x 96 DPI)

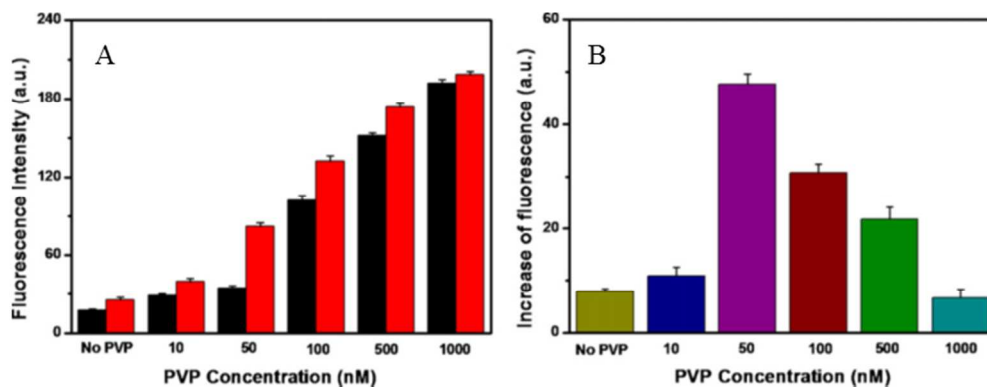


Figure 9. (A) Effect of PVP concentration on the fluorescence intensity of graphene oxide/FAM-modified aptamer without (black bar) and with (red bar) existence of ochratoxin A. (B) Columns bars were obtained by subtracting the value of black columns bars from the value of corresponding red columns bars, Error bars were obtained from three experiments. Reprinted from ref. 171, copyright 2011, with permission from Elsevier.

223x84mm (96 x 96 DPI)

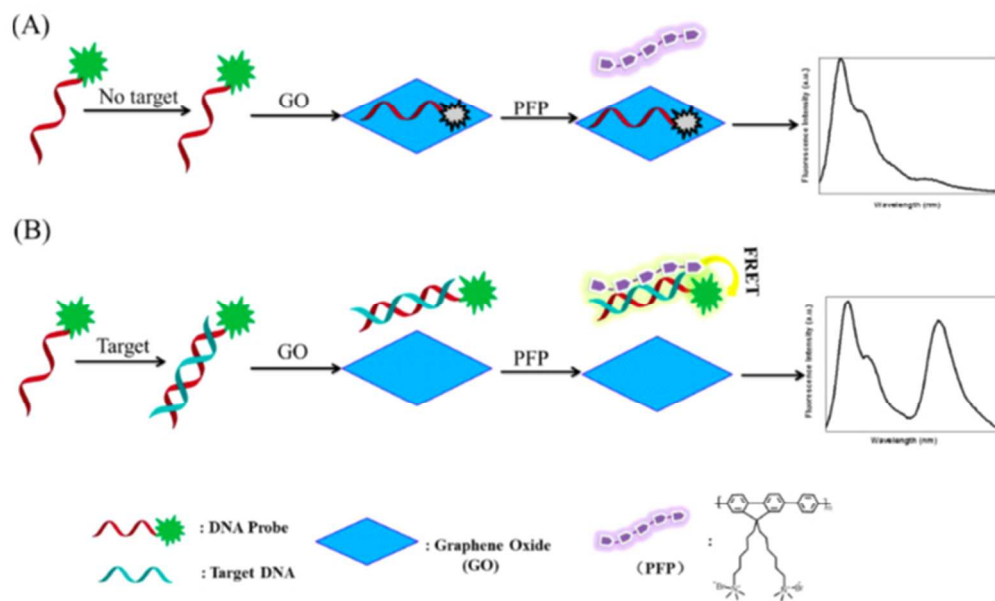


Figure 10. Schematic representation of GO-based low background-signal platform for the detection of target DNA. Reprinted from ref. 174, copyright 2012, with permission from American Chemical Society. 199x119mm (96 x 96 DPI)

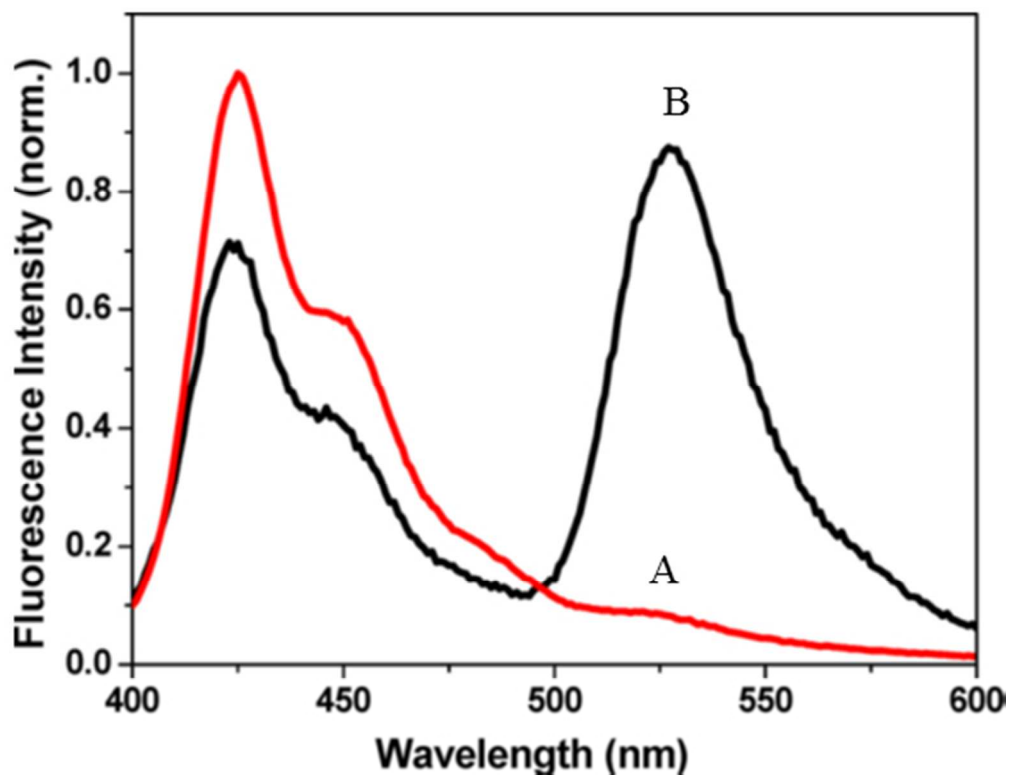


Figure 11. Normalized FRET-induced fluorescence spectra of P-GO-PFP system under different addition order: (A) addition of PFP into P/GO complex and (B) addition of P into PFP/GO complex by exciting at 370 nm. Reprinted from ref. 174, copyright 2012, with permission from American Chemical Society. 148x115mm (96 x 96 DPI)

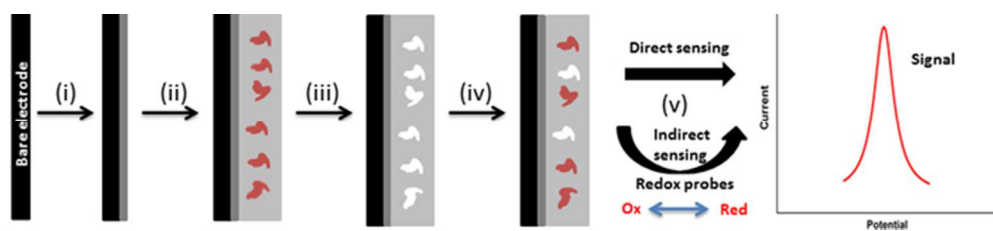


Figure 12. Schematic illustration of fabrication of a graphene/MIP-based sensor. (i) Drop casting of graphene derivatives; (ii) electropolymerization in the presence of the target; (iii) washing/elution of the template; (iv) incubation; (v) sensing.  
187x40mm (96 x 96 DPI)

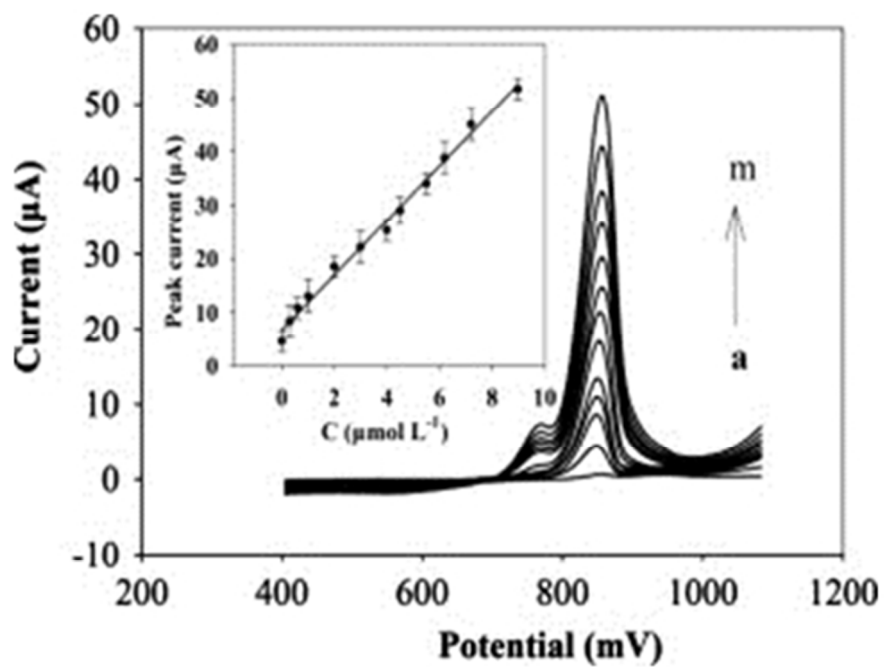


Figure 13. DPVs of the POPDA-GNWs@IL/PPNPs-RGO-COOH-GCE sensor in a Britton-Robinson buffer solution (pH 2.0) containing CEF of different concentrations:  $1.0 \times 10^{-10}$  to  $8.9 \times 10^{-6}$  mol L<sup>-1</sup>. Inset shows the calibration curve of CEF. Reprinted from ref. 207, copyright 2014, with permission from Elsevier. 115x89mm (96 x 96 DPI)

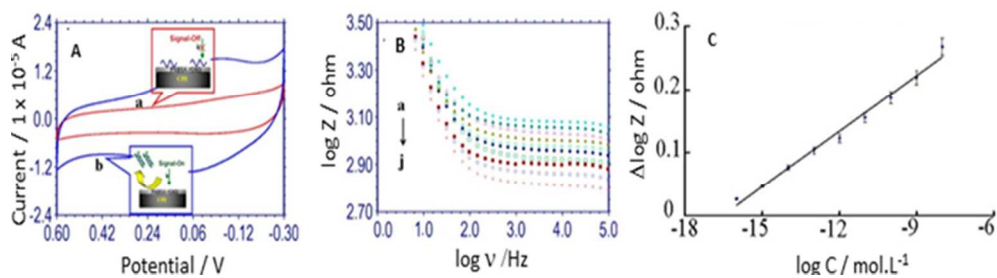


Figure 14. (A) Representative CVs of the pDNA-PABSA/RGO-CPE before (a) and after hybridization reaction (hybridized with  $1.0 \times 10^{-10}$  mol L<sup>-1</sup> cDNA, (b) recorded in 0.30 mol L<sup>-1</sup> phosphate buffer solution (pH 7.0); (B) Representative Bode plots of pDNA-PABSA/RGO-CPE before (a) and after being hybridized with its complementary PML/RARA gene sequence of different concentrations:  $1.0 \times 10^{-16}$  mol L<sup>-1</sup> (b) to  $1.0 \times 10^{-8}$  mol L<sup>-1</sup>(j). (C) The plot of  $\Delta \log Z$  vs the logarithm of target sequence concentrations. Reprinted from ref. 213, copyright 2013, with permission from American Chemical Society  
186x50mm (96 x 96 DPI)

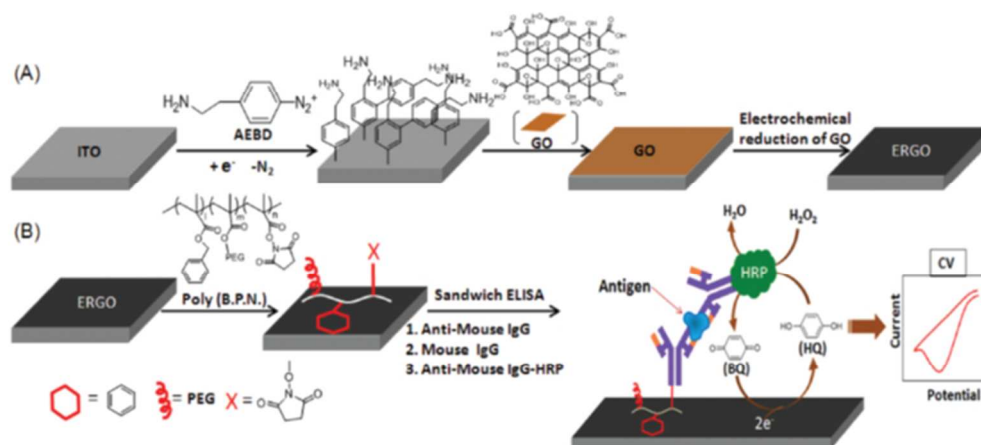


Figure 15. Schematic representation of the preparation of the electrochemical immunosensing platform. (A) Electrodeposition of AEED, deposition of GO on the AEED-modified surface, and electrochemical reduction of GO to ERGO. (B) Attachment of poly(B.P.N.) on the ERGO-modified surface, and detection of mouse IgG through a sandwich ELISA protocol, and electrochemical reduction of enzymatically produced BQ on the sensor surface. Reprinted from ref. 223, copyright 2012, with permission from American Chemical Society. 206x94mm (96 x 96 DPI)

The performance of chemical sensors based on polymer nanocomposites with CNT and graphene is revised, highlighting the role of the polymeric material.

